COMPATIBILTY PRE-SCREENING OF BENTONITE-BASED BARRIER SYSTEMS

A Thesis Submitted to the College of

Graduate Studies and Research

in Partial Fulfillment of the Requirements

for the Degree of Master of Science

in the Department of Civil and Geological Engineering

University of Saskatchewan

Saskatoon, Saskatchewan, Canada

By

Randal Osicki

Permission to Use

In presenting this thesis in partial fulfillment of the requirements for a Postgraduate degree from the University of Saskatchewan, I agree that the Libraries of this University may make it freely available for inspection. I further agree that permission for copying of this thesis in any manner, in whole or in part, for scholarly purposes may be granted by the professor or professors who supervised my thesis work or, in their absence, by the Head of the Department or the Dean of the College in which my thesis work was done. It is understood that any copying or publication or use of this thesis or parts thereof for financial gain shall not be allowed without my written permission. It is also understood that due recognition shall be given to me and to the University of Saskatchewan in any scholarly use which may be made of any material in my thesis.

Requests for permission to copy or to make other use of material in this thesis in whole or part should be addressed to:

Head of the Department of Civil and Geological Engineering
University of Saskatchewan
57 Campus Drive
Saskatoon, Saskatchewan
Canada
S7N 5A9

Abstract

Soil hydraulic conductivity is related to its internal structure, which is in turn a function of its mineralogy and placement conditions. However, this structure is not constant and changes with time as a result of chemical, physical and biological processes. Commonly, these changes result in a net increase in hydraulic conductivity.

A laboratory testing program was established to evaluate the performance and characteristics of two different bentonites. Index tests can be used to evaluate the performance of bentonite when exposed to chemical wastes. Some index tests are better than others. According to this research the author suggests that the most helpful and reliable index tests are fluid loss and plastic viscosity.

The filter press test was extended to yield an estimate of the hydraulic conductivity of the resulting filter cake. Upon comparing the relative hydraulic conductivity values obtained from the filter press and the values obtained from permeameters, similar trends were observed with DDL thickness contraction; as the DDL thickness contracts the hydraulic conductivity increases.

A new alternative pre-screening method using plastic viscosity and the filter press was outlined and compared to the existing ASTM D 6141 free swell method. The plastic viscosity method consistently reported more conservative and reliable

results that have been verified with hydraulic conductivity testing. A compatibility plot with two warning limits has been identified for the two bentonites exposed to electrolyte solutions. The first limit identifies when slight increases in the hydraulic conductivity are expected and further testing is required to determine the extent of the increase. The second limit identifies when significant increases in the hydraulic conductivity will occur and that a different liner material should be used.

A high pH, phenolic wastewater was obtained and the two pre-screening methods were used to assess the chemical compatibility of the wastewater with two different bentonite products. The plastic viscosity method returned consistently accurate results, for both bentonites, which were verified with hydraulic conductivity testing, whereas, the ASTM D 6141 method returned two different results for the two bentonites used. It was concluded that the high pH, phenolic wastewater would slightly increase the hydraulic conductivity of a bentonite-based barrier system.

The author considers the new plastic viscosity method to be better than the existing pre-screening method outlined in ASTM D 6141. Although shown to have faults, the use of ASTM D 6141 may still be continued, as it is inexpensive and easy to perform in any laboratory with a graduated cylinder. The plastic viscosity method requires a device to measure the viscosity of a soil slurry; therefore, testing is limited to laboratories that possess such a device.

Acknowledgements

I would like to thank my supervisor, Professor Ian Fleming, for his suggestions and guidance, and for financial support throughout the research project.

I would also like to thank Professor Moir Haug and Professor Jitendra Sharma, for their comments and guidance pointing me in the right direction when all direction was lost.

I am indebted to Mr. Alex Kozlow for his assistance and direction through the soils laboratory, Mr Doug Fisher for aid in chemical analysis and a constant supply of salts and distilled de-ionized water, Miss Jana Lung for her help in performing Atterberg limits.

I would like to thank Mr. Ghirmay Yisak for keeping the work area in the laboratory clean and for his daily words of wisdom to lighten the spirits. I would also like to thank my fellow graduate students for sharing their experiences and support along the way. I would also like to thank any others who I may have missed that have contributed in the preparation of this manuscript.

Thanks to my friends and family for their support and encouragement. Special thanks go out to Amanda for being there for me in times of trouble and need.

Table of Contents

Permission to Use	**i**
Abstract	**ii**
Acknowledgements	**iv**
Table of Contents	**v**
List of Figures	**x**
List of Tables	**xiii**

Chapter 1 Introduction

1.1 Subject	1
1.2 Need	2
1.3 Objectives	3
1.4 Principal Findings	5

Chapter 2 Background Information and Literature Review

2.1 Introduction	7
2.2 Origin and Composition of Bentonite	7
2.3 Uses of Bentonite in Liner Systems	10

2.4 Properties and Behavior of Bentonites 11

2.4.1 Diffuse Double Layer Model 11

2.5 Bentonite Compatibility Testing 15

Chapter 3 Laboratory Testing Program

3.1 Introduction 19

3.2 Description of Test Materials 19

3.3 Diffuse Double Layer Determination 20

3.4 Bentonite Characterization 20

3.4.1Free Swell Index 21

3.4.2 Atterberg Limits 22

3.4.3 Viscosity Testing 25

3.4.4 Hydraulic Conductivity Testing 29

3.4.4.1 Filter Press 29

3.4.4.2 Triaxial Permeability Testing 37

3.4.5 X-Ray Diffraction Testing 43

Chapter 4 Laboratory Results and Discussion

4.1 Introduction 46

4.2 Laboratory Testing Results 46

4.2.1 Diffuse Double Layer 46

4.2.2 Free Swell Index 48

4.2.3 Atterberg Limits 52

4.2.4 Viscosity Testing 52

4.2.5 Hydraulic Conductivity Testing 59

4.2.5.1 Filter Press 59

4.2.5.2 Triaxial Permeability Testing 62

4.3 Comparison of Test Results 66

Chapter 5 Development of Alternative Pre-Screening Method

5.1 Introduction 78

5.2 Alternative Method Protocol 78

5.3 Proposed Alternative Method Criteria 80

5.4 Laboratory Case Study 80

Chapter 6 Case Study and Application of the Proposed Compatibility Pre-Screening Methodology

6.1 Introduction 86

6.2 Wastewater Characteristics 87

6.3 Initial Design Compatibility Testing 88

6.4 Construction and Operation 95

6.5 Long-Term Performance and Forensic Testing 99

6.5.1 X-Ray Diffraction 99

6.5.2 Hydraulic Conductivity Testing 101

6.5.2.1 Flexible Wall Permeameter (Soil-Bentonite) 101

6.5.2.2 Flexible Wall Permeameter (GCL) 103

6.6 Application of Pre-Screening Methods to Evaluate Compatibility 106

6.6.1 Pre-Screening Methods 106

6.6.1.1 Free Swell 106

6.6.1.2 Plastic Viscosity 110

6.7 Lessons Learned 111

Chapter 7 Conclusions and Recommendations

7.1 Introduction 114

7.2 Conclusions 114

7.3 Recommendations 117

References

Appendices

A: Dielectric Constants

B: Modified Mixing Procedure

C: Free Swell Index

D: Atterberg Limits

E: Viscosity Tests

F: Filtrate Loss

G: Hydraulic Conductivity Tests

H: Odometer Tests

I: Initial Design Compatibility Tests

J: Forensic Tests

*The Appendices are contained on a CD enclosed at the back of the Thesis.

List of Figures

Figure 2.1 – Structure of montmorillonite. 9
Figure 2.2 – Gouy-Chapman model. 12

Figure 3.1 – Fall cone. 24
Figure 3.2 – Flow curves. 26
Figure 3.3 – Fann viscometer. 27
Figure 3.4 – Wyoming bentonite slurries mixed with various KCl solutions. 29
Figure 3.5 – Filter press. 30
Figure 3.6 – Filter press apparatus with electronic balance. 32
Figure 3.7 – Filter cake development with time (GCL bentonite). 35
Figure 3.8 – Hydraulic conductivity stabilization with time (GCL bentonite). 36
Figure 3.9 – Permeameter cell. 39
Figure 3.10 – Permeameter system. 40
Figure 3.11 – Steel GCL cutting shoes. 41
Figure 3.12 – GDS pressure volume controller permeameter system. 42
Figure 3.13 – X-ray diffraction. 44
Figure 3.14 – Rotation of X-ray diffraction and intensity reading. 45

Figure 4.1 – Approximate DDL thickness for electrolyte solutions used. 47
Figure 4.2 – Free swell with NaCl. 49
Figure 4.3 – Free swell with KCl. 50
Figure 4.4 – Free swell with $CaCl_2$. 50
Figure 4.5 – Changes in free swell to changes in DDL thickness (GCL bentonite). 51

Figure 4.6 – Changes in liquid limit to changes in DDL thickness. 53

Figure 4.7 – Changes in plastic viscosity over time (Wyoming bentonite). 54
Figure 4.8 – Changes in plastic viscosity with salt concentration. 55
Figure 4.9 – Relationship between plastic viscosity and DDL thickness (Wyoming bentonite). 57
Figure 4.10 – Relationship between plastic viscosity and DDL thickness (GCL bentonite). 58
Figure 4.11 – Linear relationship between hydraulic conductivity and final filtrate volume. 60
Figure 4.12 – Changes in hydraulic conductivity related to changes in the DDL thickness. 61
Figure 4.13 – Relative changes in hydraulic conductivity related to changes in DDL thickness. 64
Figure 4.14 – Changes in hydraulic conductivity related to changes in void ratio. 65
Figure 4.15 – Relative hydraulic conductivity vs. relative free swell index. 68
Figure 4.16 – ASTM D 6141 compatibility criteria, relative hydraulic conductivity vs. relative free swell index. 69
Figure 4.17 – Total amount of filtrate collected vs. relative plastic viscosity. 71
Figure 4.18 – Hydraulic conductivity vs. relative plastic viscosity. 72
Figure 4.19 – Relative hydraulic conductivity vs. relative plastic viscosity. 73
Figure 4.20 – Warning electrolyte concentrations for Wyoming bentonite. 76
Figure 4.21 – Warning electrolyte concentrations for GCL bentonite. 77

Figure 5.1 – GCL specimen after removal of confining cell. 81
Figure 5.2 – GCL specimen with rubber membrane removed. 81
Figure 5.3 – Concentrated effluent in area of failure. 82
Figure 5.4 – Even influent distribution. 83
Figure 5.5 – Relative hydraulic conductivity vs. relative free swell index (for GCL permeated with increasing $CaCl_2$). 84
Figure 5.6 – Relative hydraulic conductivity vs. relative plastic viscosity (for GCL permeated with increasing $CaCl_2$). 85

Figure 6.1 – Distilled de-ionized water (left) and synthetic wastewater (right). 88
Figure 6.2 – XRD diffractograms of polymerized Wyoming bentonite exposed to wastewater (wet). 90
Figure 6.3 – XRD diffractograms of polymerized Wyoming bentonite exposed to wastewater (air dried). 91
Figure 6.4 – XRD diffractograms of polymerized Wyoming bentonite exposed to tap water (air dried). 92
Figure 6.5 – Hydraulic conductivity vs. time, soil-bentonite initial design compatibility (polymerized Wyoming bentonite). 93
Figure 6.5 – Hydraulic conductivity vs. time, soil-bentonite initial design compatibility (untreated Wyoming bentonite). 94
Figure 6.7 – Soil-bentonite liner installation. 95
Figure 6.8 – Completed composite liner construction. 96
Figure 6.9 – Equalization lagoon resumes in operation in December of 1999. 98
Figure 6.10 – Floating geomembrane in October of 2001. 98
Figure 6.11 – Damaged geomembrane. 99
Figure 6.12 – Hydraulic conductivity vs. pore volume of exhumed soil-bentonite Shelby tube sample. 102
Figure 6.13 – Hydraulic conductivity vs. pore volume for GCL permeated with synthetic wastewater. 105
Figure 6.14 – Free swell index of GCL bentonite in distilled de-ionized water and synthetic wastewater. 108
Figure 6.15 – Relative hydraulic conductivity vs. relative free swell (wastewater data). 109
Figure 6.16 – Slurries of GCL bentonite mixed with distilled de-ionized water and wastewater. 110
Figure 6.17 – Relative hydraulic conductivity vs. relative plastic viscosity (wastewater data). 113

List of Tables

Table 4.1 – Slight changes in hydraulic conductivity. 75

Table 4.2 – Substantial changes in hydraulic conductivity. 75

Table 5.1 – Proposed plastic viscosity pre-screening criteria. 80

Table 6.1 – Wastewater characteristics. 87

Chapter 1 Introduction

This chapter is designed to acquaint the reader with the rationale and need for this research, followed by the objectives the author has set out to accomplish. The chapter then concludes with a general overview of the findings from the research study conducted.

1.1 Subject

Liner or barrier materials often rely on clay minerals to provide low hydraulic conductivity. The small particle size, high specific surface, and swelling potential of smectitic clay minerals, renders them particularly useful. Since most bentonites contain a variety of clay minerals, there are situations where the potential exists for compatibility problems between the fluid being contained (permeant) and the clay mineral (Rowe et al. 1995). Such clay/permeant interactions may result in changes in hydraulic conductivity as a result from:

1. Contraction of the diffuse double layer surrounding the clay particles as a result of interaction with chemicals dissolved in pore water ($k\uparrow$),
2. Dissolution of soil constituents by strong acids or bases ($k\uparrow$),
3. Precipitation of solids into soil pores ($k\downarrow$),

4. Soil pore blockage due to the growth of microorganisms (k↓).

The increase in hydraulic conductivity is due to a variety of processes related to the clay mineralogy and clay-colloid chemistry, including diffuse double layer contraction, potassium fixation, ion exchange and potential mineral alteration (Alther et al. 1985; Fernandez and Quigley 1988; Petrov and Rowe 1997; Shackelford et al. 2000; Shan and Lai 2002).

1.2 Need

There is a need to evaluate the susceptibility of bentonite-based barrier materials to potential increases in hydraulic conductivity when exposed to some organic and inorganic contaminants. Testing for compatibility can involve considerable time and effort; thus, the use of a compatibility pre-screening procedure has a number of advantages. Pre-screening of bentonite for potential compatibility problems typically involves the use of quick and easy index testing. The goal of simple compatibility testing is to relate the changes in elemental, easily measured and reproducible properties of the bentonite to changes in hydraulic conductivity. The American Society for Testing and Materials (ASTM) Guide for Screening the Clay Portion of a Geosynthetic Clay Liner (GCL) for Chemical Compatibility to Liquids (ASTM D 6141) is one standard guide for pre-screening the clay for compatibility. This guide is based on changes in the swelling and fluid loss characteristics of the bentonite in contact with various wastes.

Haug and Boldt-Leppin (1994), Reschke and Haug (1991), and Reschke (1991) suggested that a simple measurement of the viscosity of a bentonite slurry

may be more effective than free swell index for the assessment or comparison of the quality of various bentonites hydrated with clean water. With these findings, the proposed new guide, by Osicki et al. (2004a), followed the same criteria as ASTM D 6141, but used changes in the viscosity and changes in filter press hydraulic conductivity of a bentonite/permeant slurry as the indicator of potential compatibility effects that could be associated with increased hydraulic conductivity. The results of the two methods are compared in Chapter 4.

Potential compatibility issues may be confirmed using more detailed testing, where required. In cases where the simple screening tests do not suggest problems, the GCL products may be used with an additional degree of confidence in long-term performance and compatibility. This approach is not just limited to the clay portion of a GCL but also to any bentonite-based material or mixture requiring low hydraulic conductivity.

1.3 Objectives

The objectives of this laboratory study are threefold. Reschke (1991) developed testing procedures to characterize bentonites for use in sand-bentonite liner systems. The testing procedures used in that study consisted of the free swell index, Atterberg limits, viscosity measurements, fluid loss, hydraulic conductivity testing, etc. The tests were performed on many different bentonites hydrated with clean water to determine the relative quality of each bentonite. The primary objective of this study is to investigate the applications of the Reshcke and Haug (1991), tests to changes in hydraulic conductivity as a result of clay permeant

interactions. Using these index tests and only two different bentonite products, the changes in the behaviour of the bentonite were recorded as it was hydrated with various electrolyte solutions. As part of this objective, the Fluid Loss Index test (API Filter Press) was extended to yield an approximation of the anticipated compatibility-induced changes in hydraulic conductivity.

The second objective is to establish an alternative pre-screening method from ASTM D 6141 using viscosity measurements. Identifying index tests that provide repeatable and reliable results did this.

The final objective is to compare the existing ASTM D 6141 pre-screening method with the new alternative pre-screening method. This should give the designer another tool to use in the event that a bentonite-based barrier system being designed will contain a chemical waste.

The thesis is divided into seven chapters. In Chapter 1, the subject has been introduced, the need for this research, and the objectives of the study have been outlined. Chapter 2 contains the literature review and provides background information on the properties and behaviour of bentonite as it comes into contact with contaminated fluids. A review on the use of bentonite in liner systems and previous bentonite compatibility studies are also included. A detailed literature review on the origin and composition of bentonite is provided by Reschke (1991) and Boldt-Leppin (1995) and will not be repeated here.

The laboratory test program is described in Chapter 3. The laboratory test program consisted of index testing and hydraulic conductivity testing of two different bentonite products hydrated with electrolyte solutions. Chapter 4 presents

the results of the testing program and comparison of the different index tests. Chapter 5 presents the development an alternative pre-screening method for bentonite compatibility. A case study demonstrating the use of both bentonite pre-screening methods is provided in Chapter 6, in which it is concluded that the proposed viscosity-based method (Osicki et al., 2004a) more reliably reflects the observed behaviour. The overall conclusions from the study and recommendations for further research are provided in Chapter 7.

1.4 Principal Findings

Index tests can be used to evaluate the performance of bentonite when exposed to chemical wastes. Some index tests are better than others. According to the research described herein, the author suggests that the most helpful and reliable index tests are fluid loss and plastic viscosity.

The filter press test was extended to yield an estimate of the hydraulic conductivity of the resulting filter cake. Upon measuring the fluid loss of the bentonite slurry, additional filtrate volume measurements were taken and the test duration increased. The resulting estimates for hydraulic conductivity stabilize after less than one hour.

Upon comparing the relative hydraulic conductivity values obtained from the filter press and the values obtained from the permeameters, similar trends were observed with DDL thickness contraction; as the DDL thickness contracts the hydraulic conductivity increases.

Plastic viscosity measurements can be used as a pre-screening tool for bentonite compatibility. The method uses quick and simple measurements. The results of the testing differ from those found for the free swell index, particularly with low to moderate electrolyte concentrations. It is hypothesized that shearing in the viscometer breaks down the flocculated structure that dominated the free swell test under these conditions.

A new alternative plastic viscosity pre-screening method was outlined and compared to the existing ASTM D 6141 free swell method. The plastic viscosity method consistently reported more conservative and reliable results, which have been verified with hydraulic conductivity testing.

A high pH, phenolic wastewater was obtained and the two pre-screening methods were used to assess the chemical compatibility of the wastewater and two different bentonites. The plastic viscosity method returned consistently accurate results for both bentonites, which were verified with hydraulic conductivity testing, whereas, the ASTM D 6141 method returned two different results for the two bentonites used.

The new plastic viscosity method is considered by the author to be better than the existing pre-screening method outlined in ASTM D 6141. Although shown to have faults, the use of ASTM D 6141 may still be continued, as it is inexpensive and easy to perform in any laboratory with a graduated cylinder. The plastic viscosity method requires a device to measure the viscosity of a soil slurry; therefore, testing is limited to laboratories that possess such a device.

Chapter 2 Background Information and Literature Review

2.1 Introduction

This chapter provides background information regarding the origin, composition, and properties of bentonite. The behaviour of bentonite in contact with contaminated fluids will be reviewed. A literature survey has been performed regarding bentonite in barrier systems and previous studies of bentonite compatibility.

2.2 Origin and Composition of Bentonite

Bentonite refers to any clay that is composed predominantly of the smectite group of minerals. Smectites, characteristically, have very high plasticity and swelling potential. Bentonite is formed from the alteration of tuff or volcanic ash. Ross and Shannon (1926) defined bentonite as:

> "Bentonite is a rock composed essentially of a crystalline clay-like mineral formed by the devitrification and the accompanying alteration of a glassy igneous material, usually a tuff or volcanic ash; and it often contains variable proportions of accessory crystal grains that were originally phenocrysts in the volcanic glass."

In order for bentonite to form, an aqueous environment is considered necessary in order to provide the required water for the hydration of the ash or tuff to smectite.

The structure of a smectite mineral consists of an octahedral layer sandwiched between two silica sheets giving a 2:1 layer structure, as shown in Figure 2.1. The individual 2:1 layers are bonded together by van der Waals forces and by cations that may be present due to charge deficiencies in the structure. The bonds between 2:1 layers are weak and easily separated by cleavage or by adsorption of water or other polar liquids. The basal spacing in the c direction can range from 0.96 nm to complete separation.

Isomorphous substitution of silicon or aluminium by other cations occurs during initial formation or subsequent alteration. This substitution is what gives rise to the charge deficiency in the clay particle. The charge deficiencies are balanced by exchangeable cations that get absorbed to the clay mineral. This charge deficiency is what is important in the behaviour of the clay mineral (Mitchell, 1993).

A more detailed review on the origin and composition of bentonite is provided by Reschke (1991) and Boldt-Leppin (1995) and will not be repeated here.

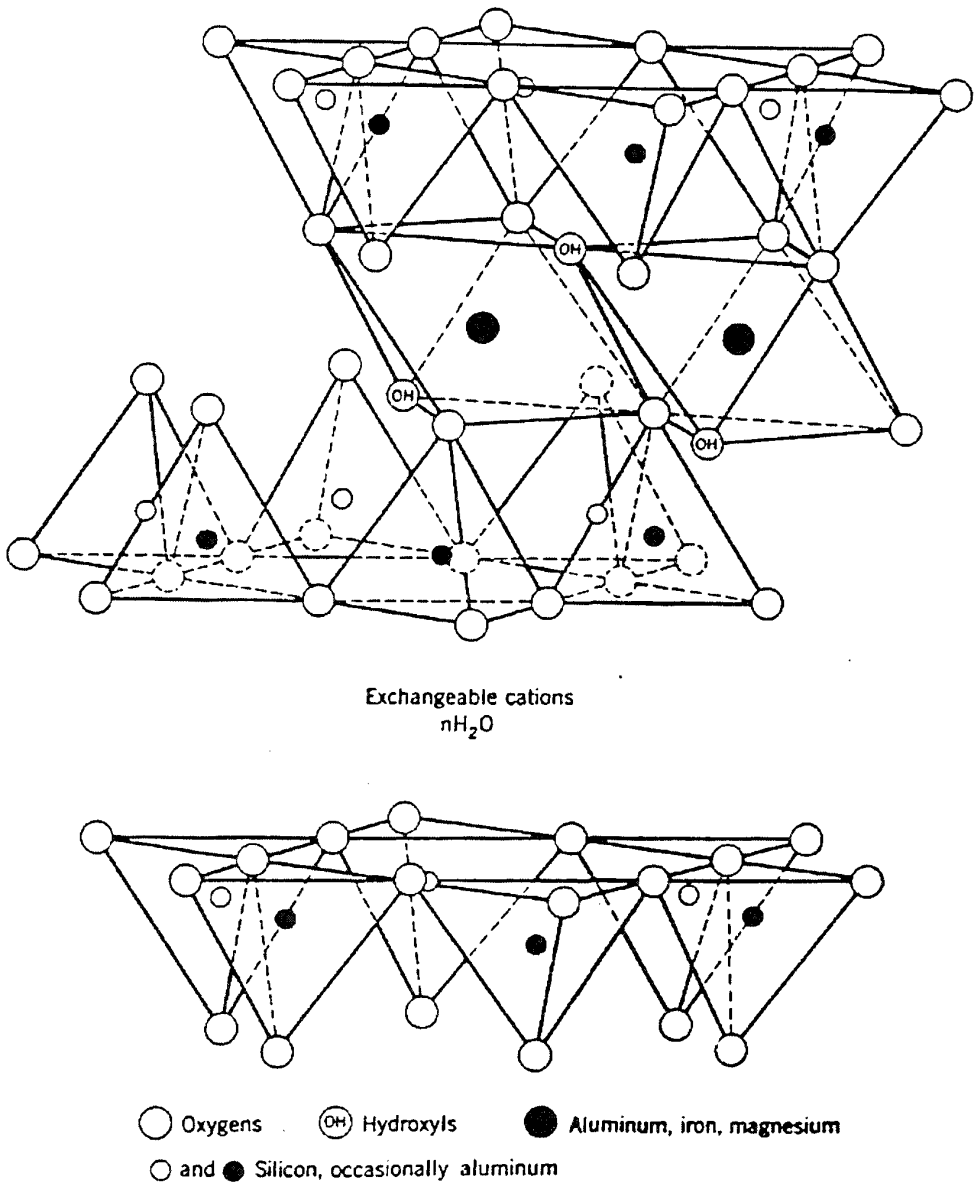

Figure 2.1 - Structure of montmorillonite (from Mitchell, 1993).

2.3 Uses of Bentonite in Liner Systems

Bentonite is widely used for a variety of purposes, ranging from drilling muds to clarification of beer and wine. Bentonite that is most common to geotechnical engineers is a highly colloidal, expansive clay that is an alteration product of volcanic ash. An attractive property of bentonite for industrial applications is its swelling capacity in water. The physical properties of the bentonite-water mixture change as its clay-to-water ratio changes. Depending on the ratio of the two components, bentonite-water mixtures are used for bonding, plasticizing, and suspending (Clem and Doehler, 1961). These outstanding physical properties give bentonite great commercial value. Its bonding qualities are applied in foundry molding sands, and in the pharmaceutical and cosmetic industries. Its high plasticity, as developed by adding water, is utilized in the ceramic and concrete industry to allow the raw materials to be easily shaped or molded. The best-known use of bentonite suspensions is in paints and drilling mud.

In geotechnical applications bentonite has additional uses because of its water absorbing characteristics that impede or stop the flow of water or aqueous solutions. It is widely used as a backfill during the construction of slurry trench walls (Haug, 1985), as a soil admixture for construction of seepage barriers (Reschke, 1991), as a grout material, as a sealant for piezometer installations, and for other special applications (Mitchell, 1993). Bentonite is also used as a low hydraulic conductivity component in geosynthetic clay liners (GCLs). In some circumstances, GCLs may have advantages over compacted clay liners, and GCLs

are often used in conjunction with polyethylene or other polymer geomembranes. The resulting composite barrier system has many advantages associated with the geomembrane in intimate contact with the low hydraulic conductivity clayey barrier material, in this case represented by the GCL.

The consideration of bentonite-based barrier systems has initiated a new field of research of the geotechnical engineer. The challenge includes the restriction of increasing environmental contamination by chemicals through the application of bentonite in contaminant barrier systems.

2.4 Properties and Behaviour of Bentonites

Bentonites tend to be highly reactive as a consequence of both their large specific surface area and their inherent charge deficiency. It is the existence of this inherent charge deficiency that is the basis of the exchange capacity and the swelling behaviour of the material (Mitchell, 1993).

2.4.1 Diffuse Double Layer Model

The properties of bentonite are greatly affected by interactions between its charged particles and the surrounding pore fluid. The charged surface and the distribution of the ions in the pore fluid are termed the diffuse double layer. Several models have been proposed for the quantitative description of ion distributions adjacent to charged surfaces. The Gouy-Chapman model of the diffuse double layer has received the greatest attention (Mitchell, 1993).

Clay particles are negatively charged. Cations are attracted to the clay surface to neutralize the electronegativity of the clay particles. In solution, cations and polar water molecules are adsorbed to the clay surfaces to maintain electrical neutrality. As a result, the adsorbed cations have a greater cation concentration at the clay surface than in the bulk solution. The resulting cation concentration gradient is associated with a resulting tendency for the cations to diffuse away from the clay surface towards the bulk solution. The net result of the electrostatic attraction of cations to the clay surface, and the diffusion away is an equilibrium situation. The area around the clay surface, in which this equilibrium is taking place, has some finite, but diffuse, thickness where the cation concentration and therefore electrochemical potential decreases with distance away from the clay surface, as shown in Figure 2.2.

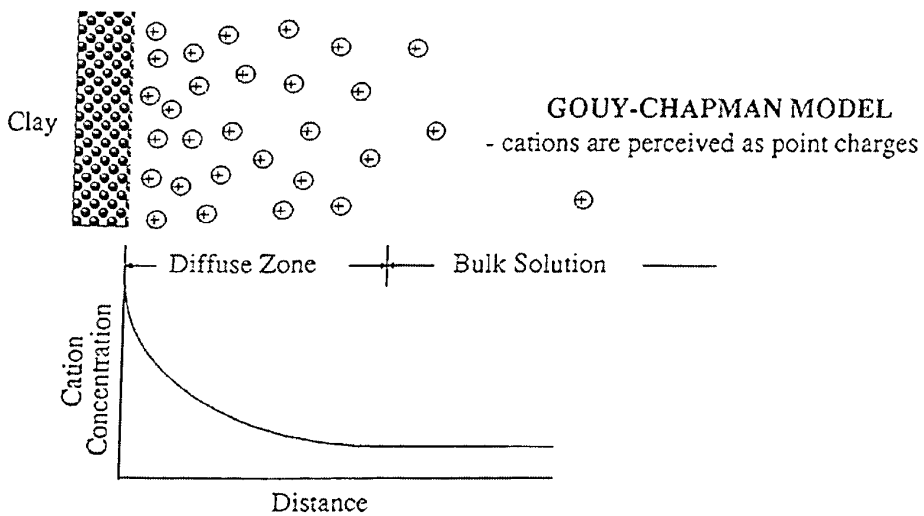

Figure 2.2 - Gouy-Chapman model (after Mitchell, 1993).

Despite the fact that this model does not account for all the factors that can influence the behaviour of the soil-water-electrolyte system, it has been useful as a generalized model for explaining clay-chemical interactions (Goldman et al., 1990 and Rowe et al., 1995). Although this model has only been shown to accurately describe the actual distribution of ions for smectite particles suspended in monovalent solutions at low concentration (McBride, 1997), it provides a useful basis for the understanding of flocculation and deflocculation and the relationship of these processes to the formation of soil structure. Despite some limitations, it will be used in this thesis.

A mathematical description of the diffuse double layer has been developed for planar clay surfaces. The approximate diffuse double layer thickness ($1/K$) is defined using the Gouy-Chapman equation (Mitchell, 1993).

$$\frac{1}{K} = \left(\frac{\varepsilon_o DkT}{2n_o e^2 v^2} \right)^{1/2} \tag{2.1}$$

where ε_o is the static permittivity of a vacuum (8.8542 x 10^{-12} $C^2J^{-1}m^{-1}$), D is the dielectric constant, k is the Boltzmann constant (1.38 x 10^{-23} $J°K^{-1}$), T is temperature (°K), n_o is the electrolyte concentration, e is the electronic charge (1.602 x 10^{-19} C), and v is the cation valence.

The following assumptions are made:

1. Ions in the double layer are point charges, and there are no interactions between them.
2. Charge on the particle surface is uniformly distributed.

3. The particle surface is a plate that is large relative to the thickness of the double layer.

4. The permittivity of the medium is independent of position.

This relationship shows that the thickness varies inversely with the valence and the square root of the concentration and directly with the square root of the dielectric constant and temperature, other factors remaining constant. However, an increase in temperature results in a decrease in dielectric constant. This tends to negate the effects of temperature change, and diffuse double layer thickness is usually not affected to any significant degree. Considerations of the influences on the dielectric constant are of great interest. Even though the pore fluid is generally water, the bentonite may be in contact with chemicals of various types when bentonite liners are used for impoundments and waste storage or by accidental spills and leaks (Mitchell, 1993).

According to the above Gouy-Chapman correlation, the thickness of the diffuse double layer influences the hydraulic conductivity and the swelling of bentonite by reducing or increasing the bound water between two clay particles, thus changing the size of the flow paths in a volume controlled environment. Using the diffuse double layer thickness to estimate the hydraulic conductivity is somewhat far-fetched, as the hydraulic conductivity is not only influenced by the diffuse double layer thickness, but also by the structure of the clay, stress level and stress history. However, the correlation does recognize the importance of the electrolyte concentration, cation valence, and dielectric constant (Egloffstein, 2001).

In general, the thicker the diffuse double layers, the fewer tendencies for the particles in suspension to flocculate and the higher the swelling pressure in expansive soils.

2.5 Bentonite Compatibility Testing

Soil hydraulic conductivity is related to its internal structure, which is in turn a function of its mineralogy and placement conditions. However, this structure is not constant and changes with time as a result of chemical, physical and biological processes. These changes may in an increase in hydraulic conductivity. Changes in hydraulic conductivity of clay soils from chemical interaction may result from:

a. Alterations in soil fabric from chemical influences on the diffuse double layer surrounding the clay particles ($k\uparrow$).

b. Dissolution of soil constituents by strong acids or bases ($k\uparrow$).

c. Precipitation of solids in soil pores ($k\downarrow$).

d. Soil pore blockage due to the growth of microorganisms ($k\downarrow$).

The alteration in soil fabric due to interactions between chemicals and clay soils has been the subject of many investigations. The results of these studies are summarized by Mitchell and Madsen (1987), and Shackelford (1994). These previous compatibility studies have shown that changes in hydraulic conductivity can be related to changes in the diffuse double layer thickness. A dispersed deflocculated soil fabric tends to have a large number of very small pore spaces. A flocculated soil fabric has relatively large inter-particle pore spaces. These large

pore spaces may cause drastic changes in the hydraulic conductivity of the clay soil since the flow rate is proportional to the square of the diameter of the flow channel. The inter-particle spacing is a function of the thickness of the diffuse double layer (Goldman et al., 1990). In theory, the change in hydraulic conductivity with varying pore fluid chemistry could be predicted if the variables that affect the thickness of the diffuse double layer are known. However, most soils contain a wide variety of minerals and particle size distributions which make chemical-soil interactions difficult to predict as a whole. Additionally, in practice, the effect of DDL contraction my be partially or completely masked by volume change associated with consolidation under high effective stress.

Even though bentonites are quite heterogeneous, the Gouy-Chapman model provides a reasonable approximation to the chemical-soil interactions. The diffuse double layer thickness decreases as the ion concentration increases, resulting in flocculation of the clay particles and larger pore channels where flow can occur (Mitchell, 1993; Gleason et al., 1997; Petrov et al. 1997; Rowe et al., 1997; Ruhl and Daniel, 1997; Stern and Shackelford, 1998; and Shan and Lai, 2002).

Compatibility studies dealing with the effects of chemicals on the hydraulic conductivity of bentonite are summarized by Alther et al. (1985), Fernandez and Quigley (1988), Gleason et al. (1997), Petrov and Rowe (1997), Shackelford et al. (2000), Jo et al. (2001), and Kashir and Yanful (2001). The results of these studies are consistent with the diffuse double layer model. Liquids with high electrolyte concentration, high cation valence and low dielectric constant, tend to increase the hydraulic conductivity.

Choosing the right permeameter type for compatibility testing is very important. Flexible wall permeameters (stress controlled) can mask hydraulic conductivity increases in cases where the soil shrinks and cracks. The confining pressure may cause cracks to close up, counteracting the effect of the permeant. Rigid wall permeameters (strain controlled) may overestimate the hydraulic conductivity in cases where the soil shrinks and pulls away from the cell wall (Filz et al., 2001).

Unfortunately, laboratory testing involves considerably shorter time frames than the design lifespan of soil liners. To compensate, lab testing should be conducted for as long a time as feasible and must be sufficiently accurate to detect subtle changes in hydraulic conductivity with time, which may indicate potential problems. In many instances this time frame is in the order of months and sometimes years. As testing for compatibility can involve considerable time and effort, pre-screening methods have been developed to determine if a laboratory compatibility study is necessary. The goal of the pre-screening methods is to relate the changes in elemental, relatively easily measured and reproducible properties of the bentonite to changes in hydraulic conductivity. These pre-screening methods expose a small amount of the bentonite to a large volume of the chemical liquid; this method allows the chemical alterations to occur quickly. By determining the relative changes in fundamental properties of the bentonite, an estimation of the chemical compatibility can be established. The American Society for Testing and Materials (ASTM) Guide for Screening the Clay Portion of a Geosynthetic Clay Liner (GCL) for Chemical Compatibility to Liquids (ASTM D 6141) is the standard guide for

pre-screening the clay for compatibility. This guide is based on changes in the free swell index (ASTM D 5890) and fluid loss (ASTM D 5891) of the bentonite in contact with various wastes.

In addition to laboratory hydraulic conductivity testing, methods such as x-ray diffraction (Kashir and Yanful, 2001), swell tests (Shackelford et al., 2000; Egloffstein, 2001; Jo et al., 2001; and Shan and Lai, 2002), Atterberg limits (Petrov and Rowe, 1997; Gleason et al., 1997; and Sivapullaiah and Savitha, 1999), and other techniques have been used to investigate chemical compatibility.

Simpson (2000) used Atterberg limits, free swell and fluid loss to correlate index tests to hydraulic conductivity. It was found that the results did not correlate well when all the different bentonite samples were grouped together. When the individual bentonites were evaluated, a correlation between the index tests and the hydraulic conductivity could be made. The liquid limit decreased, the fluid loss increased and the free swell volume decreased, which would correlate to an increase in hydraulic conductivity that did occur. The following chapters will build on these findings and explore new tests that may be used to correlate index testing and hydraulic conductivity to be used when investigating chemical compatibility.

Chapter 3 Laboratory Testing Program

3.1 Introduction

This chapter will focus on the laboratory-testing program. The laboratory test procedures will be described. The applicability of these tests using bentonite/water slurries to evaluate different raw and processed bentonite products for use in low hydraulic conductivity liner systems has been explored by Reschke and Haug (1991), and Haug and Boldt-Leppin (1994). This work, and the work described by Osicki et al. (2004b), explores the potential use of these same tests to evaluate potential compatibility problems with various electrolyte solutions.

3.2 Description of Test Materials

Two different sodium bentonites were used in the test program. The first was a granular bentonite that is used in Bentofix™ NWL Geosynthetic Clay Liners (GCL bentonite) available from Terrafix Geosynthetics Inc. The second bentonite was powdered BAKA-KADE® Standard (Wyoming bentonite), a non-treated natural Wyoming bentonite available from Bentonite Performance Minerals. The granular bentonite was ground to finer sizes (i.e. passing the #200 sieve) depending upon the particular requirements of each test method. Test samples were mixed with

various electrolyte solutions at concentrations for which increases in hydraulic conductivity have been documented in the literature. The electrolyte solutions included various concentrations of inorganic salt species; sodium chloride (NaCl), potassium chloride (KCl), and calcium chloride ($CaCl_2$) along with a distilled de-ionized water reference solution.

3.3 Diffuse Double Layer Determination

The diffuse double layer (DDL) is a region of adsorbed ions and polarized water associated with the charged surface of the clay particle. The DDL thickness is defined using the Gouy-Chapman equation (2.1). Despite the limitations of the Gouy-Chapman theory, it was used to model the approximate changes in DDL thickness for various electrolyte solutions.

Changes in the DDL thickness are easy to estimate. The dielectric constant can be measured and the electrolyte concentration of a solution can be determined from the electrical conductivity. The dielectric constants for ten of the various electrolyte solutions were measured using an HP85070A dielectric probe at the University of Western Ontario. The dielectric constants were plotted versus electrolyte concentration, and the required values for the pore water dielectric constant were interpolated from the measured data and can be found in Appendix A.

3.4 Bentonite Characterization

Bentonite characterization is performed through the use of index tests. These tests are used to characterize the quality of bentonite when hydrated with distilled

water. These tests include free swell index, Atterberg limits, viscosity testing, fluid loss, and x-ray diffraction, to name a few. These tests are described in the subsequent sections below indicating how they can be used as an indicator to the performance of, or changes to the bentonite when exposed to chemical permeants.

3.4.1 Free Swell Index

The free swell test has been developed in soil engineering investigations to serve as an indication for identification of the swelling of soils. The free swell index method gives a true picture of the soil swelling ability as it considers the type of clay minerals present in the soil and their associated repulsive and attractive forces reflected in the sediment volume of the soil in any fluid (Das, 1999). This is the case as the soil is permitted to swell in a zero effective stress environment. In this environment the soil is free to develop its desired structure, either flocculated or deflocculated depending on fluid conditions. In clean water the structure is deflocculated, while in electrolyte fluids the structure becomes flocculated.

Free swell index tests have been used to assess the potential for incompatibility between bentonite and a permeant liquid. In general, the greatest swell occurs when the hydrating liquid is de-ionized or distilled water because the interlayer and adsorbed water layer are at their maximum thickness. A decrease in the free swell index relative to that obtained with de-ionized water is indicative of shrinkage of the interlayer and adsorbed layers and a potential incompatibility between the bentonite and permeant liquid (Shackelford et al., 2000 and Simpson, 2000).

As described by the Gouy-Chapman model, the swelling of bentonite is related to the cation valence of the solute, the electrolyte concentration and the dielectric constant of the solution. The swell volume is inversely proportional to the electrolyte concentration and cation valence. On the other hand, the swell volume is directly proportional to the dielectric constant (Shan and Lai, 2002).

A standard test method has been developed for free swell index testing of bentonite. ASTM Test Method for Swell Index of Clay Mineral Component of Geosynthetic Clay Liners (ASTM D 5890) is the standard method that uses 2 g of bentonite and 100 ml of pore fluid. In a 100 ml graduated cylinder, 90 ml of the pore fluid is poured in and 0.1 g of the bentonite is added every ten minutes until all 2 g is added. The remaining 10 ml of the pore fluid is then added to wash down any bentonite that is stuck on the side of the graduated cylinder. The cylinder is covered to prevent evaporation and allowed to sit for 24 hrs. The swell volume in ml is recorded after the 24 hrs.

These tests were carried out to compare the proposed viscosity method to the ASTM D 5890 method for pre-screening the clay component of GCLs. Similar electrolyte solutions used to measure the free swell index of the GCL bentonite were also used in the viscosity testing, which is described below in Section 3.4.3. The results of the free swell testing will be summarized in Chapter 4.2.2.

3.4.2 Atterberg Limits

Atterberg limits are widely considered to be a fundamental index property of fine-grained soils. These limits are index tests that relate the water content of the

material to the termination between certain limiting or critical stages in soil behaviour.

1. Upper limit of viscous flow.
2. Liquid limit – lower limit of viscous flow.
3. Sticky limit – where the clay loses its adhesion to a metal blade.
4. Cohesion limit – where grains cease to cohere to each other.
5. Plastic limit – lower limit of the plastic state.
6. Shrinkage limit - lower limit of volume change.

Presently the most common Atterberg limits used are the liquid limit and the plastic limit. ASTM Test Methods for Liquid Limit, Plastic Limit, and Plasticity Index of Soils (ASTM D 4318) is used to determine these limits. An alternative method to determine the liquid limit is the British Standard Determination of Liquid Limit, Preferred Method using Cone Penetrometers (BS 1377-1990 Test 2(A)), which uses a Fall Cone, as shown in Figure 3.1, to determine the liquid limit. The weight and angle of the cone used are 100 g and 60°, respectively. The British method follows the same material preparation, but uses soil penetration to determine the liquid limit. The soil is mixed at various water contents as in ASTM D 4318. The water contents are such that the penetration range is between 15 and 25 mm. A straight line is best fit on a plot of water content versus penetration. The liquid limit is the water content at a penetration of 20 mm.

Liquid limits have been used to assess chemical compatibility of bentonite. The liquid limit of bentonite is primarily controlled by the diffuse double layer

(Sridharan et al., 1986). Consequently, changes in the characteristics of the pore fluid; a decrease in the dielectric constant, an increase in the electrolyte concentration, results in a decrease in the diffuse double layer thickness, and a decrease in the liquid limit (Sivapullaiah and Savitha, 1999).

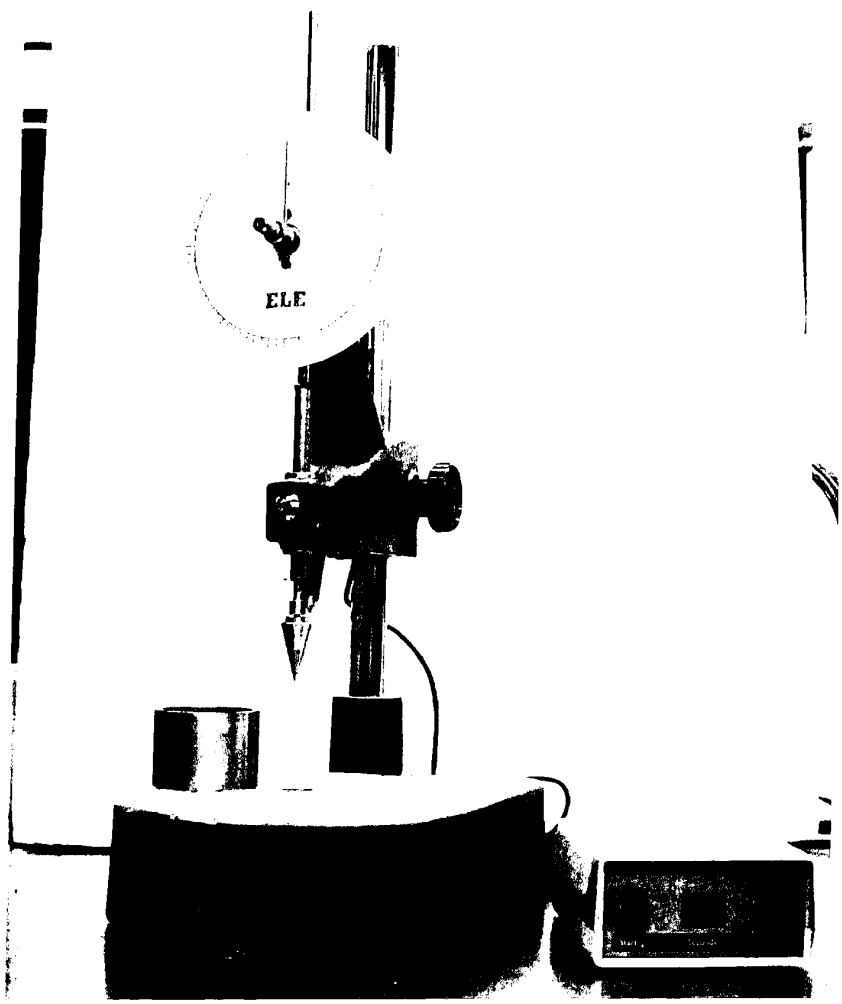

Figure 3.1 - Fall cone.

Liquid limits were performed on the two bentonites. Initial testing was conducted in accordance to ASTM D 4318. Due to difficulties of obtaining consistent results for bentonite pastes using the Casagrande Cup method, the

procedure was changed to British Standard BS 1377: Part 2: 1990, which uses a Fall Cone to determine the liquid limit. The results of liquid limit testing are summarized in Chapter 4.2.3.

3.4.3 Viscosity Testing

Viscosity is defined as the resistance of a fluid to flow. While viscosity analysis is more directly related to drilling concerns and to slurry trench excavations than to performance of bentonite liners, it provides a useful technique to examine the physical properties of the bentonite.

Fluids are classified according to the type of flow curve traced out when shear stress is plotted against shear rate, as shown in Figure 3.2. The shear stress of Newtonian fluids is directly proportional to the shear rate. If the shear rate is doubled, the shear stress is doubled. An ideal plastic is similar to a Newtonian fluid in that both exhibit straight-line relationships between shear stress and shear rate but the ideal plastic has an intercept on the shear stress axis that is called the yield point. Flow does not begin until the applied shear stress reaches the yield point after which the shear stress is directly proportional to the shear rate. The slope of this line is defined as the plastic viscosity (CSR, 1982).

Bentonite slurries are often characterized by the Bingham-plastic fluid model, which is similar to the ideal plastic model but the initial portion of the flow curve is not a straight line, as shown in Figure 3.2. The flow curve intersects the shear stress ordinate at a point that is referred to, as the gel strength of the slurry, which represents the minimum shear stress, required producing flow. When the

straight-line portion of the flow curve is extrapolated to low shear rates, it intersects the shear stress ordinate at a point designated as the Bingham yield point. As with the ideal plastic, the slope of the straight-line portion of the flow curve is referred to as the plastic viscosity (CSR, 1982).

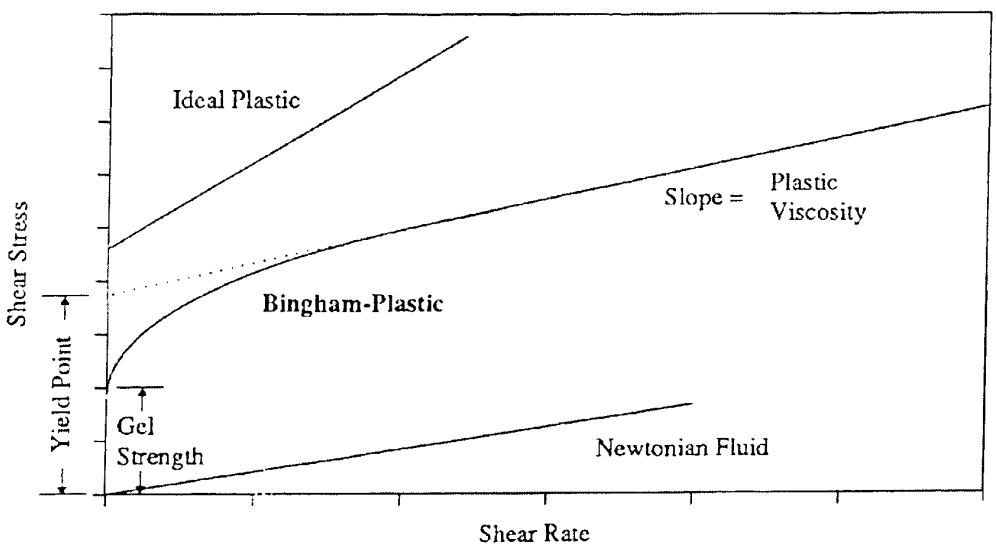

Figure 3.2 - Flow curves (from Reschke, 1991).

The values of the yield-point and the plastic viscosity are determined using a rotational Fann viscometer, as shown in Figure 3.3, according to American Petroleum Institute Recommended Practice Procedure for Field Testing Water-Based Drilling Fluids (API RP 13B). The slurry sample is contained in a cup and is sheared between two cylinders. An electric motor turns the rotor at a constant speed that imparts a torque on the bob due to the resistance of the fluid to flow. The deflection of the dial is proportional to the viscous properties of the fluid. The sleeve can be rotated at six speeds: 600, 300, 200, 100, 6, and 3 rpm.

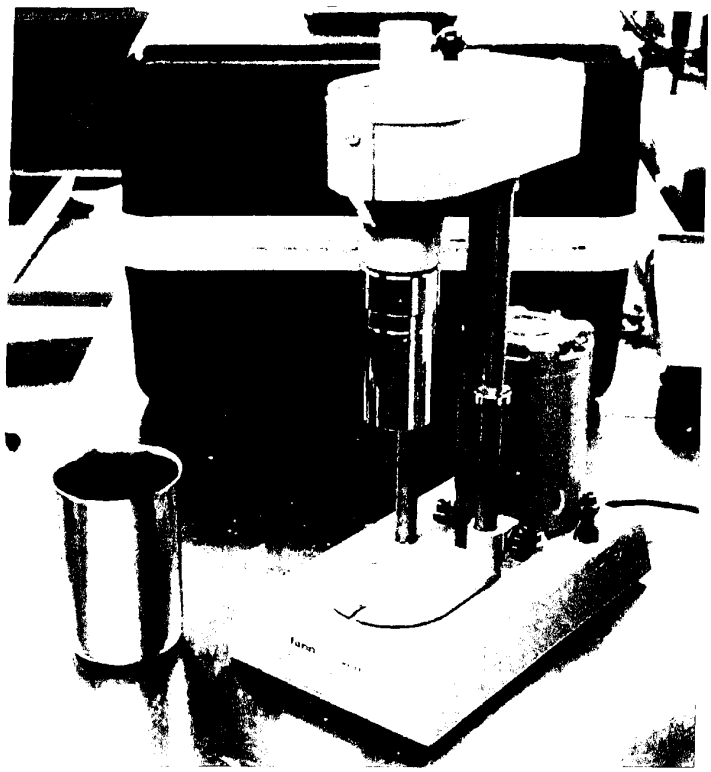

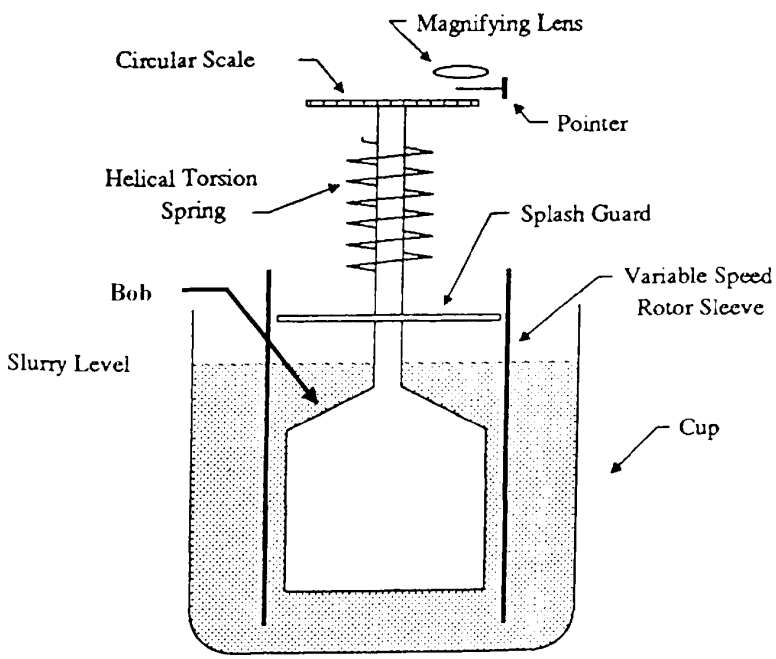

Figure 3.3 - Fann viscometer (after Reschke, 1991).

The standard rotor and bob combination is calibrated such that the plastic viscosity and yield points can be obtained directly from the 600 and 300 rpm readings as follows:

Plastic Viscosity (cP) = 600 rpm reading – 300 rpm reading (2.2)

Yield Point (cP) = 300 rpm reading – Plastic Viscosity (2.3)

The plastic viscosity and yield point can also be graphically determined from a plot of shear stress versus shear rate. The slope of the line is the plastic viscosity and the y-intercept of the straight-line portion is the yield point.

The plastic viscosity is a function of the friction between the solid particles present in the slurry and the amount of charges on those particles (Chilingarian and Vorabutr, 1981). The addition of even small quantities of electrolyte to a colloidal system can greatly alter its properties (van Olphen, 1977). In electrolyte-free systems the internal mutual flocculation imparts good viscosity and gel strength to the suspension. With even small increases in the electrolyte concentration, the internal charges are reduced and the viscosity is decreased. As the electrolyte concentration is increased further, the liquid and solid phases start to separate due to neutralization of the negative charges on the clay surface and the structure of the bentonite becomes increasingly flocculated and settles out (Chilingarian and Vorabutr, 1981).

A 7% by weight, bentonite slurry was prepared with each electrolyte solution. This slurry was chosen as it was found to be thin enough to provide easy mixing and yet thick enough to observe compatibility effects. The slurry preparation

method, which uses a BRAUN™ handmixer, was a method modified from API RP 13B and can be found in Appendix B. The rheological properties of the bentonite slurries were measured in accordance with API RP 13B using a Model 35A Fann Viscometer.

The slurry was stored, following mixing, in glass mason jars to allow for thorough hydration and for other chemical effects to take place. Figure 3.4 shows the Wyoming bentonite slurries that were stored for three day before viscosity testing. The results of the viscosity testing are summarized in Chapter 4.2.4.

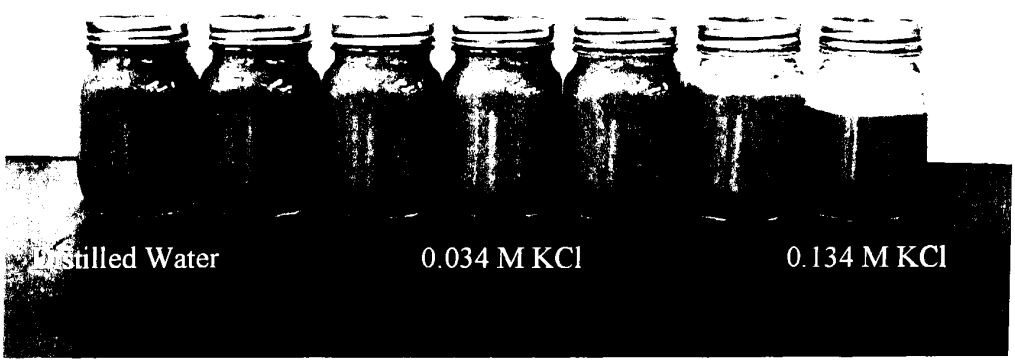

Figure 3.4 – Wyoming bentonite slurries mixed with various KCl solutions.

3.4.4 Hydraulic Conductivity Testing

3.4.4.1 Filter Press

Filtration properties of drilling fluids provide an estimate of the hydraulic conductivity. Thus a low fluid loss during the filter press test is taken to indicate a low hydraulic conductivity (Xanthakos, 1979). A standard filter press determines

fluid loss. It consists of a mud cup, filtering medium, filtrate collection and pressure source, as shown in Figure 3.5. The cell, top cap, screen, rubber gaskets and base cap make up the mud cup. The filtering medium is a sheet of special hardened filter paper with an opening size of 0.5 μm that is placed on the screen. A graduated cylinder is used to collect the filtrate. Compressed air or nitrogen, CO_2 cartridges, high-pressure air or water systems may be used as the pressure source.

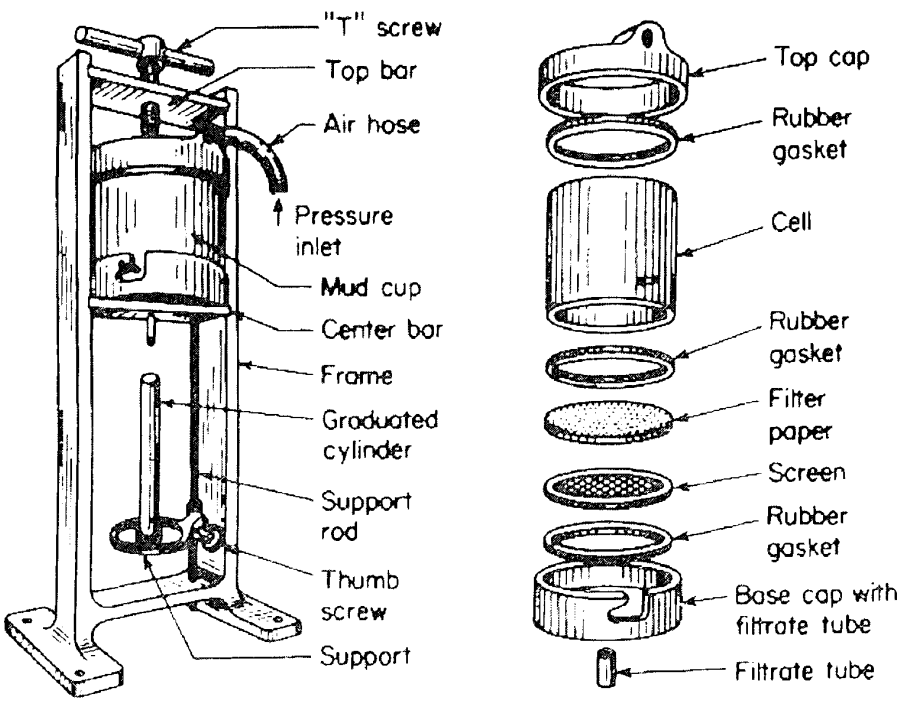

Figure 3.5 - Filter press (from Chilingarian and Vorabutr, 1981).

The standard test procedures are contained in API RP 13B and ASTM Test Method for Fluid Loss of Clay Component of Geosynthetic Clay Liners (ASTM D 5891) which was adapted from API RP 13B. The standard filtration test requires the sample to be exposed to a pressure of 690 ± 5 kPa for 30 minutes. The mud cup is assembled with the filter paper. The cup is filled with the sample to be tested to

within 10 mm of the top. This is done only to conserve the amount of compressed gas that is used. The mud cup is then secured with the T-screw. The graduated cylinder is placed beneath the filtrate tube. The 690 kPa pressure is applied and the timer is started. At the end of the 30 minutes, the pressure is relieved and the volume of filtrate collected in the graduated cylinder is read. The volume of filtrate is reported in ml as the API filtrate loss. The mud cup is disassembled and the filter cake thickness is measured.

The cumulative volume of the filtrate is directly proportional to the square root of time (Chilingarian and Vorabutr, 1981). This has also been confirmed by experimental results (Henry et al., 1998). Therefore, it is possible to estimate the API filtrate loss after 30 minutes by running the test for a shorter period of time.

Fluid loss increases with increasing electrolyte concentration in solutions due to the neutralization of negative charges on the clay platelets and their subsequent flocculation, which results in the formation of a more permeable filter cake (Chilingarian and Vorabutr, 1981).

The slurry samples mixed with various salt solutions were placed in the API filter press and tested according to API RP 13B (ASTM D 5891). The slurry was placed in the cell and subjected to a pressure of 690 kPa ± 5 kPa for 30 minutes with the filtrate being collected in a graduated cylinder. Measurement of the filtrate quantity was improved by weighing the filtrate with an electronic balance (Figure 3.6) and then converting the mass to volume (Minase et al. 2001).

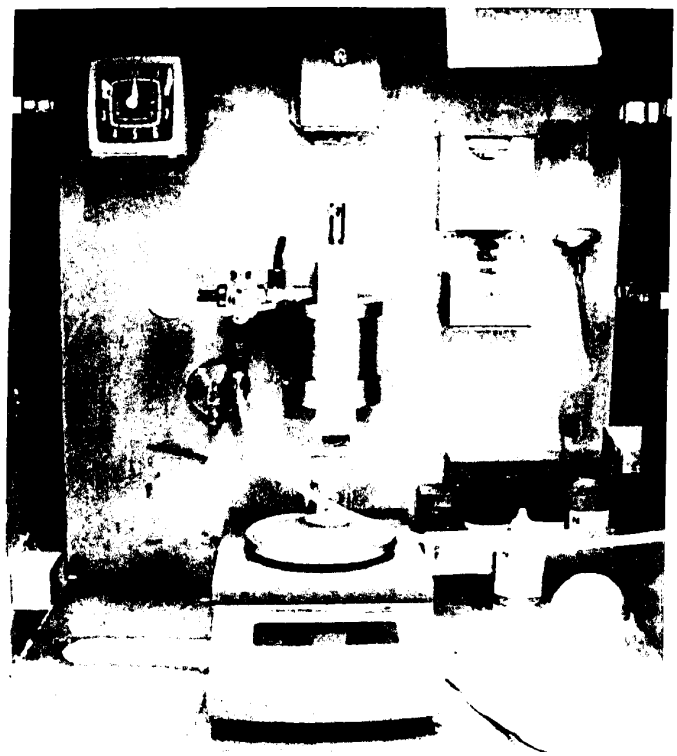

Figure 3.6 - Filter press apparatus with electronic balance.

At the end of the test the slurry was decanted and the filter cake thickness and mass were measured. The cake was then dried and weighed again. The void ratio of the cake was determined using the water content and the specific gravity of the bentonite.

Alther et al. (1985) calculated the hydraulic conductivity of the resulting filter cake according to API RP 13B, which is based on the volume of filtrate collected during the entire 30 minutes of filtration. The filtrate collection rate is not constant over the entire 30 minutes due to consolidation and sedimentation of the slurry. The filtrate collection rate decreases with time resulting in a higher than expected hydraulic conductivity value calculated according to API RP 13B. In this research program, the determination of the hydraulic conductivity of the filter cake

was improved by recording the filtrate volume after 25 and 30 minutes, to obtain a hydraulic conductivity value reflecting the end of test conditions. The filtrate collection rate over this smaller increment is believed to be more stable resulting in a constant hydraulic conductivity. The end of test filter cake thickness was used, assuming that the thickness is relatively constant over the final five minutes. Equation (3.2) uses the filter cake thickness, five minute filtrate volume and filter press pressure along with Darcy's Law to calculate an approximate value of hydraulic conductivity, k.

$$k = \frac{QL}{HAT} \tag{3.2}$$

where
Q= filtrate volume
L= filter cake thickness
H= pressure head
A= cross-sectional area of filter cake
T= time of filtrate collection

Replicate filter press tests were interrupted at shorter time intervals during the test in order to obtain measurements of the filter cake thickness and filtrate volumes with time. Figure 3.7 shows the variation of the filter cake thickness with time. A finite difference scheme was developed to estimate the evolution of hydraulic conductivity over time in the filter press. The finite difference solution incorporated the measured thickness of the filter cake and the measured filtrate volume over time. Considering the finite difference calculations, it can be seen that the inferred hydraulic conductivity stabilizes with time, as seen in Figure 3.8. Therefore, it appears justified to take filtrate volume measurements near the end of the test in order to obtain a more representative hydraulic conductivity value.

Given the above considerations, the increment in filtrate volume recorded over the last five minutes was used along with measured end of test filter cake thickness to estimate the hydraulic conductivity at the end of the test. All laboratory results can be found in Appendix F. Since the filtrate volume increases linearly with the square root of time (Henry et al. 1998), only two separate filtrate volume readings need to be made; the filtrate volume for any other time can be calculated. This could be beneficial as a smaller incremental filtrate volume could be used to calculate the hydraulic conductivity of the final filter cake thickness. The results of the filter press tests are summarized in Chapter 4.2.5.1.

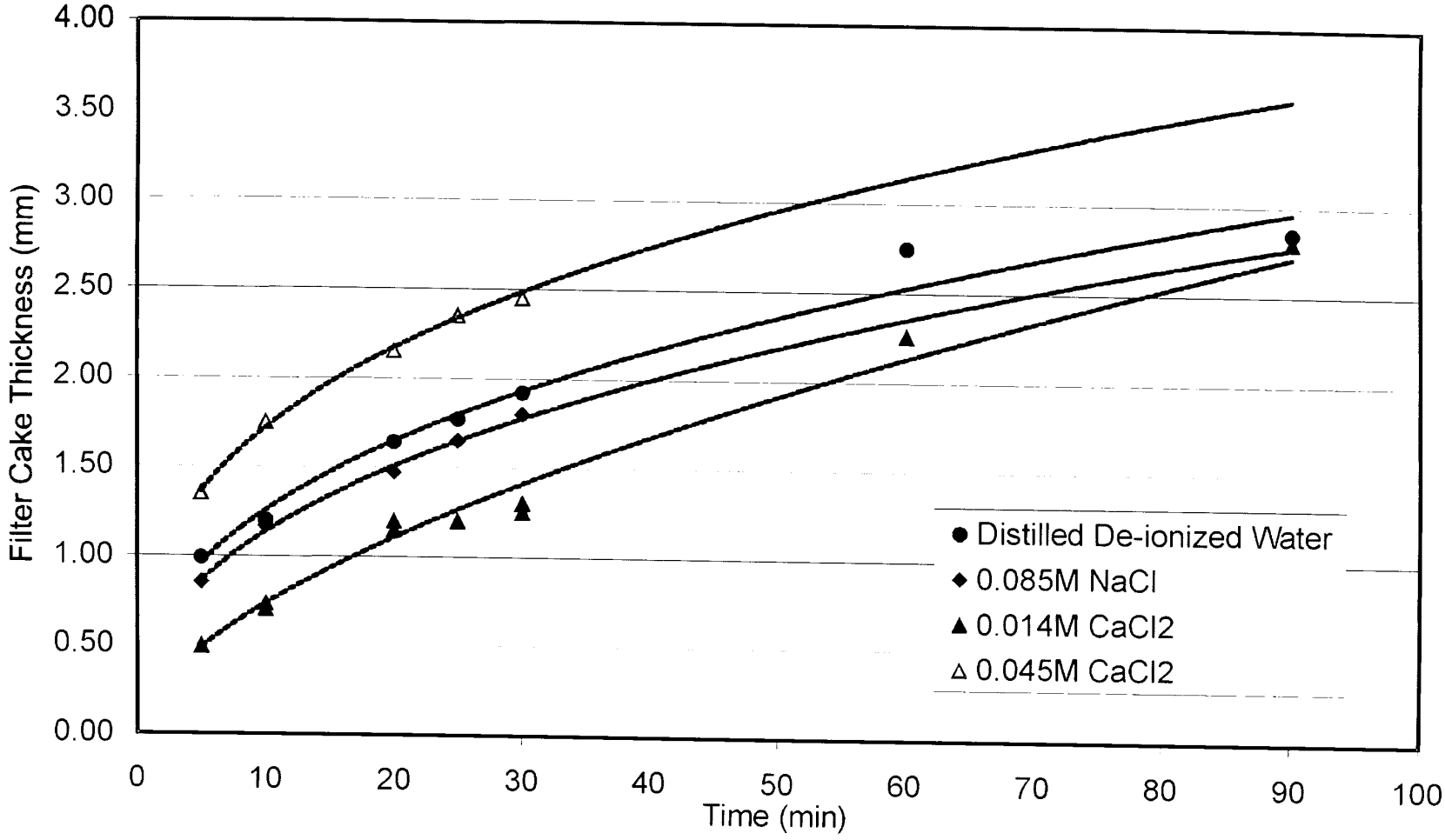

Figure 3.7 - Filter cake development with time (GCL bentonite).

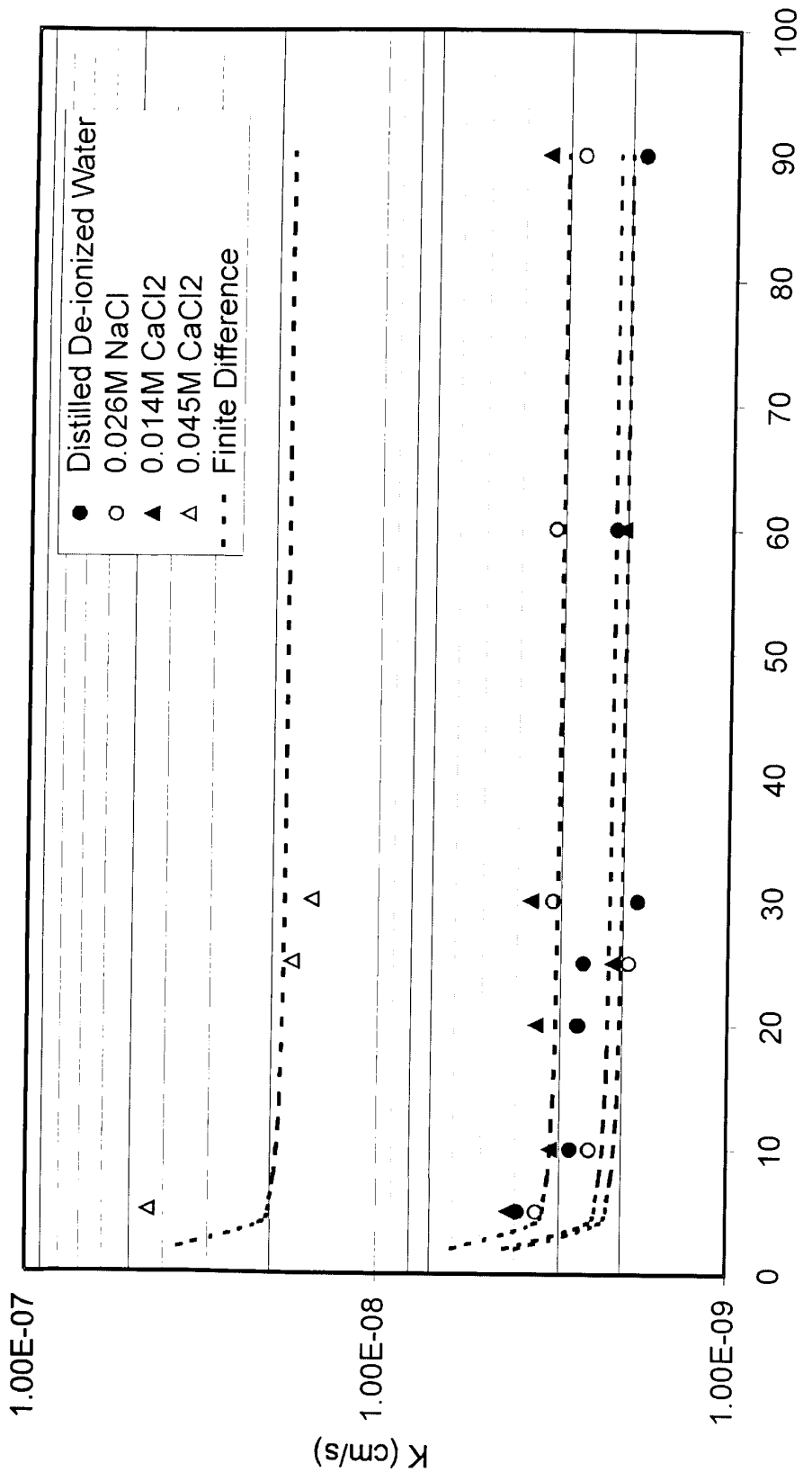

Figure 3.8 - Hydraulic conductivity stabilization with time (GCL bentonite).

3.4.4.2 Triaxial Permeability Testing

Hydraulic conductivity testing involves the measurement of fluid flow through a soil sample. Hydraulic conductivity testing of low permeability clayey barrier materials is used for design, construction quality control and for clay/chemical compatibility. Hydraulic conductivity can be calculated using Darcy's Law as follows:

$$Q = -kiA \tag{2.5}$$

where, Q is the discharge (cm^3/s), k is the hydraulic conductivity (cm/s), i is the constant hydraulic gradient, and A is the cross-sectional area of the sample (cm^2).

There are various means of measuring the hydraulic conductivity of soils. One of the more common methods is the use of a flexible wall triaxial permeameter, as shown in Figure 3.9. The cells, used in the work described herein, were fabricated from stainless steel. The interchangeable base and top cap are spirally grooved to ensure uniform distribution of the entering permeating liquid (influent) and exiting permeating liquid (effluent) collection. The sample is placed between two porous stones and surrounded by a flexible membrane. The flexible membrane is attached to the interchangeable base and top cap using O-rings. The effluent line is connected to the top cap and to the base. All the pressure lines are passed through the base to the cell. Transducers located on the base of the permeameter monitor pressures applied to the sample. A differential transducer is used to measure the head loss across the sample. The influent and effluent are measured using a twin tube, double

acting burette system, connected between the reservoirs and the sample. The tubes are graduated 25 ml or 10 ml burettes with resolutions of 0.05 ml and 0.02 ml respectively. The movement of a water kerosene interface, as shown in Figure 3.10, indicates the volume change.

Hydraulic conductivity tests are performed by passing influent upwards into the sample under pressure. The effluent exits the top of the sample where the backpressure can be maintained at a lower level to impose a hydraulic gradient. A confining cell pressure, greater than the influent pressure, is applied to press the membrane firmly against the sample. The confining pressure prevents sidewall leakage (Edil and Erickson, 1985), and it in conjunction with the influent and effluent pressures imposes an effective stress on the sample. If the sample shrinks, the flexible membrane will remain in contact with the sample, thus avoiding fluid flow between the sidewalls and the sample.

In a typical test, distilled water is passed though the sample to establish a stable initial hydraulic conductivity before the test permeant liquid is introduced. Hydraulic conductivity, effluent volume, and time increment are reported for each volume of influent passed though the sample. These values are then used to plot hydraulic conductivity versus pore volumes of permeant passed.

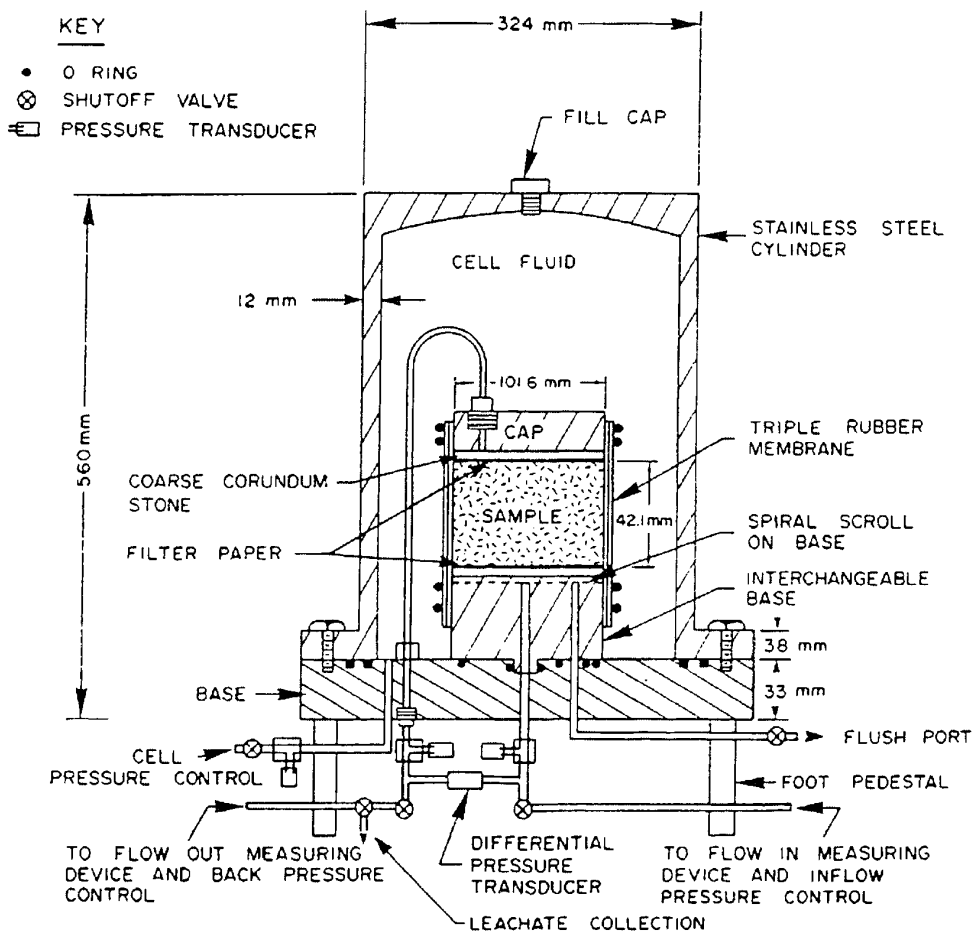

Figure 3.9 - Permeameter cell (from Reschke, 1991).

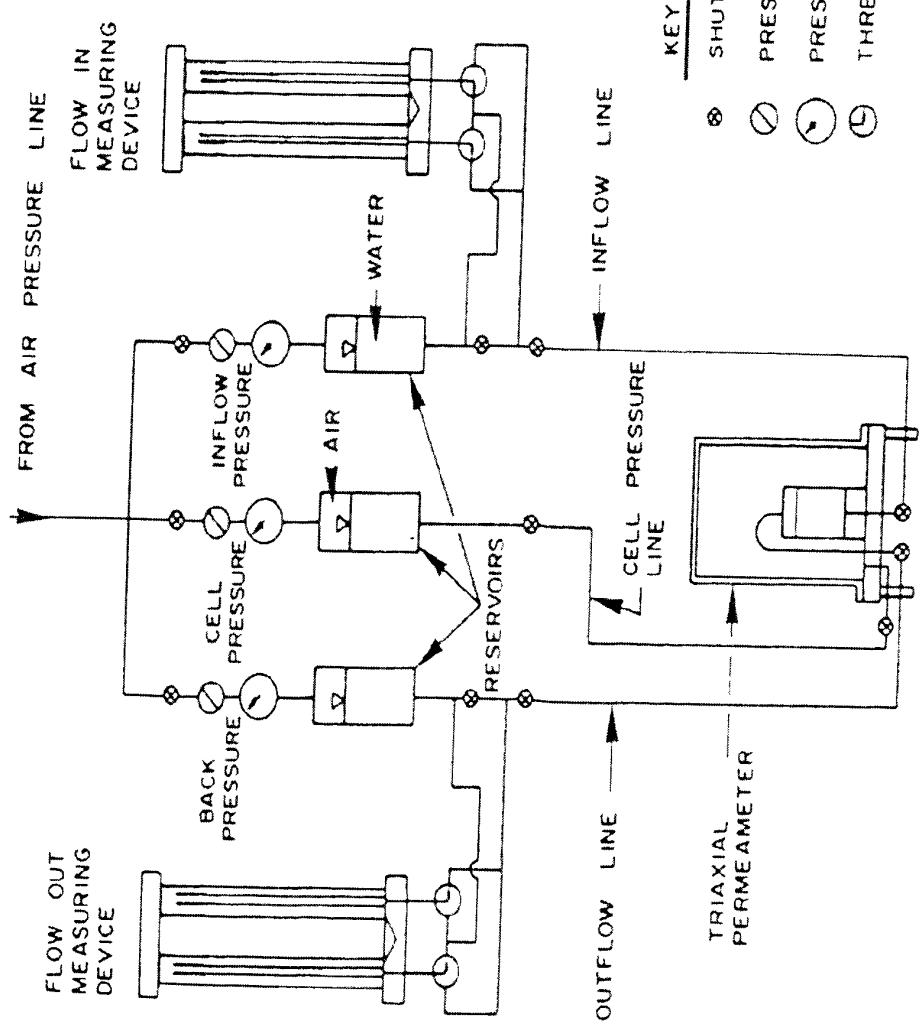

Figure 3.10 - Permeameter system (from Reschke, 1991).

Large diameter flexible wall permeameters were used to test GCLs using the same electrolyte solutions from the slurry testing as permeants. The GCL test specimens were cut using a sharp circular steel cutting shoe as described by Rowe et al. (1997). A square piece of GCL was cut from the roll. The GCL was then placed on a solid wood block with the grain facing up. The wood block used was a 300 mm long and 400 mm diameter log. The cutting shoe was placed on top of the GCL and the whole setup was placed in a hydraulic press. The cutting shoe was pressed through the GCL into the wood block. Once the GCL was cut, the inner edge of the shoe was wetted with water. This procedure allowed the GCLs to be cut to the required size without the loss of bentonite. Two cutting shoes were fabricated with diameters of 150 and 200 mm, as shown in Figure 3.11.

Figure 3.11 – Steel GCL cutting shoes.

The large diameters were used in order to reduce the effect of sidewall leakage and to increase the total flow through the specimens. The increased total flow through the specimens combined with the use of low gradients and a precise

flow in and out measuring apparatus was intended to provide a high level of precision and confirmation that chemical equilibrium had been achieved or at least approached (Haug et al. 1994). The twin burette system initially used was exchanged for two GDS Advanced Pressure Volume Digital Controllers, as shown in Figure 3.12.

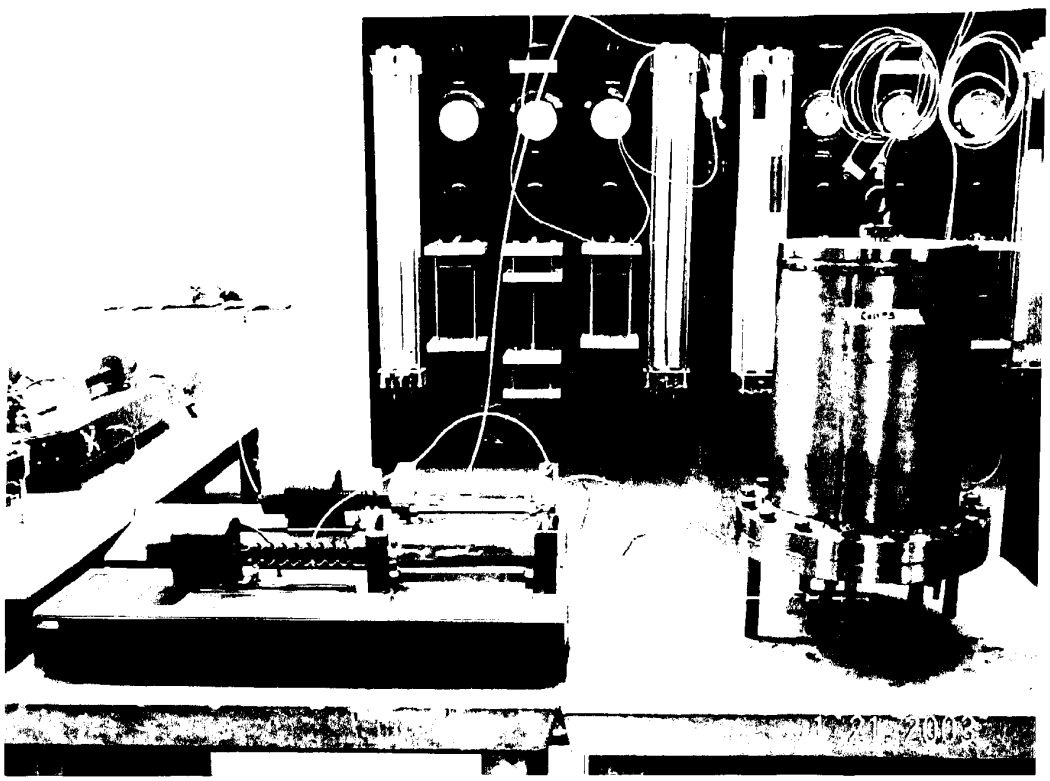

Figure 3.12 – GDS pressure volume controller permeameter system.

The pressure volume controllers have a digital readout that displays the controller pressure in kPa and the volume in mm^3. The controllers eliminated the use of individual pressure transducers and a data acquisition system to obtain the

voltage readings from the pressure transducers. The controllers also eliminated the dependence of the twin burettes to be changed in order to record the cumulative volume beyond the volume of the individual burettes. The controllers, depending on their size, can record the volume up to 200 cm^3 or 1000 cm^3. The results obtained from the use of the controllers produce a more accurate and stable measurement of hydraulic conductivity. The results of the large diameter flexible wall permeameters are summarized in Chapter 4.2.5.2.

3.4.5 X-Ray Diffraction Testing

Bentonites are composed of many minerals. The most important aid in the identification of the mineral species and quantitative estimation of their relative proportions is the application of x-ray diffraction (XRD) analysis.

The x-rays, entering the mineral at changing angles on a number of regular network levels, are bent in different directions and at different intervals. The diffraction is amplified by interference at particular angles and registered as a peak on the decoder. The interplanar spacing, d, specific to the mineral may be calculated from the critical diffraction angle, θ, at which rays scattered from successive planes will be in phase along a front as they leave the mineral, as shown in Figure 3.13. Knowing the wavelength of the x-ray, λ, the interplanar spacing can be defined using the Bragg's Law:

$$n\lambda = 2d \sin\theta \qquad (2.4)$$

The integer n is called the order of reflection and is related to the path difference between rays scattered from adjacent planes. The critical diffraction angle

is determined not by moving the x-ray source but by rotating the sample in the path of the beam. The detector, used to measure the diffracted rays, also moves in such a way as to maintain an angle with the sample which is equal at all times to the angle of incidence of the primary beam. Geometrically, this implies that the decoder must rotate 2θ degrees for θ degrees of sample rotation, as shown in Figure 3.14. It is this 2θ value that appears on x-ray diffractograms (Egloffstein, 1995).

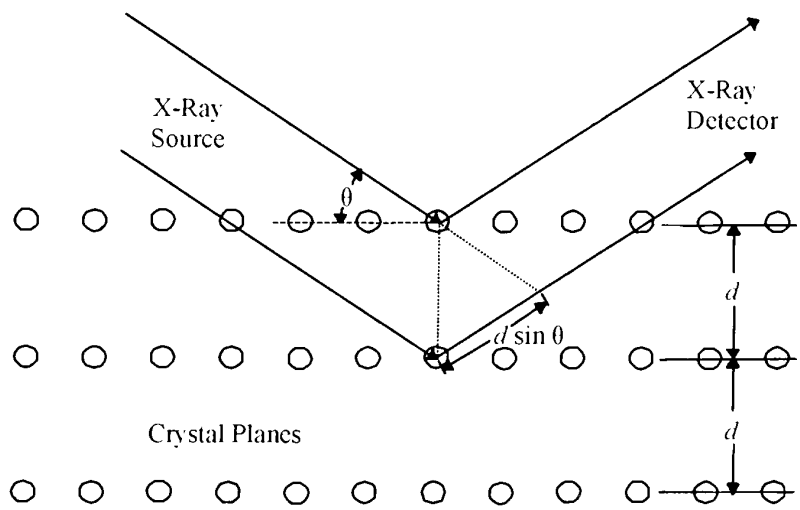

Figure 3.13 - X-ray diffraction (after Mitchell, 1993).

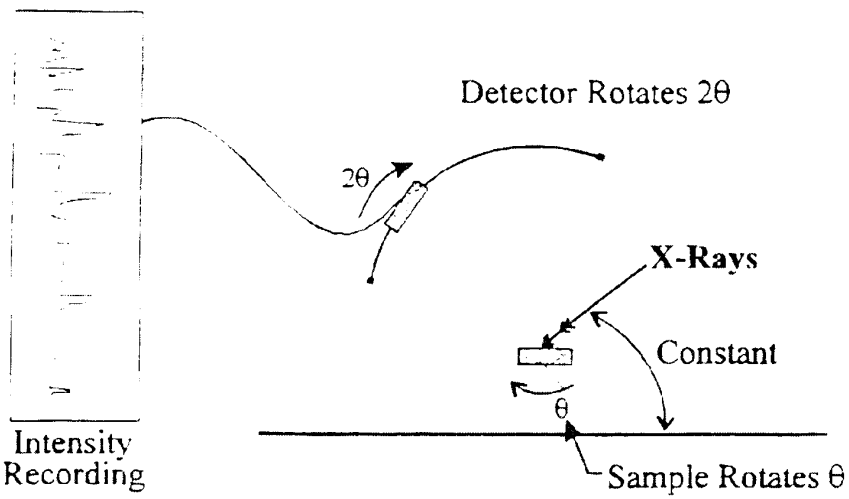

Figure 3.14 - Rotation of X-ray diffractometer and intensity reading (after Mitchell, 1993).

In order to identify smectites, whose d-spacing varies, depending on the water content and occupancy of cations, pre-treatment techniques have been used. The use of glycol is recommended for pre-treatment of smectites. Pre-treating with glycol forms a layer two molecules thick between the planes of the smectite particles and will give spacings varying from 1.64 to 1.72 nm (Haug, 2003).

X-ray diffraction analysis is well suited to examine the structural changes in clay minerals after contact with chemicals that impair their structure (Egloffstein, 1995). The XRD analysis will pick up any changes that occur to the basal spacing in the c direction. The basal spacing can contract to 1.0 nm from the fixation of potassium between the mineral layers or can expand from the absorption of organic molecules between the mineral layers. Either way, the alteration of the basal spacing in the smectite mineral may indicate chemical compatibility problems. XRD testing was conducted in the case study presented in Chapter 6.

Chapter 4 Laboratory Results and Discussion

4.1 Introduction

This chapter presents results from the laboratory-testing program. A comparison of the free swell and viscosity testing results for compatibility testing are examined. The free swell indices will be used following the guidelines set out in ASTM D 6141 for the pre-screening of bentonite for chemical compatibility. The plastic viscosity will be used in a new proposed method for the pre-screening of bentonite for chemical compatibility.

4.2 Laboratory Testing Results

4.2.1 Diffuse Double Layer

The approximate DDL thickness was calculated using equation (2.1) for the three salt species, as shown in Figure 4.1.

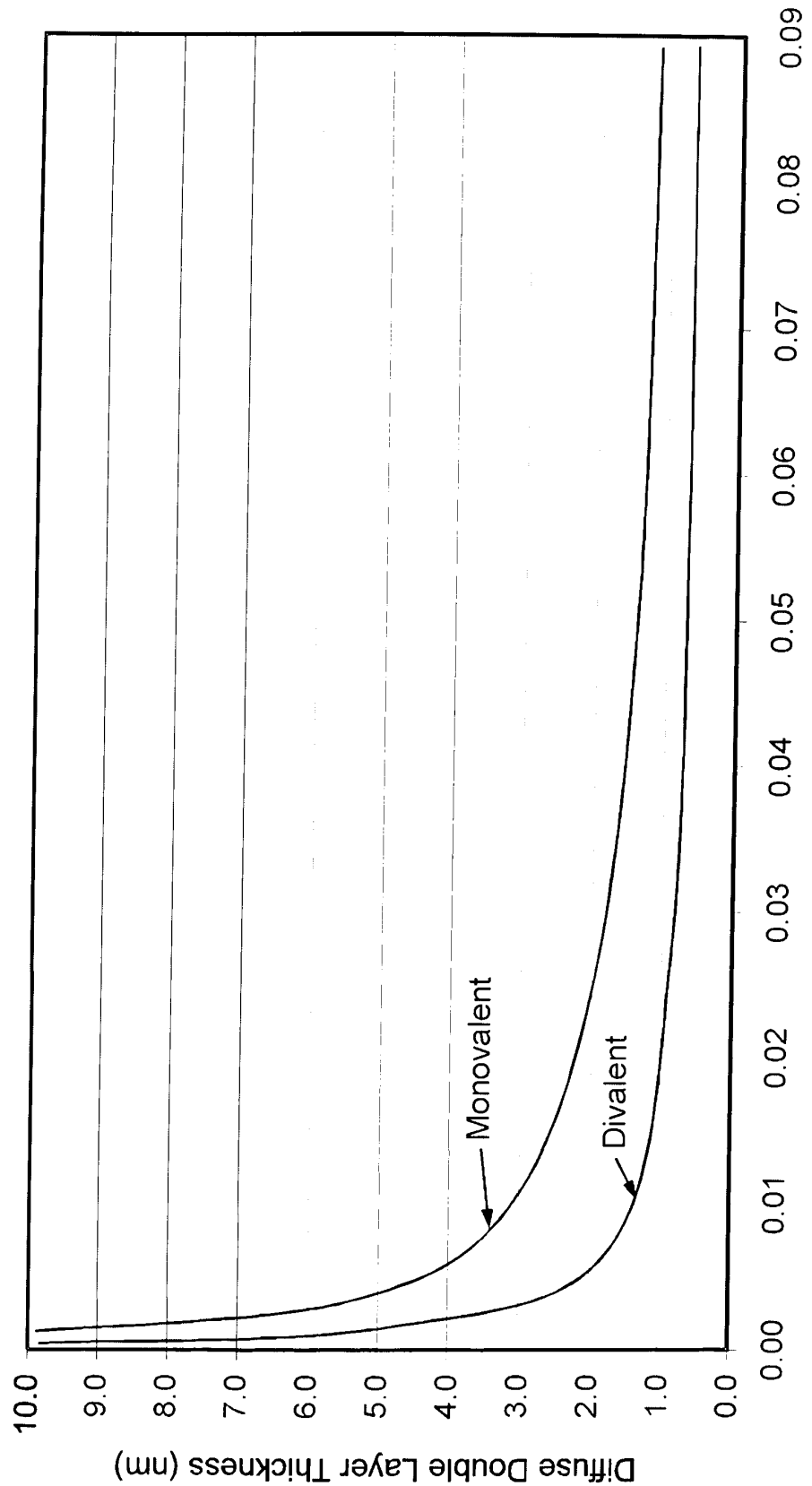

Figure 4.1 - Approximate DDL thickness for electrolyte solutions used.

The effect of species valence is evident on the DDL thickness by comparing the difference between the curves for the divalent $CaCl_2$ to those for the monovalent NaCl and KCl salts. The same DDL thickness can be produced for each salt by selecting the appropriate electrolyte concentration. A 0.003 M NaCl or KCl concentration and a 0.001 M $CaCl_2$ concentration all produce a DDL thickness of 5.0 nm. By selecting concentrations that result in the same DDL thickness, similar compatibility effects associated with changes in the thickness of the DDL can be examined for each salt species.

4.2.2 Free Swell Index

The visual results of the free swell testing can be seen in Figure 4.2 to Figure 4.4. The free swell test produces a flocculated clay fabric in most cases where electrolyte solutions are used. This is most apparent at low concentrations where the DDL is still relatively thick. The effect of DDL thickness on the free swell index can be seen in Figure 4.5. The results of the free swell index testing are presented in detail in Appendix C. The free swell index decreases as the electrolyte concentration increases due to the decrease in DDL thickness. During this study the free swell index increased from the reference distilled de-ionized water, then decreased. Accordingly, the tests were repeated two, and in some cases, three times. The results obtained from the repeated tests were consistent. This phenomenon has not been described in the literature (i.e. Shackelford et al., 2000; Egloffstein, 2001; or Jo et al., 2001). This increase in the free swell index is hypothesized to reflect an increasing degree of flocculation in the clay as it is exposed to a dilute to moderately concentrated electrolyte solutions. At high concentrations, a sharp

decrease in the free swell index is likely associated with a decrease in the DDL thickness.

Distilled de-ionized water 0.026 M 0.083 M 0.171 M

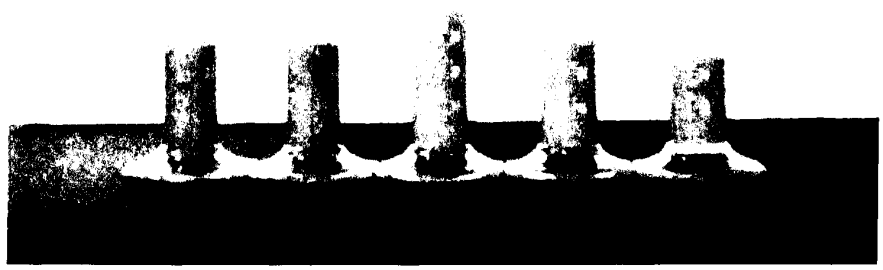

Figure 4.2 - Free swell with NaCl.

Distilled de-ionized water 0.008 M 0.013 M 0.067 M

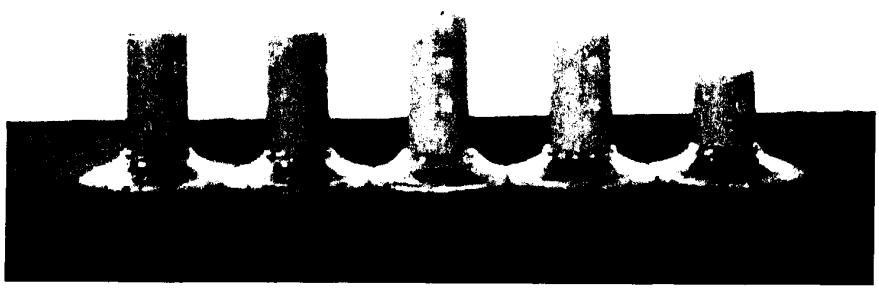

Figure 4.3 - Free swell with KCl.

Distilled de-ionized water 0.005 M 0.009 M 0.023 M

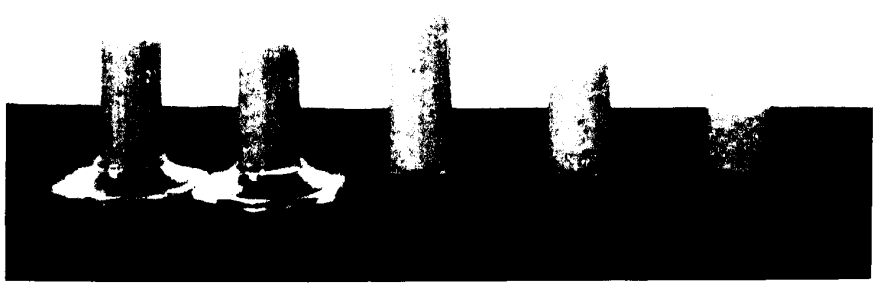

Figure 4.4 - Free swell with $CaCl_2$.

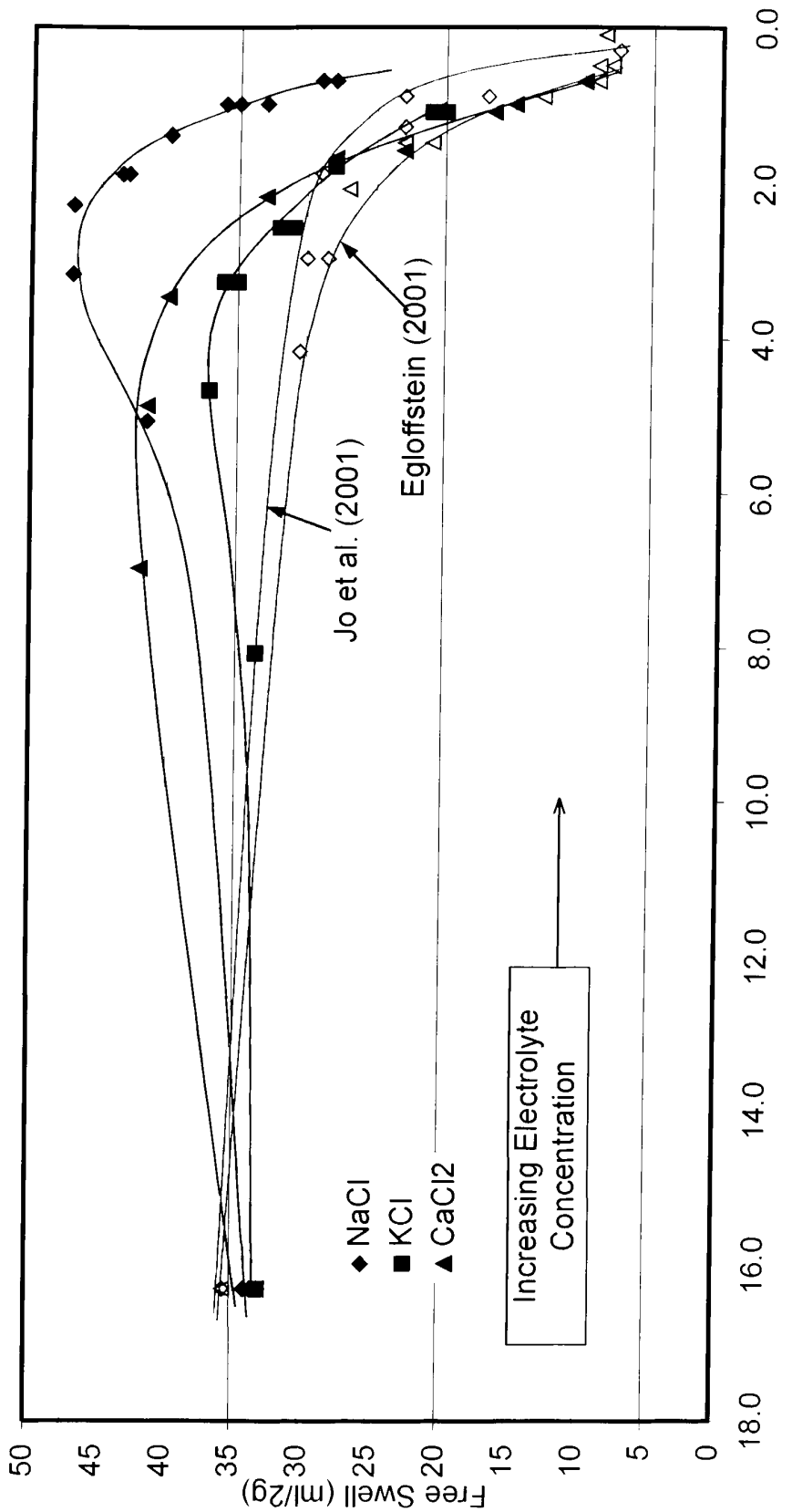

Figure 4.5 - Changes in free swell index to changes in DDL thickness (GCL bentonite).

4.2.3 Atterberg Limits

The effect of DDL thickness on the liquid limits can be seen in Figure 4.6. Similar trends have been observed by Petrov and Rowe (1997) and Gleason et al. (1997). The liquid limit of bentonite, when exposed to increasing electrolyte concentrations, decreases rapidly. This decrease is consistent with the three salt species used. There is also an added decrease in liquid limit with the increase in KCl concentration. This same effect was observed in viscosity testing, as discussed in Section 4.2.4 below, and may be attributed to potassium fixation within the bentonite. A detailed summary of the liquid limit result is presented in Appendix D.

4.2.4 Viscosity Testing

Figure 4.7 presents data for Wyoming bentonite showing that after about three days of hydration, the measured plastic viscosity and chemical effects stabilize. The slurries were mixed, stored for three days and stirred again for further testing. The higher PV associated with hydration by distilled de-ionized water may take slightly longer to develop completely, reflecting the greater DDL thickness in the absence of electrolyte. Similar trends were observed for GCL bentonite when mixed and stored.

Figure 4.8 presents the observed change, over three days, in the plastic viscosity for both GCL and Wyoming bentonite slurries mixed with various concentrations of NaCl. The plastic viscosity after three days for a slurry made using distilled de-ionized water is referred to as "PV_o" and was repeatedly measured in order to establish values of 30 cP and 16 cP respectively for the GCL and Wyoming bentonites.

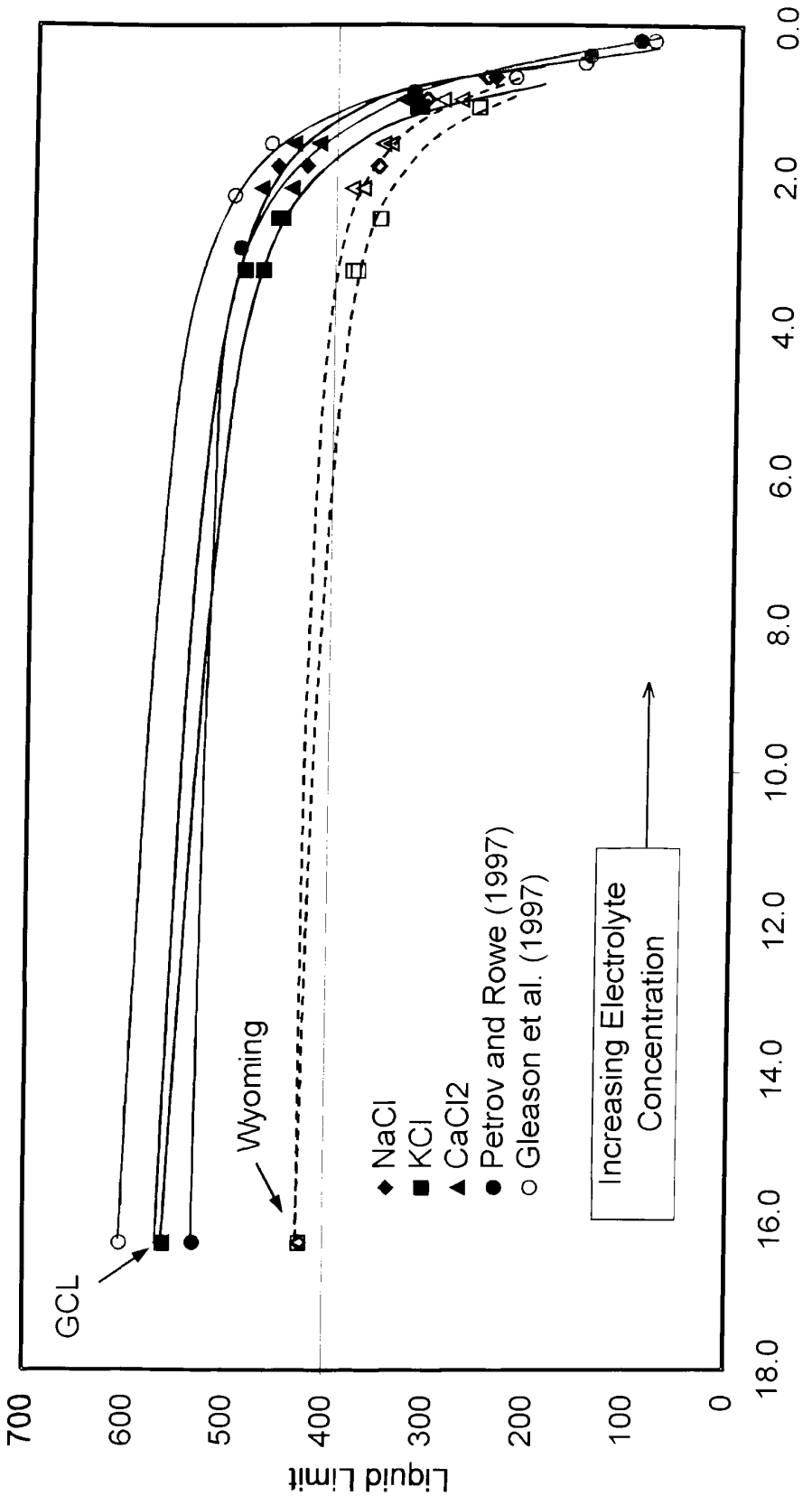

Figure 4.6 - Changes in liquid limit to changes in DDL thickness.

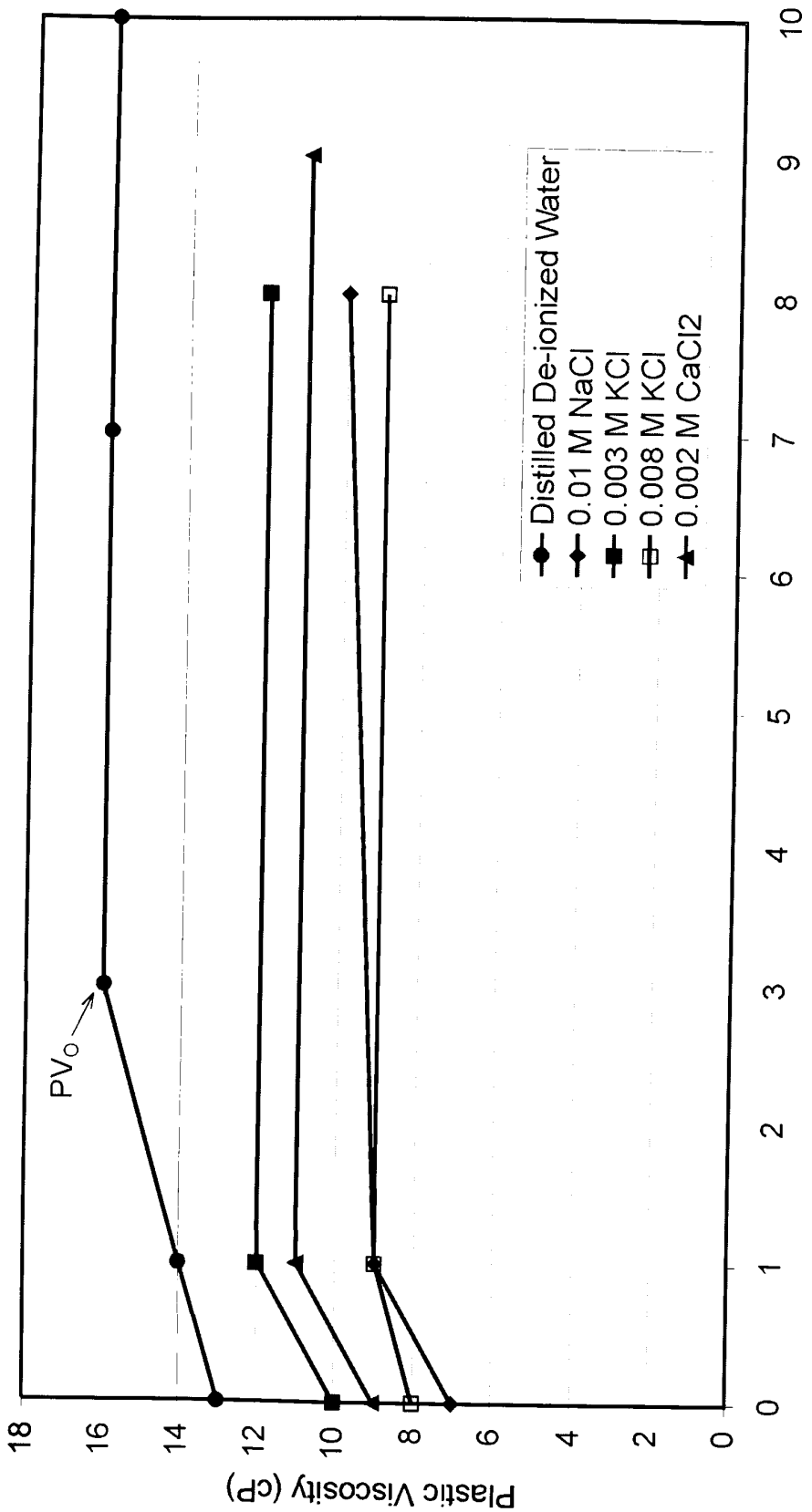

Figure 4.7 - Changes in plastic viscosity over time (Wyoming bentonite).

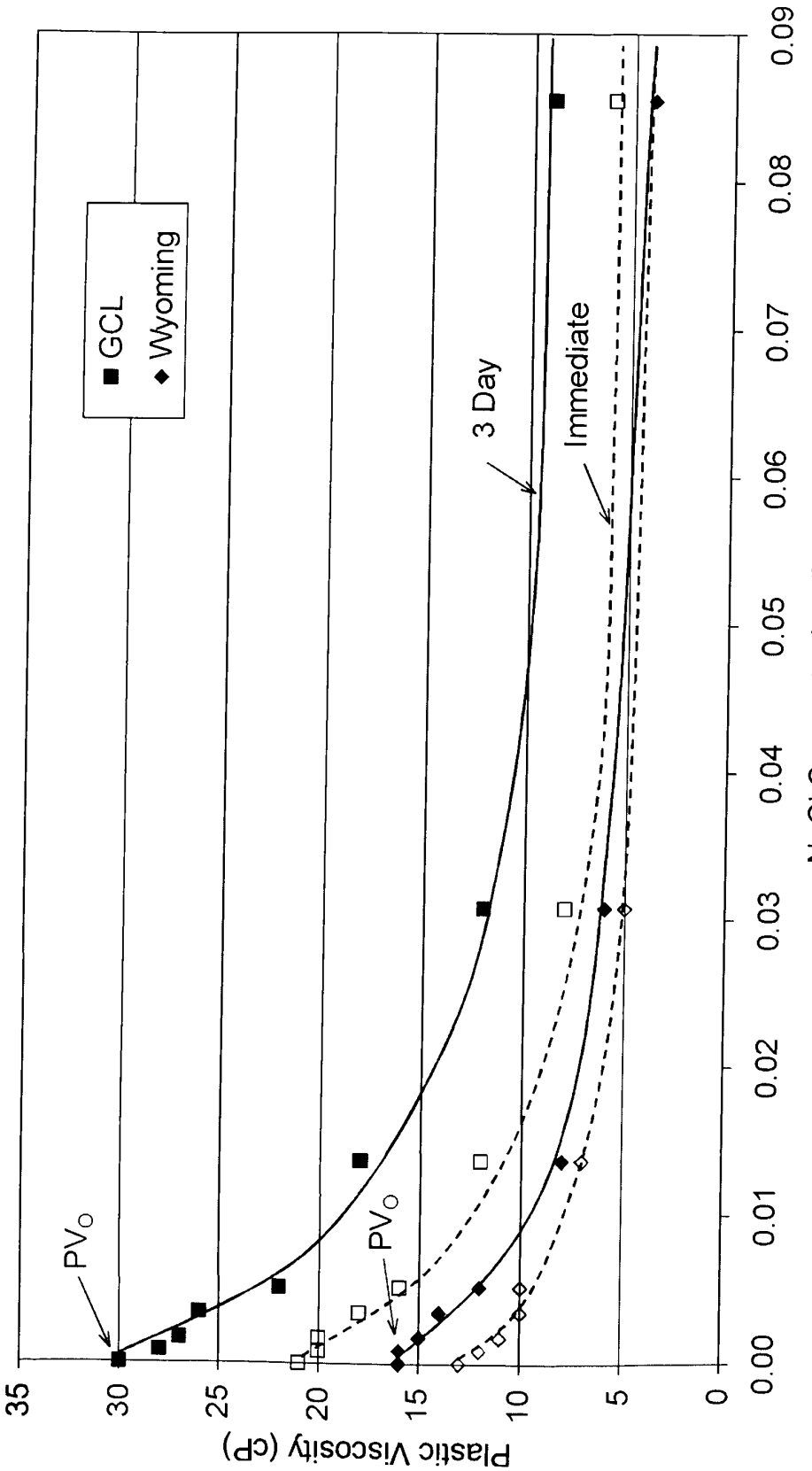

Figure 4.8 - Changes in plastic viscosity with salt concentration.

PV_o will be used in subsequent chapters to normalize measured PV values. The difference in the plastic viscosity of the two bentonites indicates that the composition of the bentonites is not the same. The bentonite used in the GCL may be of higher quality, or may have been treated, or otherwise modified.

Changes in the DDL thickness of the clay in the slurry appear to be reflected in a change in the plastic viscosity, as shown in Figures 4.9 and 4.10. The detailed summary of the viscosity testing data is presented in Appendix E. This is not surprising as decreased DDL thickness is associated with reduced inter-particle forces and a consequent reduction in viscosity. There is a steady decrease in PV with decreasing DDL thickness, as shown in Figures 4.9 and 4.10. In comparison, with increasing electrolyte concentration, the free swell index, Figure 4.5, initially increased and subsequently decreased. It is hypothesized that shearing by the viscometer tends to minimize the effects such as flocculation that led to the observed behaviour of Figure 4.5. The deflocculated structure may be more representative of the in-situ oriented fabric found in GCLs and compacted clay liners. Under the effective stress associated with field conditions, the flocculated structure may not develop. The relationship between PV and DDL thickness vary slightly for the different cationic species tested. This might suggest ion exchange of $CaCl_2$. There is also an added decrease in the plastic viscosity in the slurries mixed with moderate concentrations of KCl, evident in Figures 4.9 and 4.10, which may reflect potassium fixation within the bentonite.

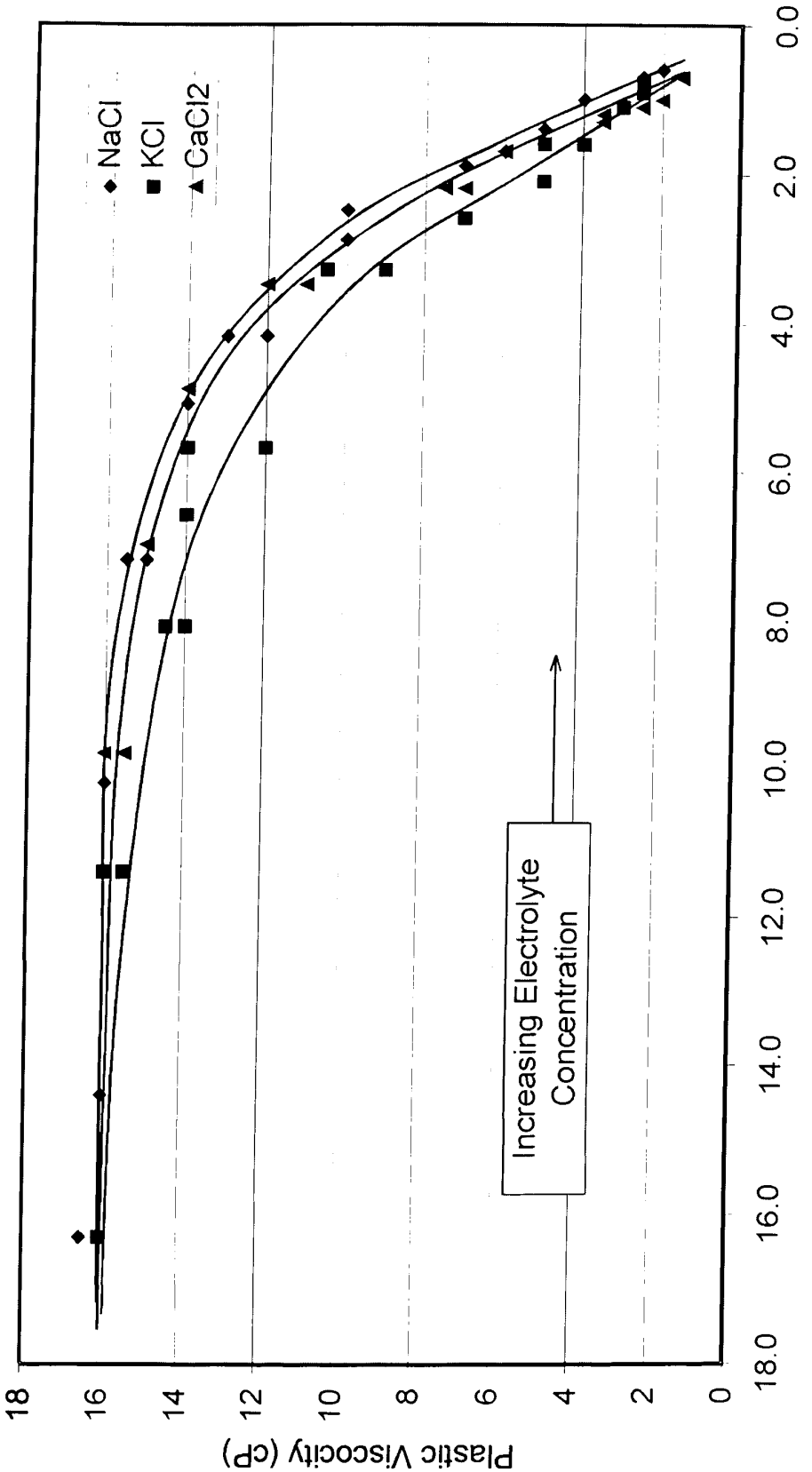

Figure 4.9 - Relationship between plastic viscosity and DDL thickness (Wyoming bentonite).

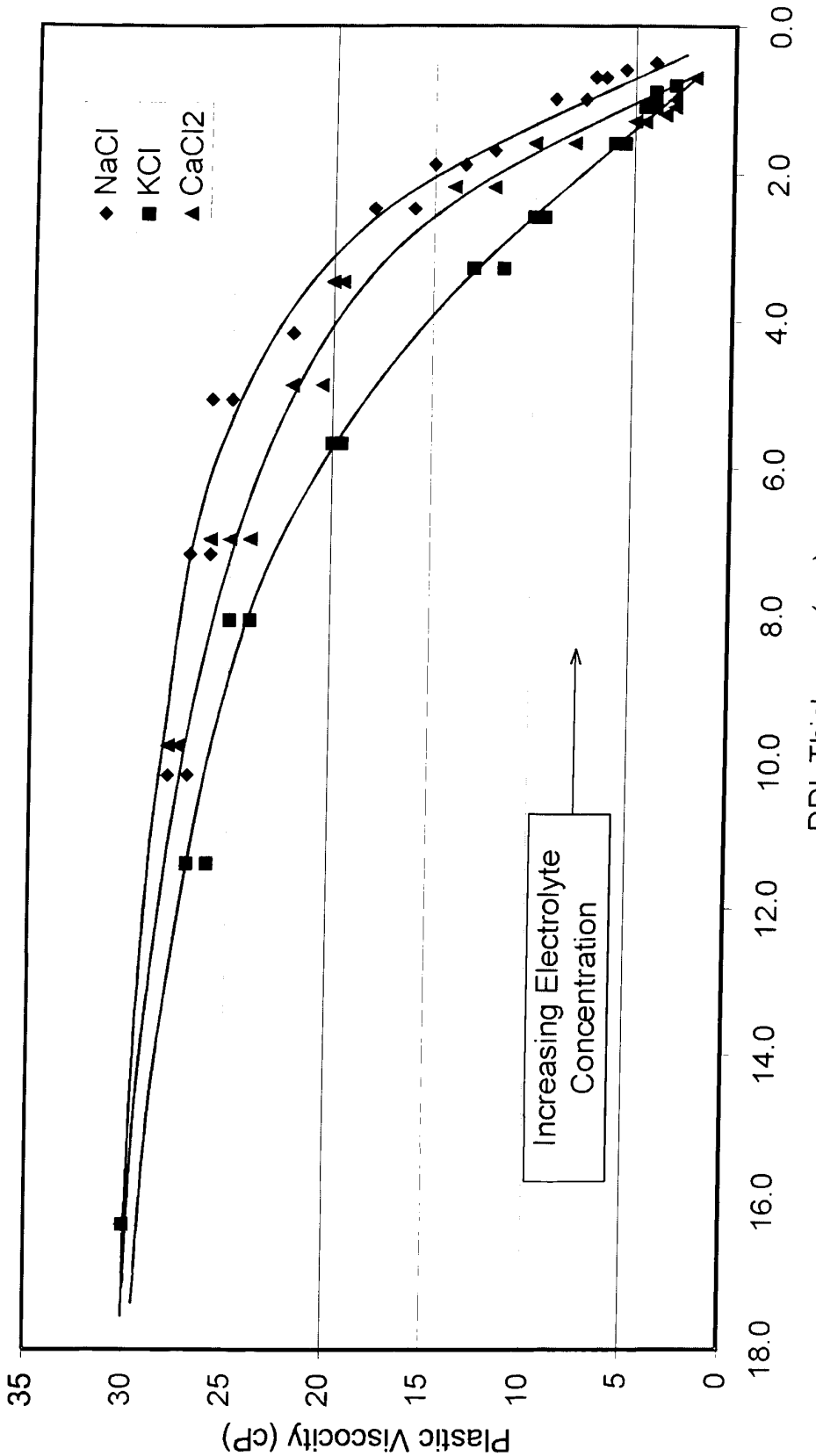

Figure 4.10 - Relationship between plastic viscosity and DDL thickness (GCL bentonite).

4.2.5 Hydraulic Conductivity Testing

4.2.5.1 Filter Press

Figure 4.11 shows a linear relationship between the hydraulic conductivity of the filter cake (as calculated from the increment of filtrate volume over the final five minutes) and the total filtrate volume. The open symbols represent the hydraulic conductivity of the filter cake using the total 30-minute filtrate volume in the calculations; whereas, the solid symbols used the final five-minute filtrate volume. A detailed summary of the filter press data is presented in Appendix F.

The data presented in Figure 4.12 suggests that as the DDL thickness decreases, the hydraulic conductivity increases. As discussed in Chapter 2.4.1, the DDL thickness is controlled in part by the electrolyte concentration and the species valence. An increase in concentration or an increase in valence will result in a decrease in the DDL thickness, which in turn results in an increase in hydraulic conductivity. Similar trends have been observed by Alther et al. (1985), Gleason et al. (1997), Ruhl and Daniel (1997), Stern and Shackelford (1998), and Egloffstein (2001). Data from theses studies described in the literature have been added to Figure 4.12 in which, it should be noted, a number of the re-plotted points from the literature reflect soil/bentonite mixtures, with corresponding higher hydraulic conductivity values. Not all test specimens had the same initial hydraulic conductivity (DDL = 16.3 nm). The test conditions may have been different or different materials may have been used.

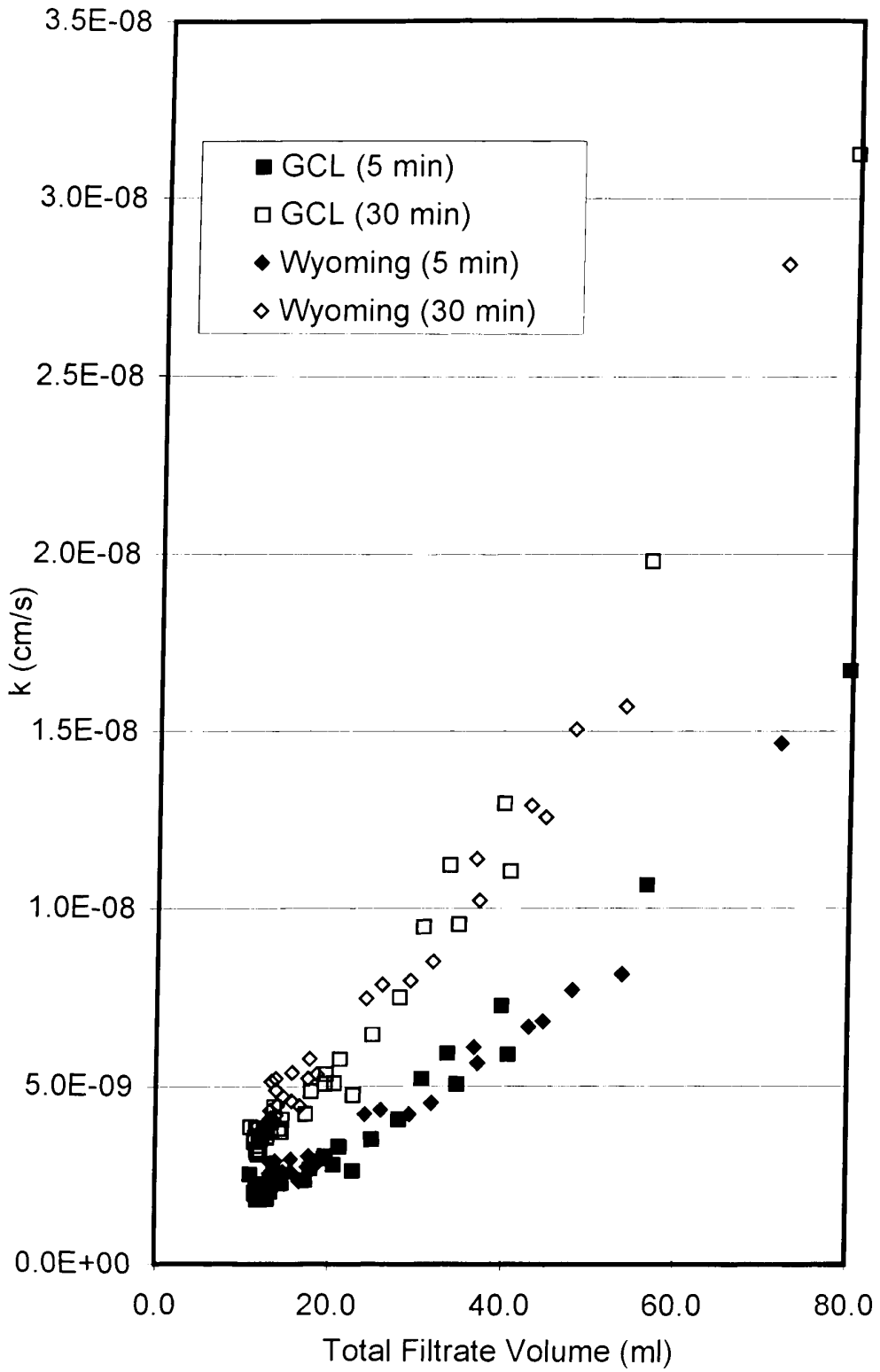

Figure 4.11 – Linear relationship between hydraulic conductivity and final filtrate volume.

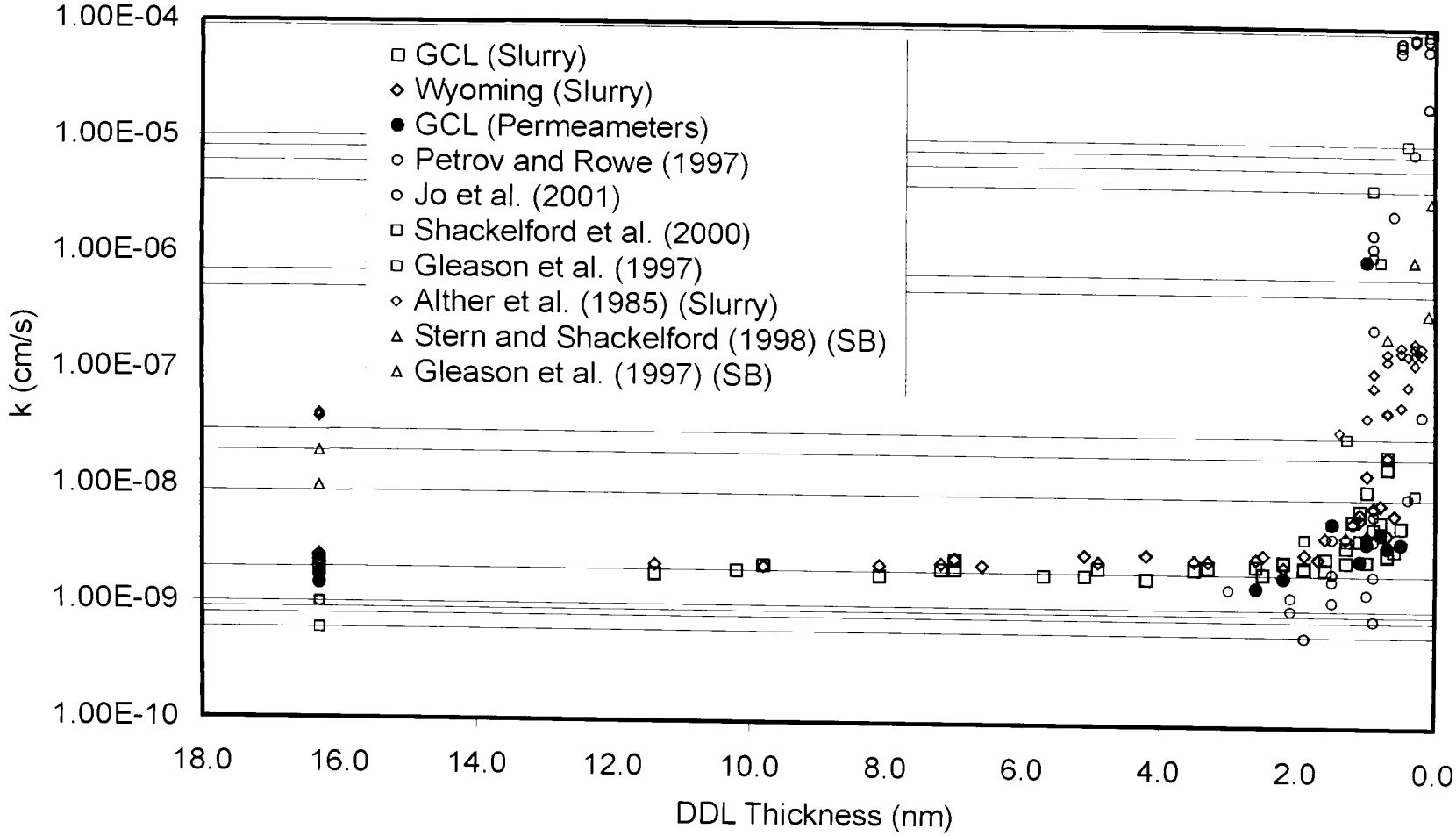

Figure 4.12 - Changes in hydraulic conductivity related to changes in the DDL thickness.

The hydraulic conductivity does not seem to be affected until the DDL thickness is less than 3 nm which corresponds to an electrolyte concentration greater than 0.003M; wastewaters and leachates commonly exhibit electrolyte concentration above 0.01M. Petrov and Rowe (1997) permeated GCLs with NaCl concentrations of 0.01, 0.1, 0.6, and 2.0M and observed small to large increases in hydraulic conductivity for 0.01M and 2.0M, respectively.

4.2.5.2 Triaxial Permeability Testing

The hydraulic conductivity for 11 of these tests involving various electrolyte solutions can also be seen as solid circles in Figure 4.12. A detailed summary of the hydraulic conductivity tests is presented in Appendix G. In order to compare the results from the literature, in which tests were carried out with varying sample preparation and under various stress conditions, the hydraulic conductivity was reduced to relative changes within each individual test. Figure 4.13 illustrates these relative changes expressed as the ratio k/k_o. It is evident that similar effects occur in all the test specimens. This figure suggests that different test samples can be compared as long as the relative changes are considered.

Figure 4.14 shows that the overall hydraulic conductivity values were lower in the permeameters, reflecting the higher effective stress and resulting lower void ratios in the permeameter tests. The effective stress in the filter press could not be determined. The effective stress is initially zero with a gradual increase to half of the applied pressure as the filter cake consolidates. The consolidation rate is not known therefore, effective stress could not be determined. Confined swell tests were conducted on smaller GCL samples in order to obtain the thickness and void ratio of

the GCL in the permeameters. The results and test description of the confined swell tests are contained in Appendix H.

In general, the filter press test tends to yield magnified changes in hydraulic conductivity compared to subtle changes in hydraulic conductivity in the permeameter tests. The subtle changes in hydraulic conductivity may reflect the fact that the higher effective stress causes consolidation within the GCL, reducing the void ratio, and countering the effect of mineral alteration, DDL contraction or other such compatibility effects.

It can also be seen, in Figure 4.14, that the data from the filter press testing suggest an increase in hydraulic conductivity with a decrease in void ratio. Petrov and Rowe (1997) also observed similar trends in GCLs permeated at a constant, low effective stress. However, increasing the effective stress on a sample caused consolidation and no change or a decrease in hydraulic conductivity was observed (Petrov and Rowe, 1997). The void ratios of the GCL specimen remained relatively constant due to the low effective stress as the hydraulic conductivity increased when the electrolyte concentration was increased. This is consistent with DDL contraction where a reduction in the volume of bound water occurs (Jo et al., 2001).

It can be seen from the laboratory testing and previous studies that the mechanisms influencing the index properties and hydraulic conductivity of bentonite are similar. The next section brings together the index tests and hydraulic conductivity tests to provide a possible quantitative correlation between the changes in the index properties to the changes in hydraulic conductivity with regards to chemical compatibility.

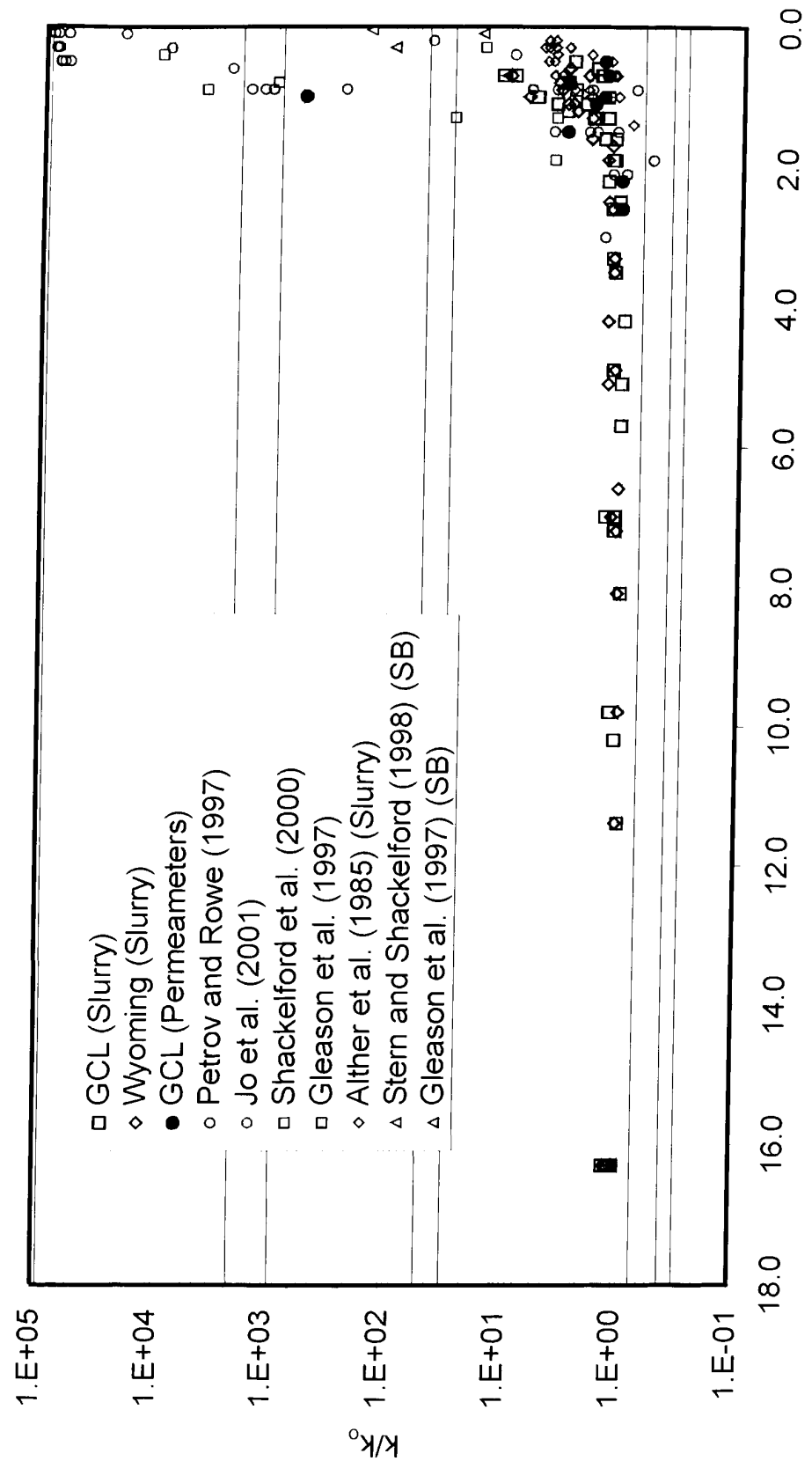

Figure 4.13 - Relative changes in hydraulic conductivity related to changes in the DDL thickness.

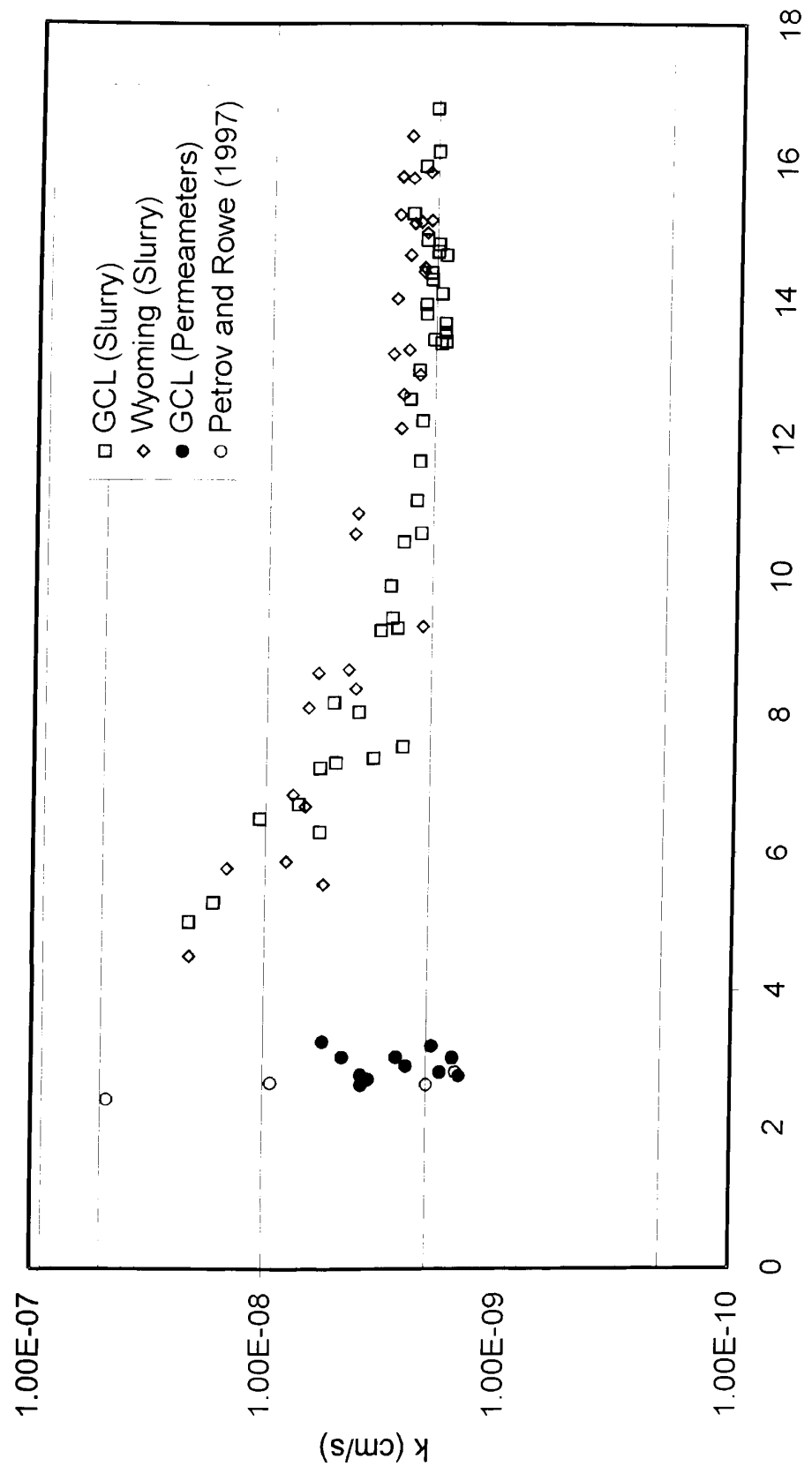

Figure 4.14 - Changes in hydraulic conductivity related to changes in void ratio.

4.3 Comparison of Test Results

Pre-screening for chemical compatibility, by the use of index tests, is beneficial to relate the changes in fairly simple, relatively easily measured and reproducible properties of the bentonite to changes in hydraulic conductivity. The free swell index values were compared to a reference free swell index according to ASTM D 6141. Instead of directly using fluid loss, the filter press interpretation was extended as described in Chapter 3.4.4.1 and relative hydraulic conductivities were calculated. The relative hydraulic conductivity is given by the hydraulic conductivity of the slurry, k, over the hydraulic conductivity of the slurry with distilled de-ionized water, k_o. Figure 4.15 and Figure 4.16 shows k/k_o versus S/S_o, where S is the free swell index with an electrolyte solution and S_o is the baseline free swell index with distilled de-ionized water.

Figure 4.16 represents the same data as Figure 4.15 but the k/k_o scale has been increased. This is helpful in comparing Figure 4.16 with a similar plot (Figure 4.19) using plastic viscosity instead of free swell index. As the electrolyte concentration increases, the relative free swell index decreases along with a consistent increase in relative hydraulic conductivity. At low free swell indices there are dramatic increases to the hydraulic conductivity. In Figure 4.15, S/S_o values around 0.4 to 0.3 show some variation in the relative hydraulic conductivity between the values reported in the literature and those determined from the laboratory testing in this research program. There appears to be a discontinuity in the relative hydraulic conductivity values. There is either little change in the hydraulic conductivity or large change in the hydraulic conductivity; there are no

moderate changes. Figure 4.16, shows that slight changes ($k/k_o \sim 1.5$) in the hydraulic conductivity start to occur at an S/S_o value of 0.7 and substantial changes ($k/k_o \sim 3$) occur at S/S_o values less than 0.5, thus resulting in two warning criteria.

As shown above in Figure 4.5, the laboratory data shows an increase in free swell index then a subsequent decrease, whereas, the data from literature showed only decreases in free swell indices. In Figure 4.16 there seems to be a general trend in the relative hydraulic conductivity as the free swell index decreases. This figure also exhibits some scatter among the data points.

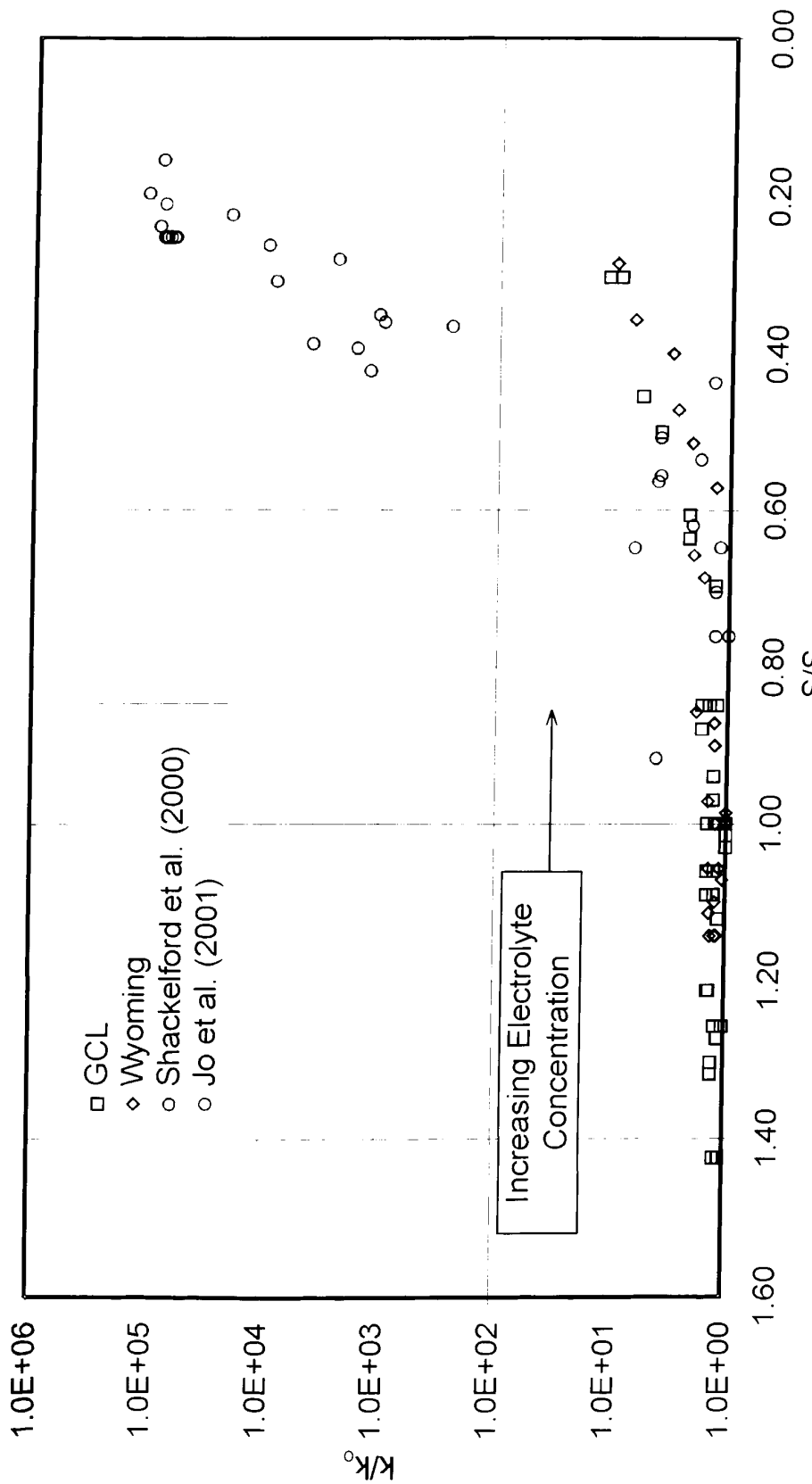

Figure 4.15 - Relative hydraulic conductivity vs. relative free swell index.

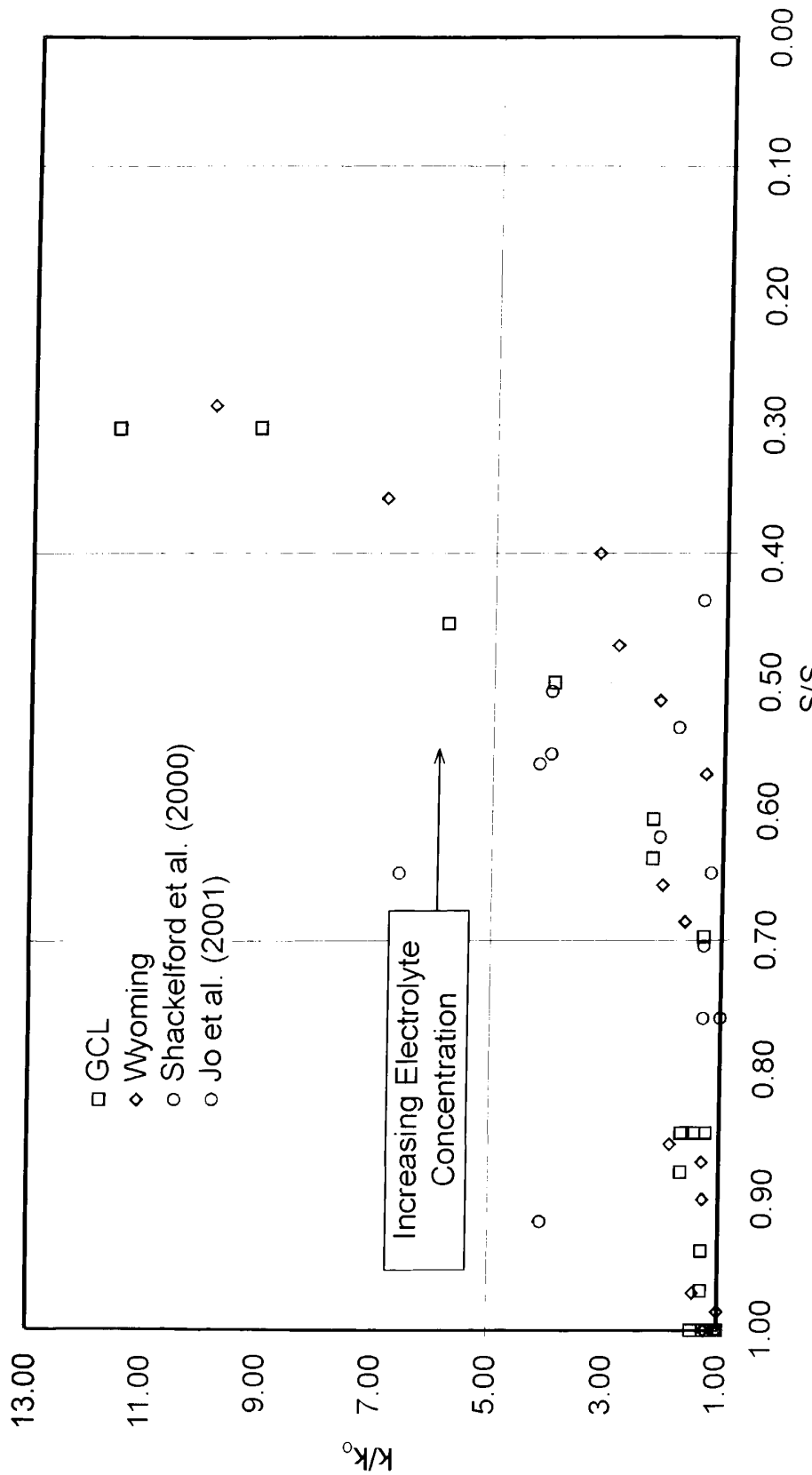

Figure 4.16 - ASTM D 6141 compatibility criteria, relative hydraulic conductivity vs. relative free swell index.

The plastic viscosity values were compared to a reference plastic viscosity, PV_o, value. A relation between the decrease in measured plastic viscosity and the total filtrate volume is shown in Figure 4.17. PV/PVo where PV is the plastic viscosity of the slurry and PVo is the plastic viscosity of the slurry mixed with distilled de-ionized water represents the relative change of the plastic viscosity. In slurries with low PV/PV_o values, the volume of filtrate collected is greatest which corresponds to a higher hydraulic conductivity.

A slight increase in the total filtrate volume can be seen at a PV/PV_o value of about 0.5 and a substantial increase in the total filtrate volume occurs when PV/PV_o is less than 0.2, as shown in Figure 4.17. In Section 4.2.5.1, Figure 4.11 shows a linear relationship between the total filtrate volume and the hydraulic conductivity. Substituting the filtrate volume with hydraulic conductivity in Figure 4.17 produces Figure 4.18. The scatter in the data can be attributed to some differences between the two types of bentonites used.

In an attempt to eliminate the effect of the two different types of bentonite, a relative change in hydraulic conductivity, as expressed earlier, is used in Figure 4.19 to describe the results. From this figure slight changes in hydraulic conductivity are observed at a PV/PV_o value of 0.5 and substantial changes occur at PV/PV_o values less than 0.2, as seen before. The wide band has been reduced and relative changes in hydraulic conductivity of the two bentonites follow similar patterns.

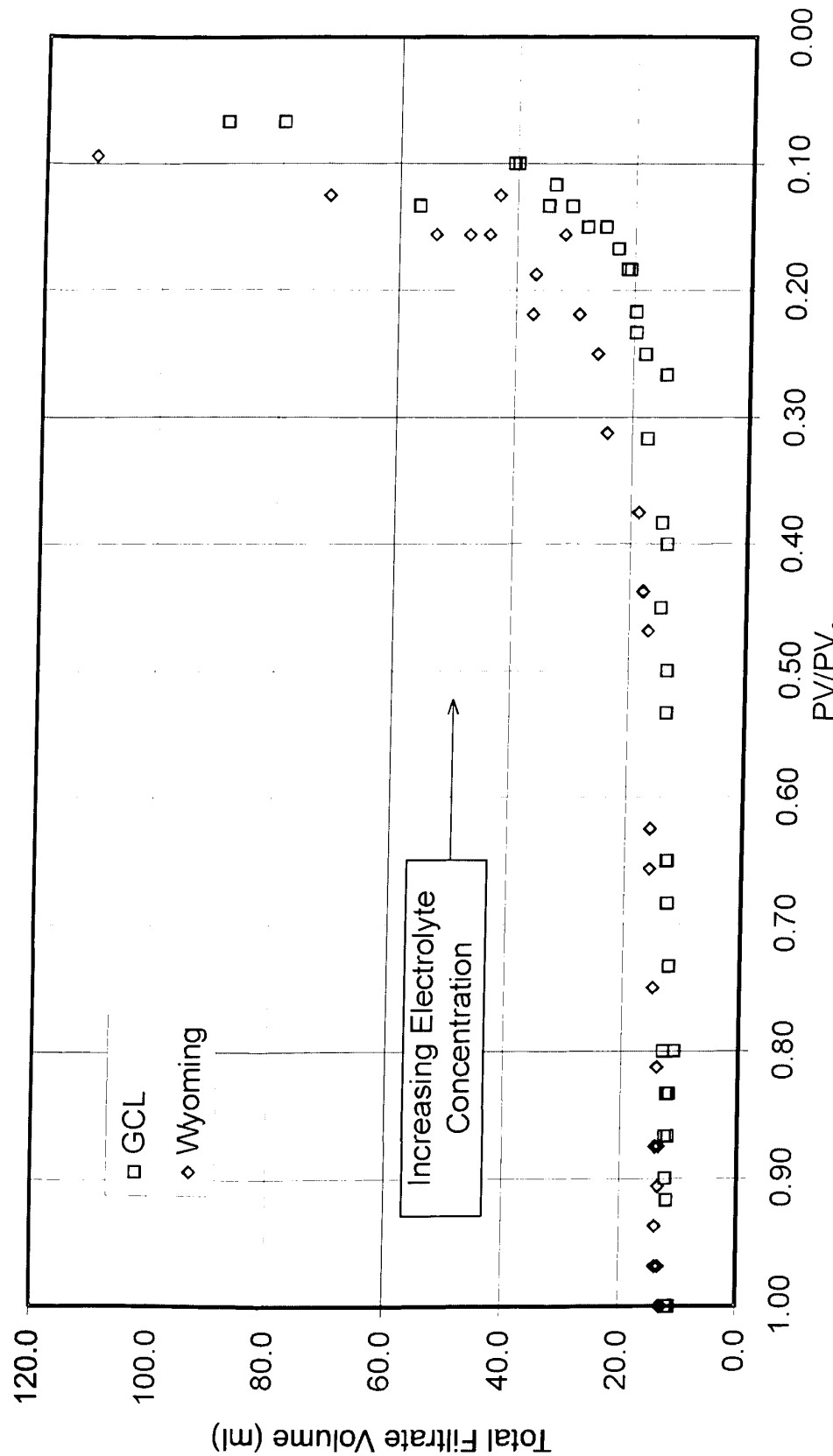

Figure 4.17 - Total amount of filtrate collected vs. relative plastic viscosity.

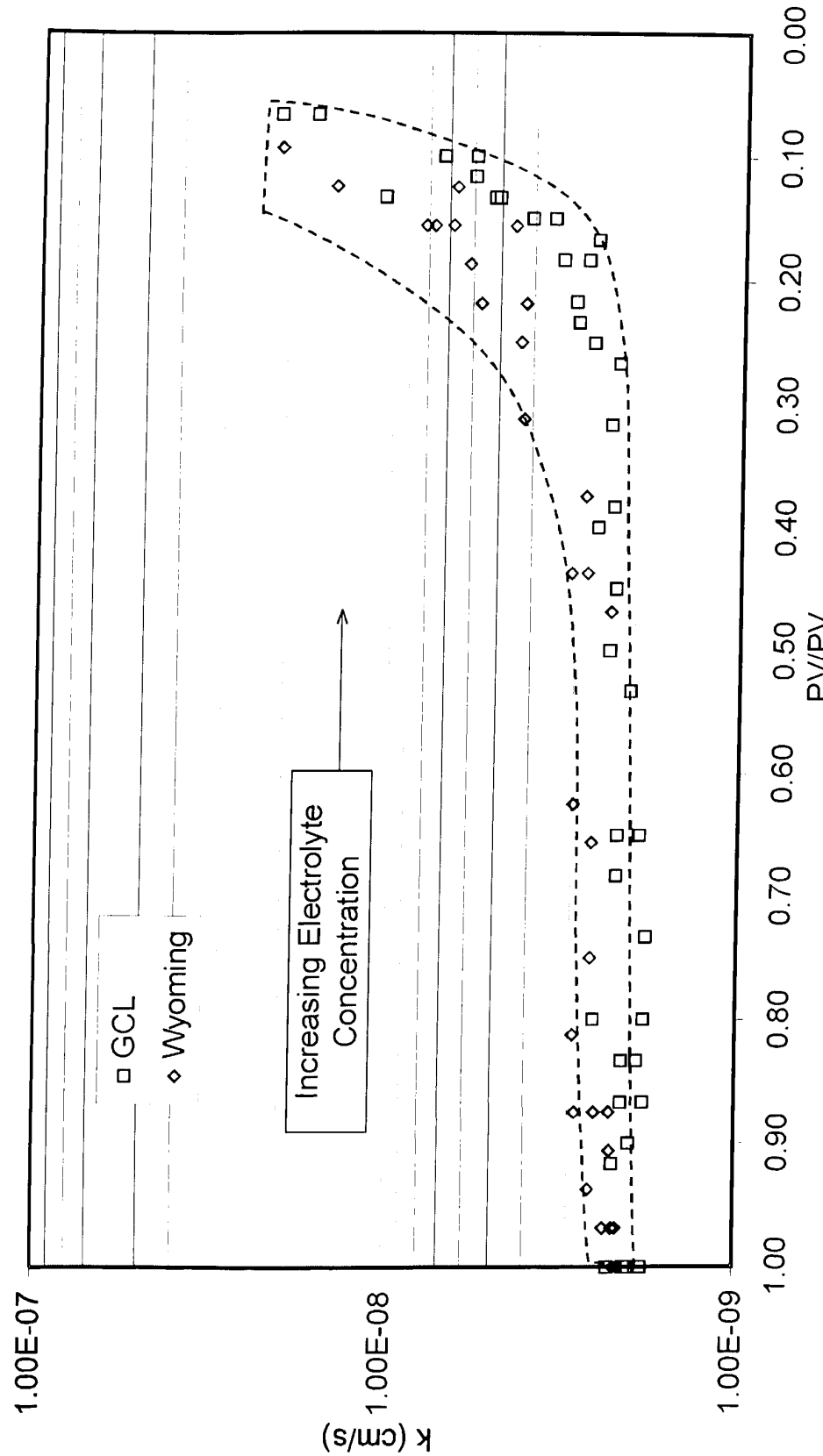

Figure 4.18 - Hydraulic conductivity vs. relative plastic viscosity.

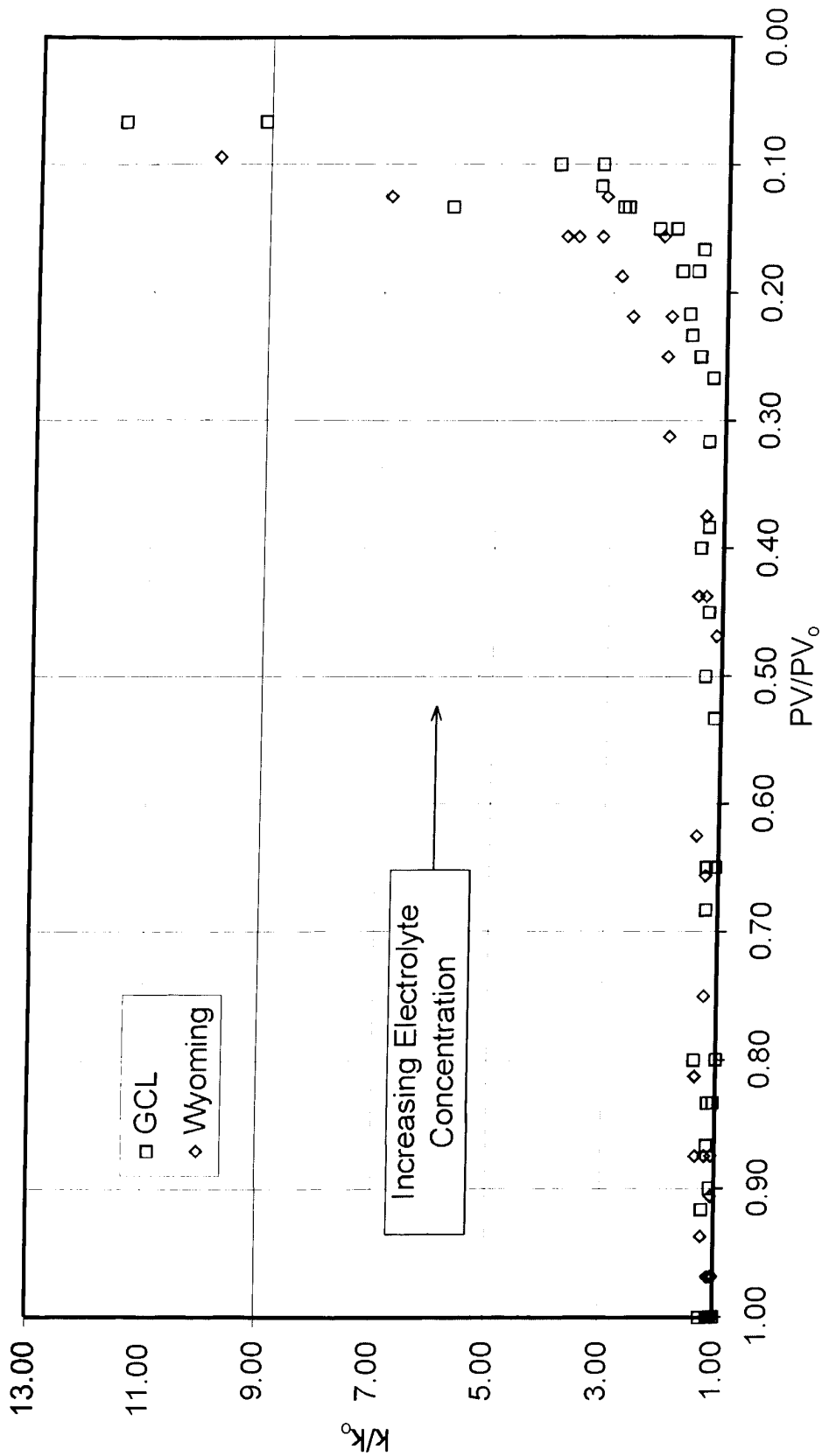

Figure 4.19 - Relative hydraulic conductivity vs. relative plastic viscosity.

The shape of the plot in Figure 4.19 is similar to the k/k_o versus S/S_o plot, in Figure 4.16, but using plastic viscosity seems to produce more consistent results. There is less scatter in the data and this makes the general trend more pronounced. The shearing of the slurry during viscosity testing has eliminated the effects of flocculation. In the free swell test, the index value includes the effects of flocculation. This is evident as previously shown in Figure 4.5 where the free swell index at low electrolyte concentrations is greater than distilled de-ionized water. The relative free swell values, in Figure 4.16; seem to be higher than the relative plastic viscosity values in Figure 4.19 for the same relative hydraulic conductivity value.

Comparing the two pre-screening methods, the electrolyte concentrations at which the two warning criteria are met - slight ($k/k_o \sim 1.5$) and substantial ($k/k_o \sim 3$) changes to the hydraulic conductivity - is higher for the free swell index than for the plastic viscosity, as shown in Tables 4.1 and 4.2. Figures 4.20 and 4.21 reflect the data presented in the two tables. In both tables the $CaCl_2$ concentration at which these changes take place is approximately the same for both methods. Taking all the electrolyte solutions into account, the warning concentrations obtained from the free swell method are all higher than the warning concentrations from the plastic viscosity method except the one $CaCl_2$ which is practically the same. This holds true for both bentonite products used. In Figure 4.21, the electrolyte concentrations for substantial changes in the hydraulic conductivity indicated by plastic viscosity are lower than slight changes indicated by free swell. Using the free swell pre-screening method, at these concentrations, one would anticipate very little change, but an increased hydraulic conductivity would be expected to develop based upon the

results of the plastic viscosity testing. The warning concentrations based on plastic viscosity are lower than those based on free swell. Therefore, using plastic viscosity measurements, the results obtained are more conservative and reliable.

Table 4.1 - Slight changes in hydraulic conductivity warning concentrations.

$k/k_o \sim 1.5$						
Bentonite	Electrolyte Concentration, M					
	NaCl		KCl		$CaCl_2$	
	Free Swell	Viscosity	Free Swell	Viscosity	Free Swell	Viscosity
GCL	0.3	0.026	0.05	0.007	0.009	0.005
Wyoming	0.07	0.017	0.02	0.004	0.006	0.002

Table 4.2 – Substantial changes in hydraulic conductivity warning concentrations.

$k/k_o \sim 3$						
Bentonite	Electrolyte Concentration, M					
	NaCl		KCl		$CaCl_2$	
	Free Swell	Viscosity	Free Swell	Viscosity	Free Swell	Viscosity
GCL	0.6	0.2	0.1	0.02	0.02	0.015
Wyoming	0.17	0.1	0.06	0.03	0.009	0.01

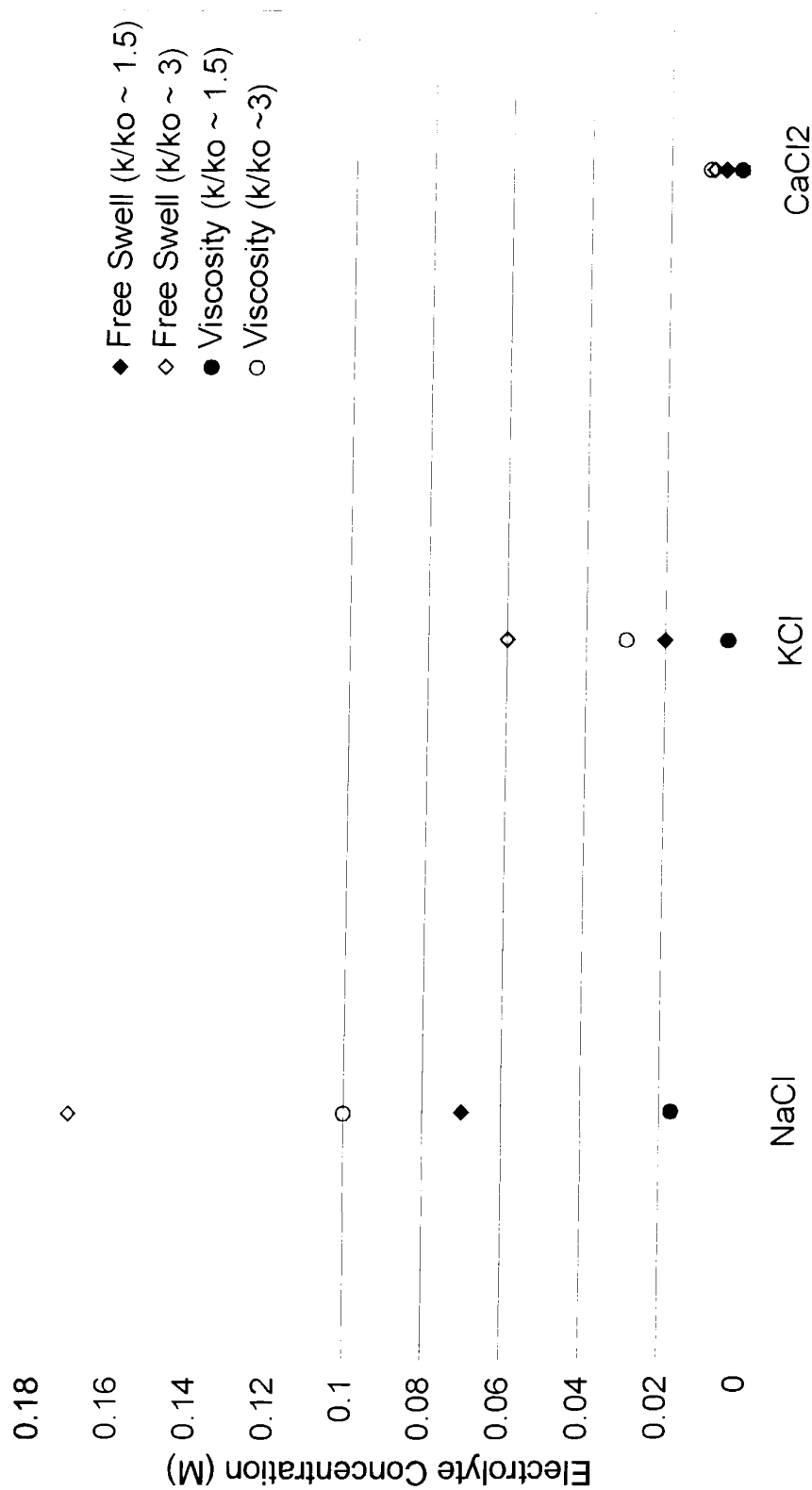

Figure 4.20 - Warning electrolyte concentrations for Wyoming bentonite.

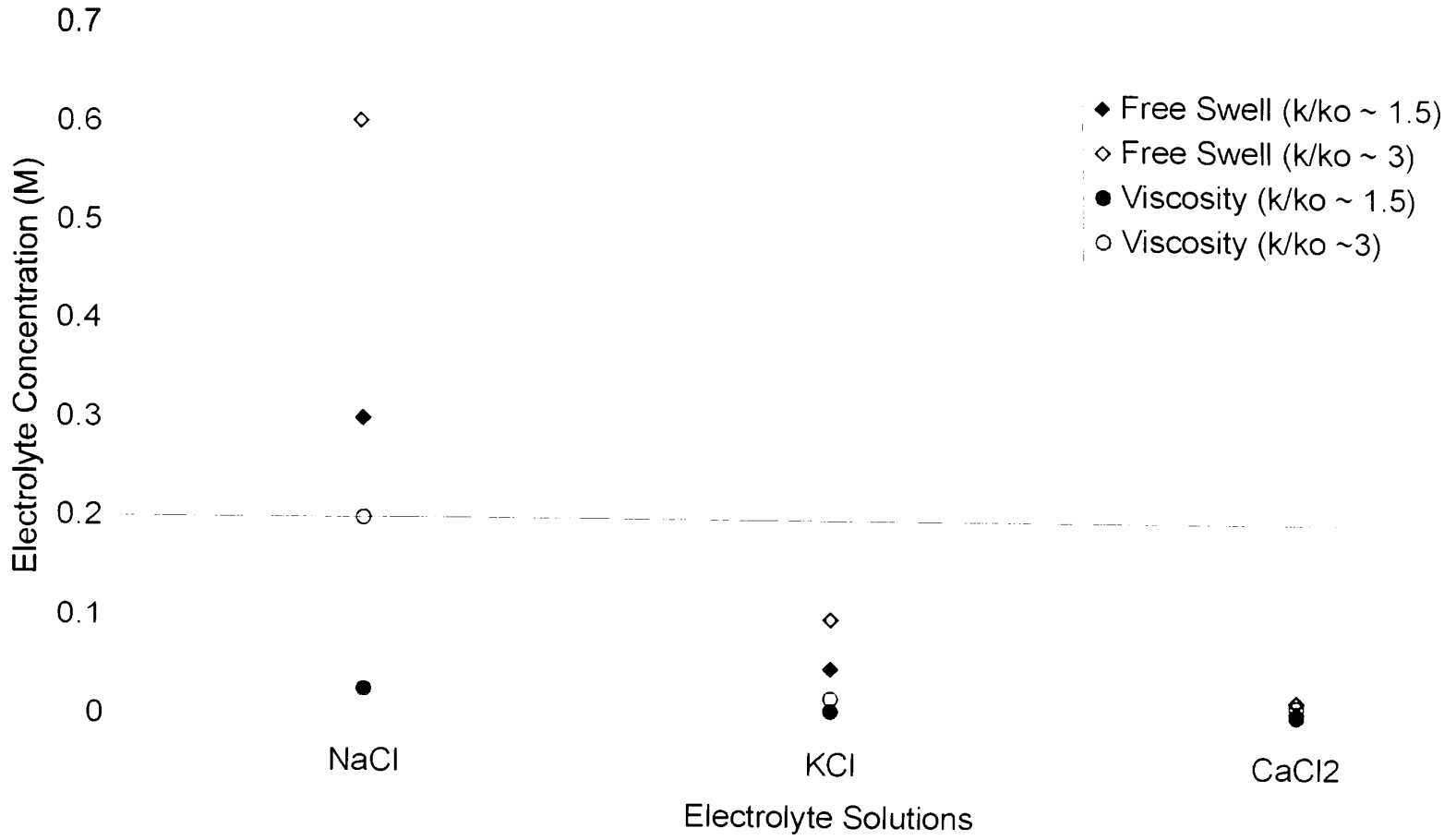

Figure 4.21 - Warning electrolyte concentration for GCL bentonite.

Chapter 5 Development of Alternative Pre-Screening Method

5.1 Introduction

A step-by-step test procedure for a new pre-screening method is outlined in this chapter. This alternative test method pre-screens the bentonite based on changes to the plastic viscosity and hydraulic conductivity of a slurry mixed with a chemical solution. A discussion and the verification of the alternative pre-screening method is also provided.

5.2 Alternative Method Protocol

1. Obtain sample of wastewater or chemical solution and bentonite to be used in construction.
2. Prepare a 7%, by weight, 500 ml slurry with the bentonite and chemical solution.
3. Mix the slurry with a BRAUN™ handmixer for about ten minutes and store the slurry in a container for three days. A 500 ml mason jar works well.

4. After three days, stir the slurry again and place a sample of the slurry in the viscometer cup. Start the viscometer and record the required viscosity readings (600 and 300 rpm).

5. Once the viscosity testing is finished, pour the slurry into the mud cup of the filter press. Assemble the filter press and apply the 690 kPa ± 5 kPa pressure for 30 minutes. During the filter press testing collect the filtrate below and record the volume of filtrate at two different times.

6. Since the volume of filtrate collected varies linearly with the square root of time, the filtrate volume can be determined at whatever time is needed.

7. After the 30 minutes, relieve the pressure and remove the mud cup from the filter press.

8. Pour off the remaining slurry from the cup and gently wash the top of the resulting filter cake on the filter paper. Measure the thickness of the filter cake; the filter cake is used in the determination of the hydraulic conductivity.

9. Repeat the same procedure using distilled de-ionized water to produce the slurry.

10. Once complete, determine the relative plastic viscosity, PV/PV_o.

11. Compare the PV/PV_o value to the warning criteria and determine which scenario the value falls under and take appropriate action in the design of the barrier system (See Table 5.1).

5.3 Proposed Alternative Method Criteria

Table 5.1 - Proposed plastic viscosity pre-screening criteria.

PV/PV_o	≥ 0.50	$0.50 - 0.20$	≤ 0.20	≤ 0.15
	Little to no change in hydraulic conductivity anticipated	Find alternative bentonite or alternative to bentonite, or if bentonite is to be used carry out careful long-term hydraulic conductivity tests using the actual permeant that is anticipated in the field	Use bentonite very cautiously with expert advice and extensive monitoring etc.	Do not use bentonite

5.4 Laboratory Case Study

During laboratory testing a failure occurred in one of the GCL specimens in a permeameters. The GCL specimen was initially hydrated with distilled water until it was saturated and the hydraulic conductivity stabilized at 1.55×10^{-9} cm/s. A 0.005 M $CaCl_2$ solution was introduced and this caused little change to the hydraulic conductivity. A 0.009 M $CaCl_2$ solution was subsequently added and the hydraulic conductivity increased to slightly more than three times its original value. Once the hydraulic conductivity was stable the permeant was changed to a 0.023 M $CaCl_2$ solution. After a few minutes the GCL sample had failed with the last measurable hydraulic conductivity of 1×10^{-6} cm/s, approximately 570 times its original value.

The test was terminated and a tracer dye was permeated through the specimen to determine the mode of failure. The confining cell was removed and the rubber membrane surrounding the specimen was in good condition as shown in Figure 5.1. Removal of the membrane did not show any evidence of sidewall leakage (Figure 5.2).

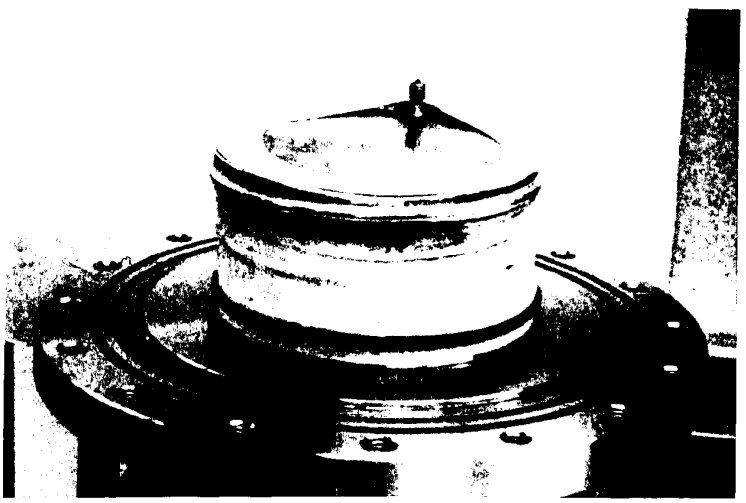

Figure 5.1 – GCL specimen after removal of confining cell.

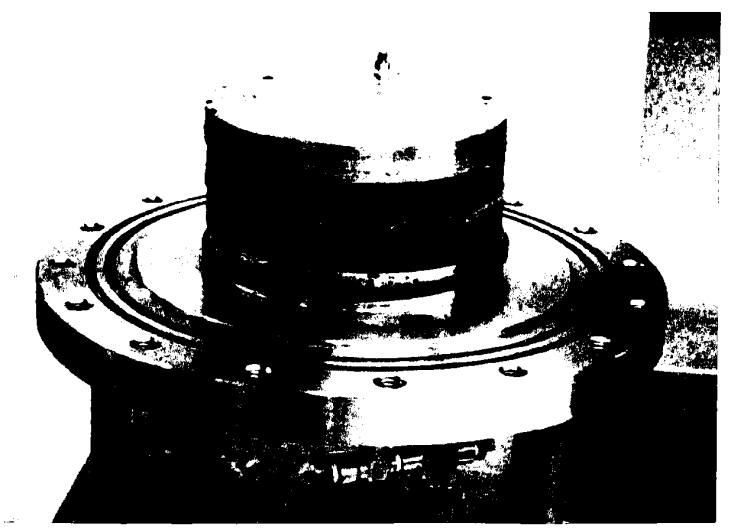

Figure 5.2 – GCL specimen with rubber membrane removed.

The top cap and porous disk were removed exposing the effluent side of the GCL. The tracer dye was concentrated at one location in the GCL as shown in Figure 5.3.

Figure 5.3 - Concentrated effluent in area of failure.

The specimen was turned over and the dye was evenly distributed over the entire surface as shown in Figure 5.4. It was concluded that the mode of failure was internal by causes not determined. The GCL may have had a thin spot at that location, the bentonite may have undergone shrinkage and pulled away from a stitch in that location, or the bentonite may have cracked due to double layer contraction. Any of these are possible and failure was most likely a combination of all three.

Figure 5.4 - Even influent distribution.

Increased hydraulic conductivities were observed for each increase in $CaCl_2$ concentration. These results have been related to their respective free swell index and plastic viscosity. Using the pre-screening methods mentioned above the results of the GCL permeameters permeated with a $CaCl_2$ solution are plotted on the compatibility criteria (Figures 4.16 and 4.19) as shown in Figures 5.5 and 5.6. From the GCL permeameter testing mentioned above, the 0.009 M $CaCl_2$ solution produces significant ($k/k_o > 3$) increases in the hydraulic conductivity, using the free swell pre-screening method would suggest little to no change as shown in Figure 5.5. When these results are used with the proposed viscosity pre-screening method, as shown in Figure 5.6, the coupled relative hydraulic conductivity and plastic viscosity values plot in the appropriate warning zones where the correct assessment of the chemical compatibility can be made. Once again it has been shown that the use of plastic viscosity as a pre-screening tool appears to be more reliable compared with the free swell index.

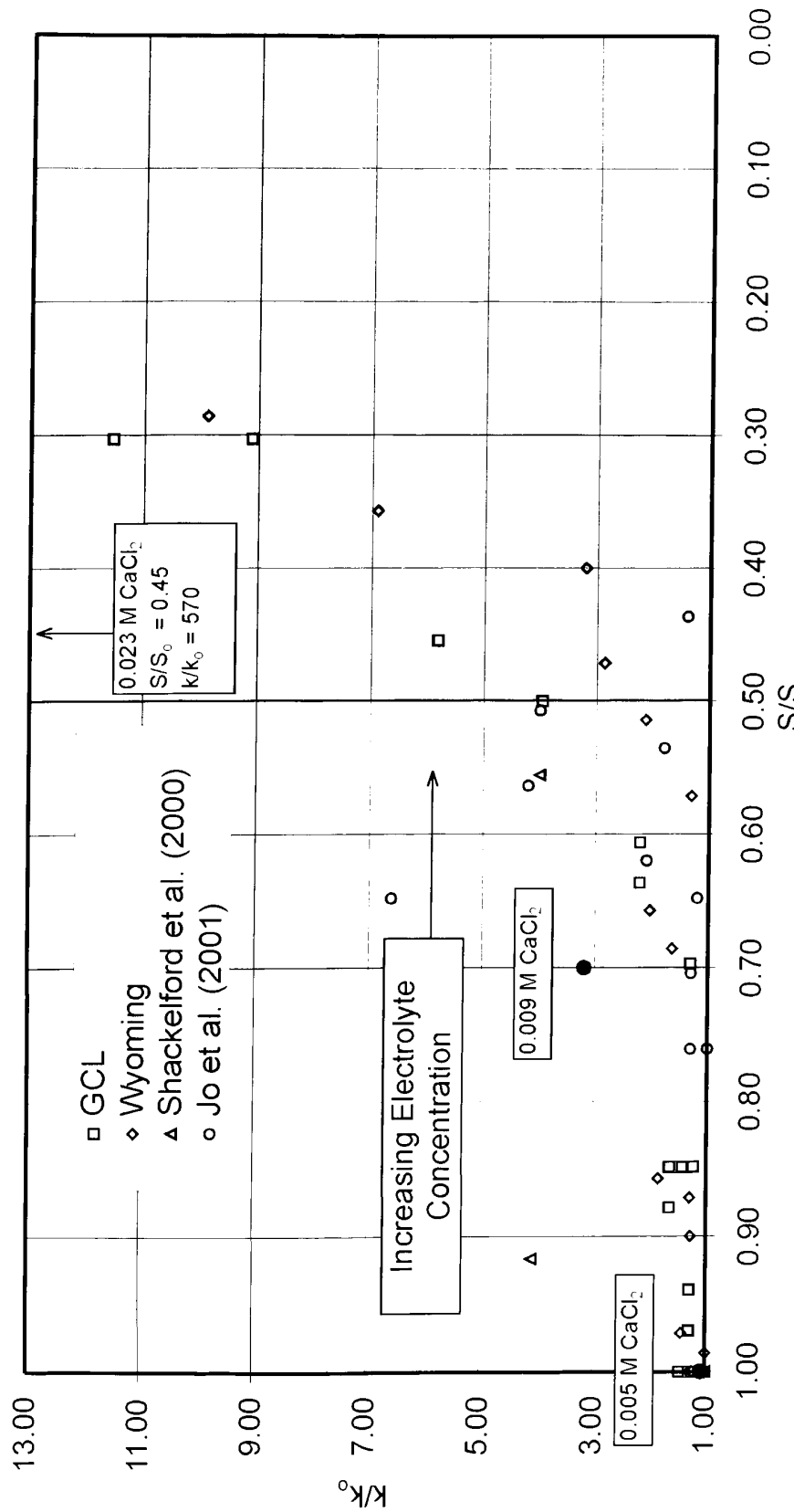

Figure 5.5 - Relative hydraulic conductivity vs. relative free swell index (for GCL permeated with increasing $CaCl_2$).

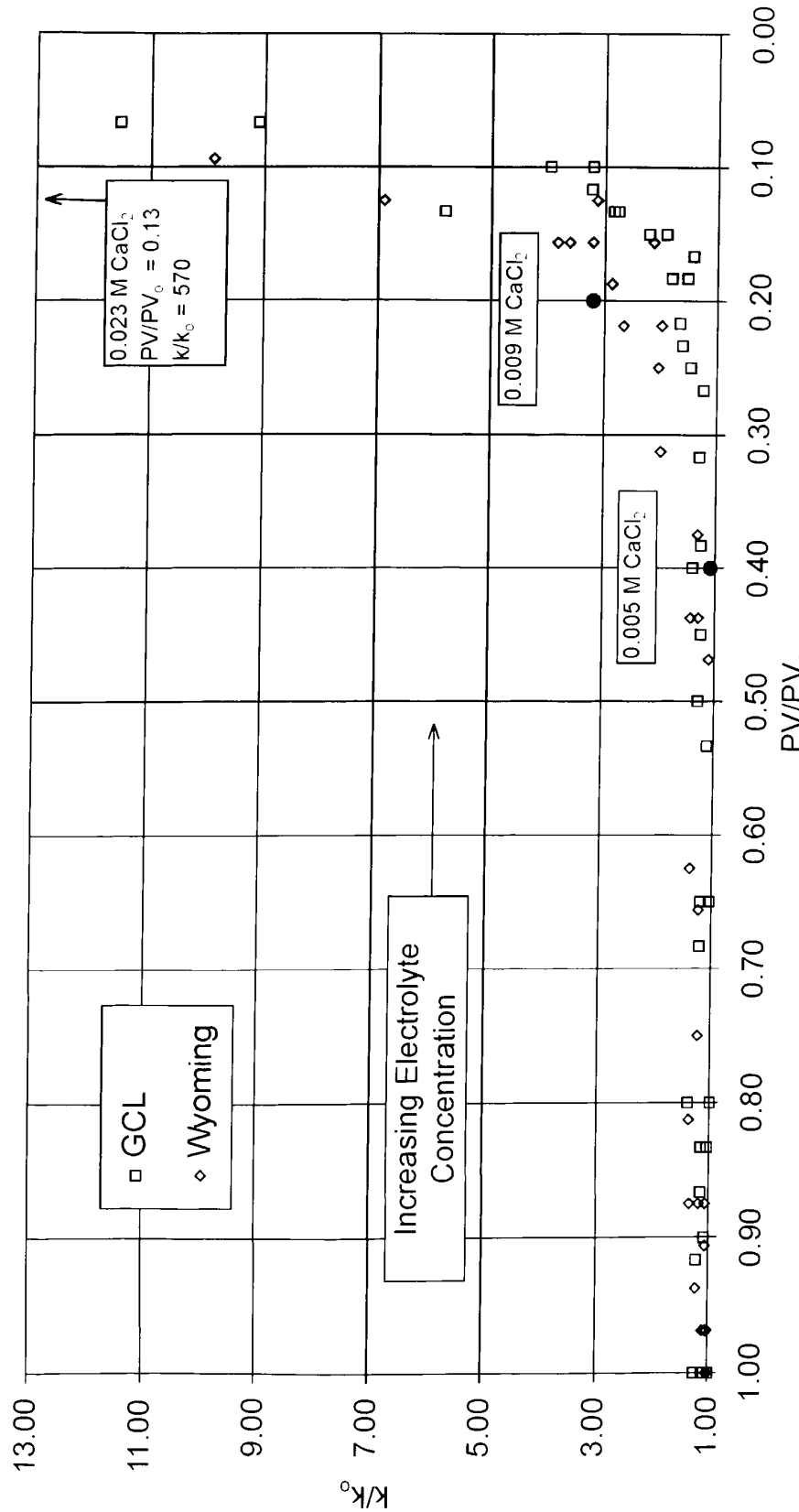

Figure 5.6 - Relative hydraulic conductivity vs. relative plastic viscosity (for GCL permeated with increasing $CaCl_2$).

Chapter 6 Case Study and Application of the Proposed Compatibility Pre-Screening Methodology

6.1 Introduction

This chapter presents an overview of a case study involving a soil-bentonite material installed as part of a composite liner for an industrial wastewater equalization lagoon upgrade at a chemical plant in Canada. The wastewater was diverted to a temporary storage lagoon. The equalization lagoon composite liner was constructed in December 1999 with a geomembrane overlying the compacted soil-bentonite material. For chemical compatibility design purposes, the wastewater composition assumed is shown in Table 6.1.

A consultant, prior to construction performed a compatibility study, but as with most compatibility studies, time was an issue and only a few pore volumes of permeant were passed through the samples in the course of carrying out fixed-wall permeameter tests. Hydraulic conductivity and X-ray diffraction testing were performed to assess the chemical compatibility of the wastewater and the soil-bentonite liner. The X-ray diffraction testing was performed by the GRC at the University of Western Ontario under the guidance of Dr. Ernest Yanful. The GRC report can be found in Appendix I.

The geomembrane was damaged as a result of operating conditions in the lagoon and the chemical wastewater came into contact with the soil-bentonite liner. This gave an opportunity in 2003 to investigate the unknown long-term performance of the soil-bentonite liner after about three years of exposure to the chemical wastewater. This chapter will review the initial design compatibility study performed by the consultant and comment on the performance of the soil-bentonite liner. This case study will also provide a means of demonstrating the usefulness of pre-screening methods, in industrial applications, for barrier design in the containment of chemical wastewaters.

6.2 Wastewater Characteristics

The table below presents the concentrations of the selected parameters used to assess the chemical compatibility of the wastewater.

Table 6.1 - Wastewater characteristics.

		Measured Range or Maximum Concentration in Wastewater	Design Concentration
pH		8.5 – 11.5	12
Formaldehyde	mg/l	4800	4800
Total Phenolics	mg/l	986	1000
Ammonia	mg/l	424	500
Total Alcohols	mg/l	3.8	500
Total MAH	mg/l	1.7	1000

At the time of construction, it was anticipated that future upgrades to the stormwater drainage facilities at the plant would reduce the amount of storm runoff and therefore increase the concentrations of key wastewater parameters. Some of the

key species listed above were, therefore, conservatively increased to ensure that the measured concentrations in the future do not exceed the design concentrations. Figure 6.1 shows a photograph of the synthetic wastewater used in the course of this study.

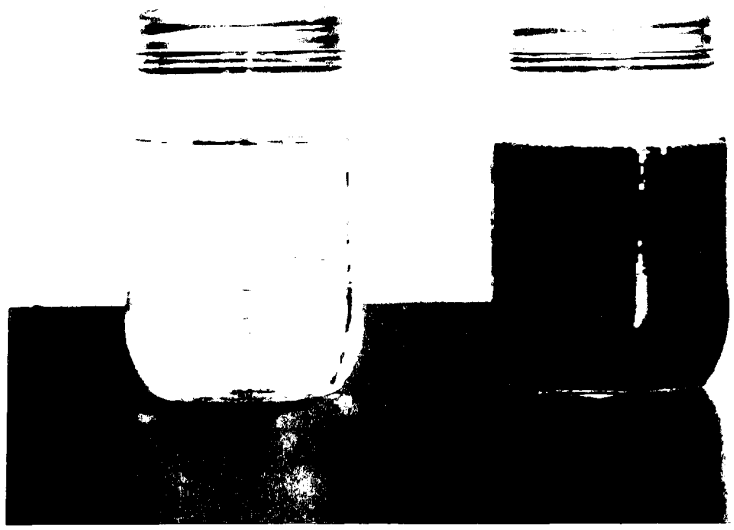

Figure 6.1 – Distilled de-ionized water (left) and synthetic wastewater (right).

6.3 Initial Design Compatibility Testing

During initial design X-ray diffraction (XRD) was conducted on three bentonite samples mixed with tap water and wastewater. The XRD test methods used were described previously in Chapter 3.4.5. The three bentonites were a polymerized Wyoming bentonite (ENVIRO-SEAL® - Bentonite Performance Minerals), an untreated Wyoming bentonite and an untreated Saskatchewan

bentonite. Figure 6.2 shows that the wastewater induced swelling (interlayer spacing greater than 4.4 nm) when wet. This swelling was apparently caused by the adsorption of organic molecules present in the wastewater. When the samples were air dried the organic substance appeared to volatize, resulting in a collapse of the interlayer. In all three bentonites, the samples treated with wastewater displayed lower air dried inter-layer spacings (1.20-1.30 nm) as shown in Figure 6.3 than the tap water sample shown in Figure 6.4, indicating slight collapse due to hydration with the wastewater. It was concluded that the wastewater likely was the cause of some mineral alteration within the Na-montmorillonite. Figures 6.2 to 6.4 show just three of the many XRD diffractograms. The remaining initial XRD diffractograms are contained in Appendix I.

Additional testing was recommended to assess the extent of the structural change in the bentonite. Fixed-wall permeameter testing was carried out for selected soil-bentonite mixes using the wastewater as permeant to determine the hydraulic conductivity. The samples consisted of a 4% soil-bentonite mix with either the polymerized or untreated Wyoming bentonite. The hydraulic conductivity initially decreased then experienced slight increases but remained stable and was less than $1x10^{-8}$ cm/s for both soil-bentonite mixes, as shown in Figures 6.5 and 6.6. In addition, the absence of an observed increase in hydraulic conductivity during the tests indicates that no short-term increase in hydraulic conductivity of the soil-bentonite liner would result from exposure to the wastewater. The soil-bentonite mixes were deemed acceptable, provided the bentonite was hydrated first with fresh water. The data for the fixed-walled permeameters and the compatibility report

prepared by Dr. Ernest Yanful at the University of Western Ontario is contained in Appendix I.

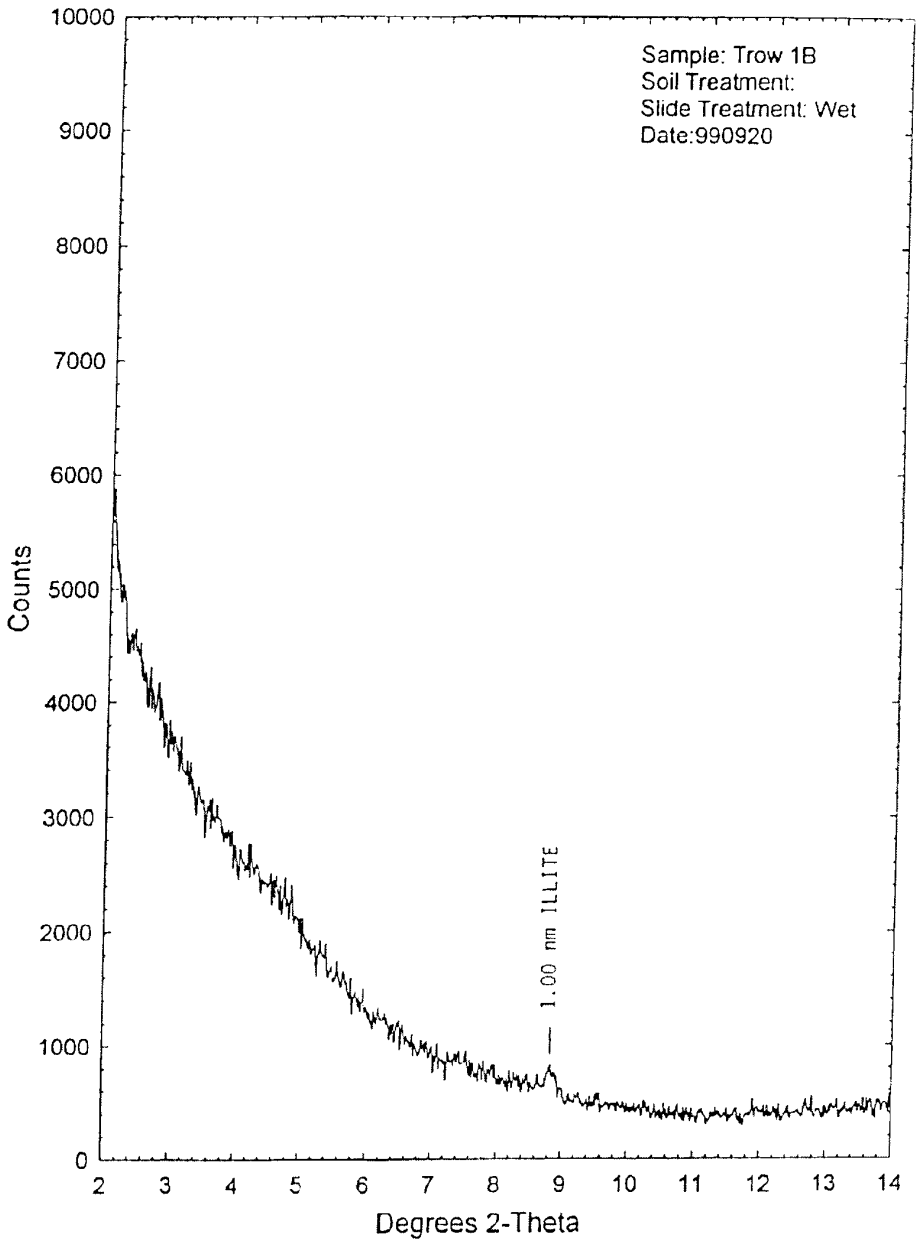

Figure 6.2 - XRD diffractogram of polymerized Wyoming bentonite exposed to wastewater (wet).

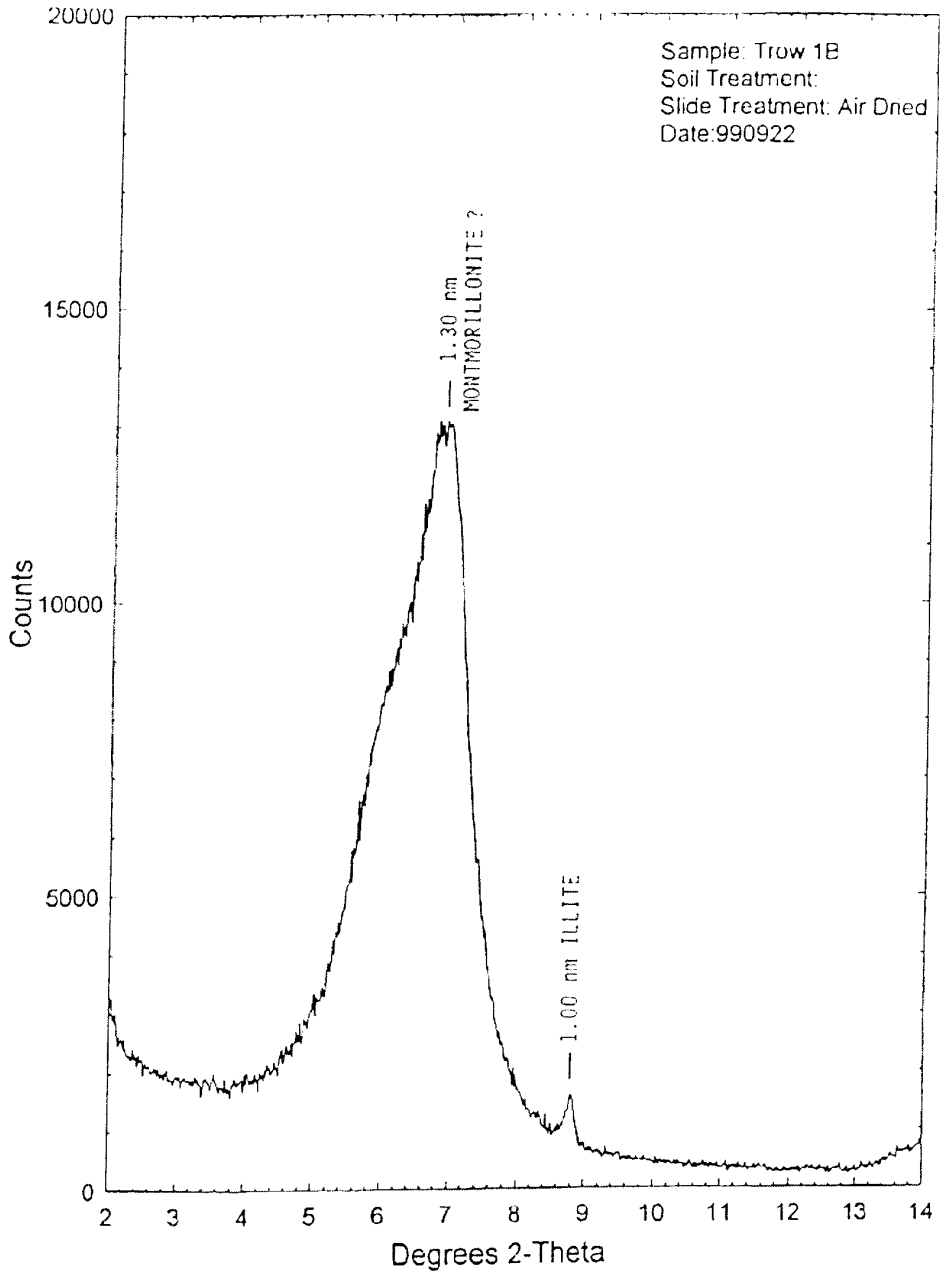

Figure 6.3 - XRD diffractogram of polymerized Wyoming bentonite exposed to wastewater (air dried).

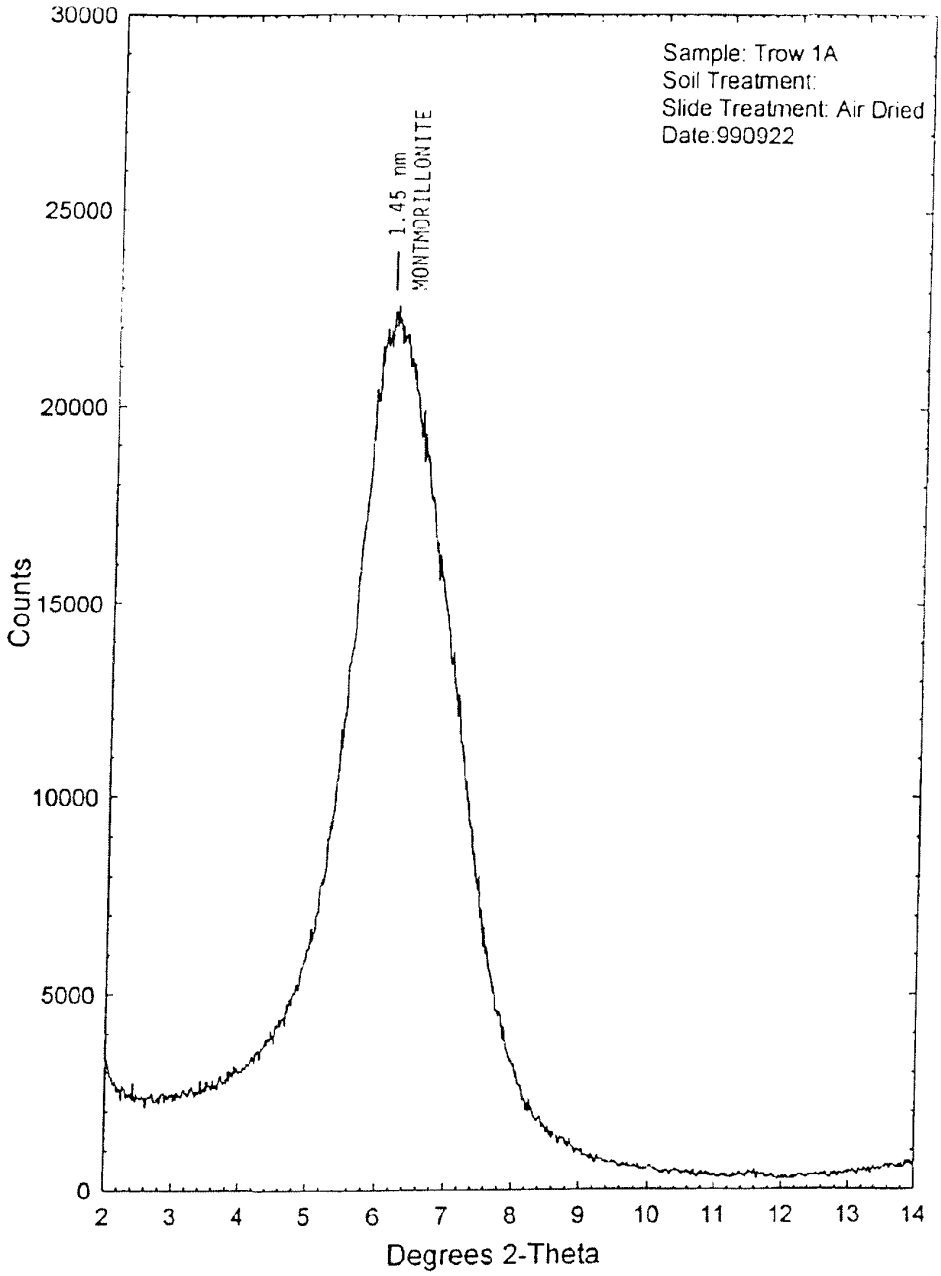

Figure 6.4 - XRD diffractogram of polymerized Wyoming bentonite exposed to tap water (air dried).

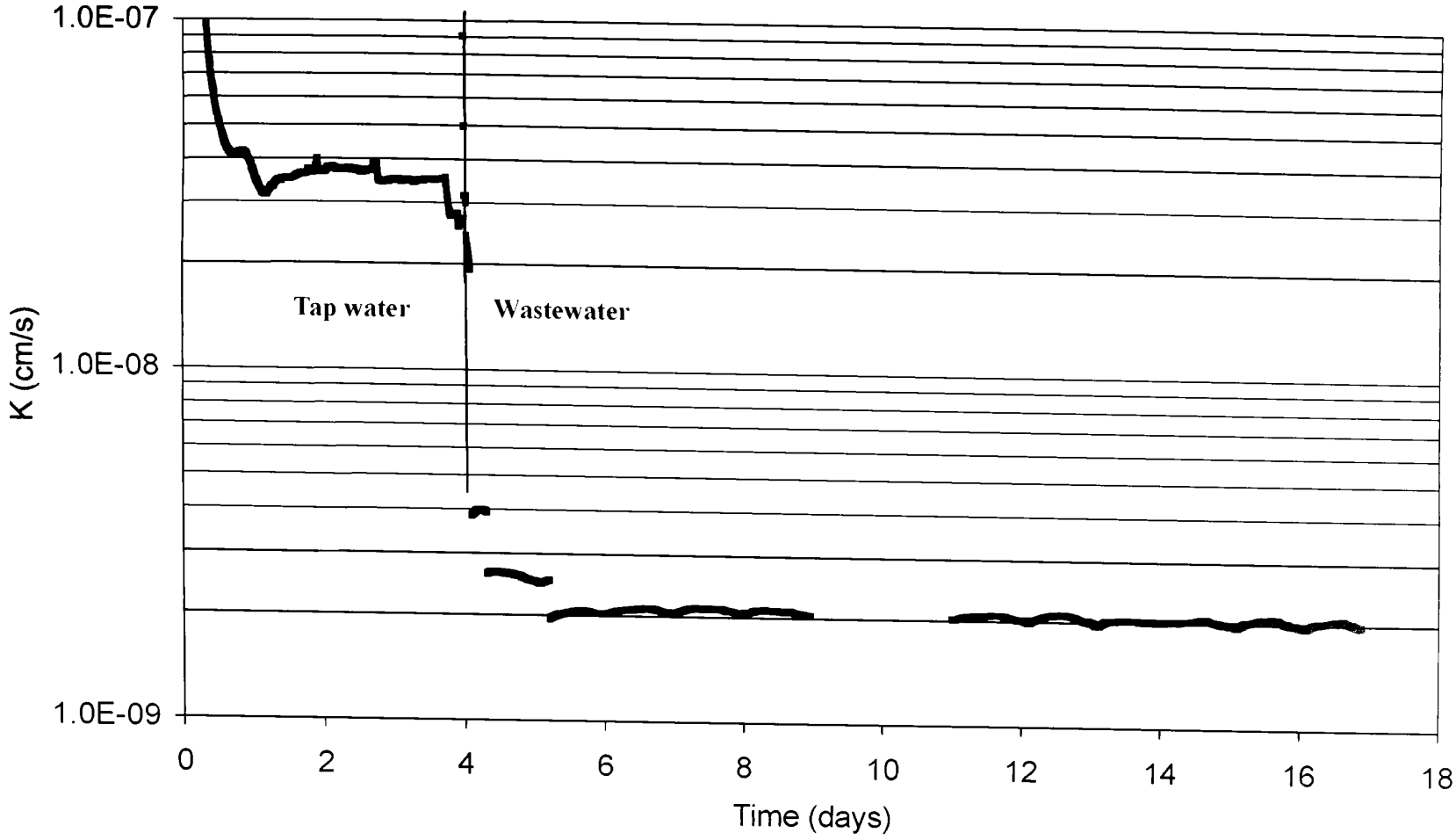

Figure 6.5 - Hydraulic conductivity vs. time, soil-bentonite initial design compatibility (polymerized Wyoming bentonite).

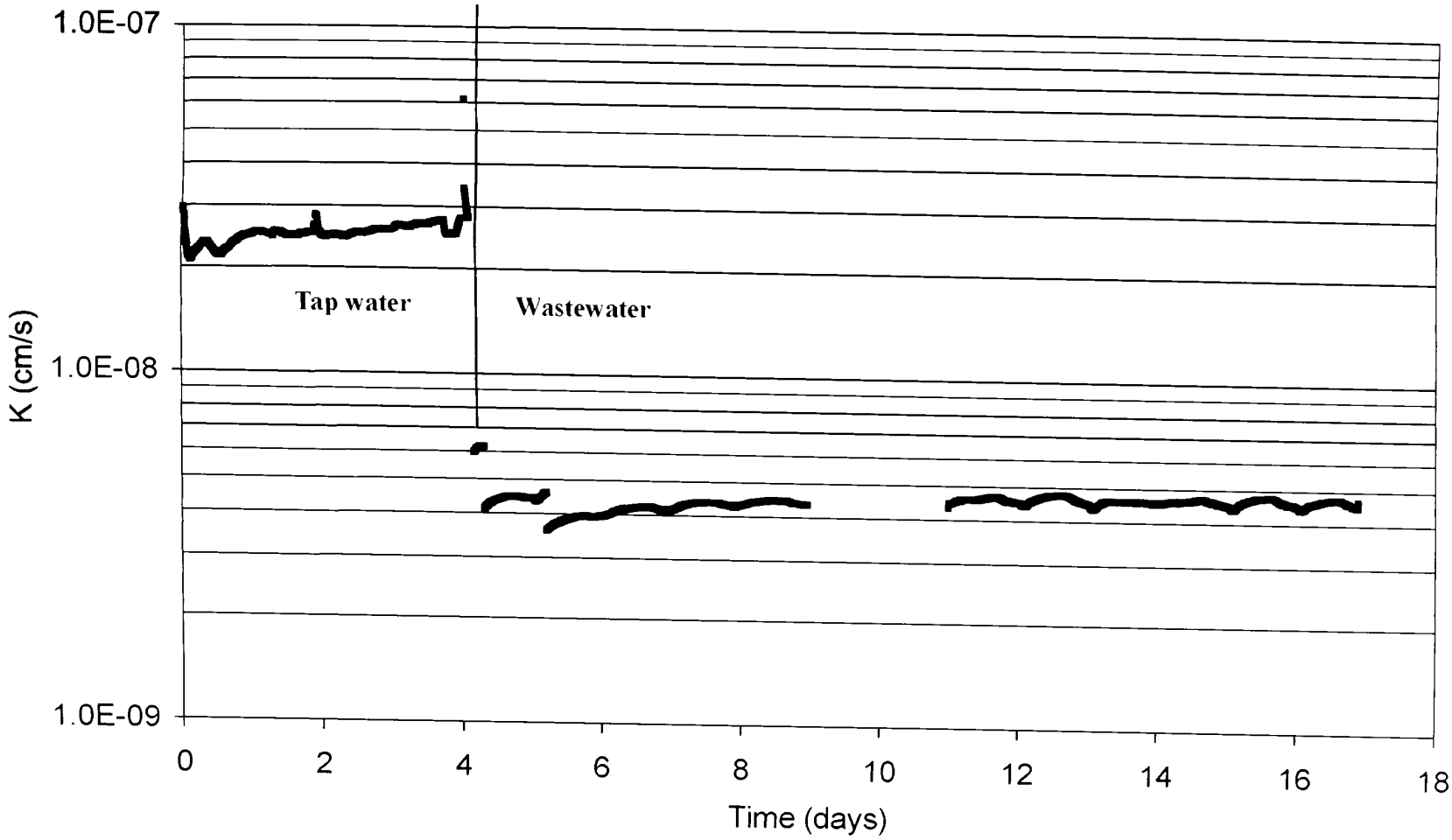

Figure 6.6 - Hydraulic conductivity vs. time, soil-bentonite initial design compatibility (untreated Wyoming bentonite).

6.4 Construction and Operation

The final design of the composite lining system for the wastewater equalization lagoon consisted of a geomembrane immediately overlaying a 200 mm thickness of compacted soil-bentonite. The soil-bentonite mixture consisted of 6% polymerized ENVIRO-SEAL® bentonite in graded silty soil. The installation of the soil-bentonite liner can be seen in Figure 6.7. The geomembrane completely covered the soil-bentonite liner and was in contact with the wastewater. The completed equalization lagoon liner can be seen in Figure 6.8. There was no requirement for a cover soil to protect the geomembrane from UV photo degradation, as the equalization lagoon is covered and therefore the lagoon base is not exposed to sunlight.

Figure 6.7 - Soil-bentonite liner installation.

Figure 6.8 - Completed composite liner construction.

The wastewater was diverted back to the equalization lagoon and resumed operations in December 1999, as shown in Figure 6.9. With the now installed composite liner system, the soil-bentonite layer would only be exposed to the chemicals in the wastewater in the immediate zone surrounding small defects in the geomembrane. In October of 2001, as shown in Figure 6.10, the geomembrane was

floating on the surface of the equalization lagoon in three places. The lagoon was drained in the spring of 2002 in order to investigate the problem. The geomembrane had been damaged during operation and holes were observed throughout the lagoon, as seen in Figure 6.11. It appears that excessive agitation and aeration of the lagoon was associated with oversized mixers installed into the lagoon after its initial construction in 1999. With the extent of the damage to the geomembrane, the underlying soil-bentonite liner was directly exposed to the chemical wastewater. Since the density of the geomembrane is less than the wastewater, the membrane floated to the surface creating a cavity below and exposing the wastewater to the soil-bentonite liner. If a cover soil had been placed over the geomembrane, the weight of the cover soil would have kept the geomembrane at the bottom thus eliminating the "early warning" and the problem might not have been identified until much later. On the other hand, if a cover soil had been used for protection, the geomembrane may not have been damaged during operations. Even if damaged, the geomembrane would not have lifted away from the soil-bentonite liner and allowed the free flow of wastewater through to contact the soil-bentonite. Considering all of the above, this case history suggests that the placement of cover soil over a geomembrane is in most cases beneficial to maintain intimate contact with the underlying material.

Figure 6.9 - Equalization lagoon resumes operation in December of 1999.

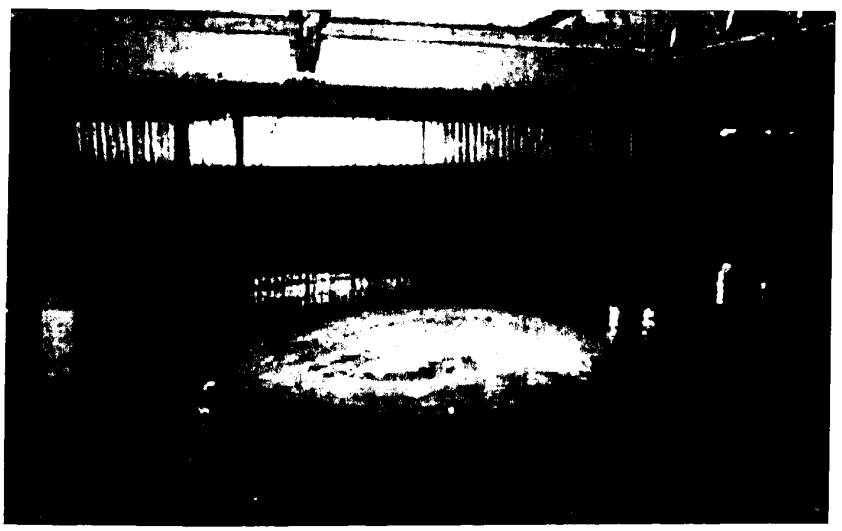

Figure 6.10 - Floating geomembrane in October of 2001.

Figure 6.11 - Damaged geomembrane.

6.5 Long-Term Performance and Forensic Testing

6.5.1 X-Ray Diffraction

The consultant exhumed the composite liner and shipped samples of the soil-bentonite liner to the University of Saskatchewan. Both Shelby tube samples and bulk grab samples were taken of the soil-bentonite material. In addition, several "sludge" samples were taken of the soft material above the soil-bentonite liner; it was hypothesized that this material likely contained soil-bentonite material that had

been scoured from the lagoon base during the period of operation because of excess agitation. Grain size and XRD analysis were performed to determine the clay fraction, which was inferred to equal the bentonite content of the Shelby tube samples. It was concluded from grain size analysis that the bentonite content in the Shelby tube samples was 2-3%, whereas the design called for 6% bentonite content. XRD testing was conducted by the Saskatchewan Research Council and followed the procedures outlined in Chapter 3.4.5. XRD was conducted on the Shelby tube samples and found that the bentonite content was 2-7%, which was similar to the grain size analysis. The results of the grain size and XRD testing can be found in Appendix J.

XRD was conducted on the grab and sludge samples as well. The bentonite content of the grab samples was found to be 0-2%, which is also lower than what was initially specified. There was some bentonite present in the sludge samples tested (0-3%). It is not clear whether the amount of bentonite present in the sludge can account for the generally low bentonite contents found in the Shelby and grab samples.

X-ray diffraction was conducted on what was assumed to be the same three bentonites used in the initial design compatibility testing. The three bentonites were ENVIRO-SEAL® a treated Wyoming bentonite, BARA-KADE® Standard an untreated Wyoming bentonite (both from Bentonite Performance Minerals) and an untreated Saskatchewan bentonite. During this round of testing, the glycolated diffractograms were similar to those obtained during the initial design compatibility testing. During the initial (1999) compatibility testing, the X-ray diffraction was

carried out from 2 to 15 degrees. During the later (2002) forensic testing, the diffractograms were taken from 5 to 35 degrees. Looking at the diffractograms of the bentonites mixed with the wastewater, there appears to be some additional calcite and dolomite, which is inferred to represent precipitation. The precipitation along with the organic absorption into the interlayer could explain the initial decrease in hydraulic conductivity as shown in Figures 6.12 and 6.13.

6.5.2 Hydraulic Conductivity Testing

6.5.2.1 Flexible Wall Permeameter (Soil-Bentonite)

Hydraulic conductivity tests were performed on the Shelby tube samples. The samples were first permeated with the wastewater to assess the long-term performance of the liner after it had been exposed to the wastewater for the three years. The results of the hydraulic conductivity testing can be found in Appendix J. The hydraulic conductivity was slightly higher than $1x10^{-7}$ cm/s after three pore volumes of wastewater had passed through, as shown in Figure 6.12. At this point, the permeant was changed to distilled de-ionized water (MegaPure) in order to investigate the potential for a decrease in the hydraulic conductivity due to reversible processes such as diffuse double layer swelling. The hydraulic conductivity decreased slightly to about $6x10^{-8}$ cm/s after three pore volumes of MegaPure had passed through. The permeant was changed back to the wastewater and the hydraulic conductivity initially decreased then increased slightly similar to that of the initial design compatibility in Figures 6.5 and 6.6.

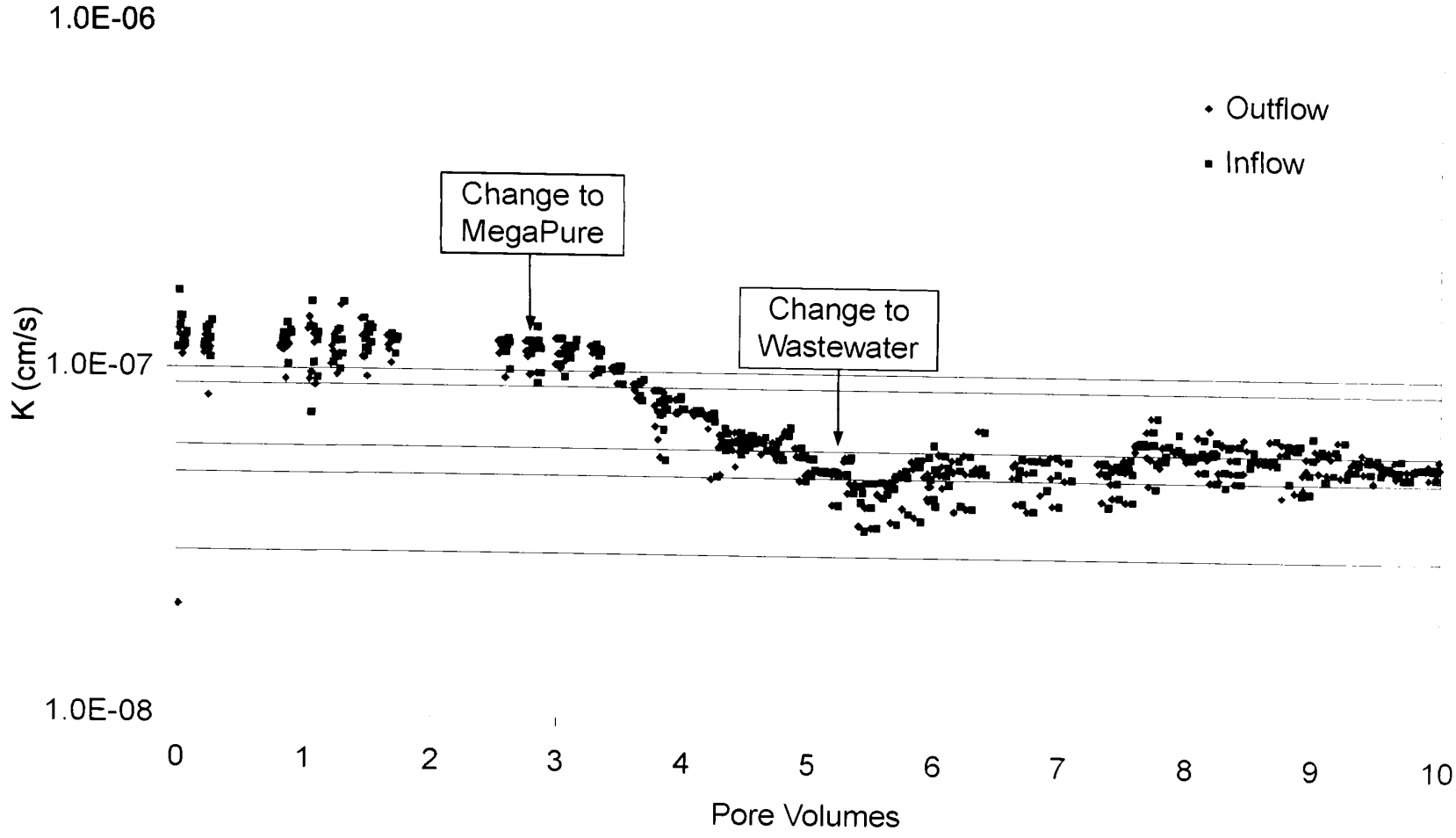

Figure 6.12 - Hydraulic conductivity vs. pore volumes of exhumed soil-bentonite Shelby tube sample.

The hydraulic conductivity obtained in the initial design compatibility was less than $1x10^{-8}$ cm/s. The hydraulic conductivity of the exhumed sample was slightly higher than $1x10^{-7}$ cm/s. The difference in the two values is likely attributable to the lower than specified bentonite content found in the exhumed liner (about 2% bentonite content). It may also be that a long-term increase in the hydraulic conductivity had occurred, but this cannot be verified with the existing data.

6.5.2.2 Flexible Wall Permeameter (GCL)

Long-term compatibility testing was performed on a large diameter GCL sample. The sample was prepared as described in Chapter 3.4.4.2. The flexible wall permeameter system used for testing made use of the GDS pressure volume controllers, as shown before in Figure 3.12. The GCL was hydrated with distilled de-ionized water for 1.6 pore volumes to obtain a baseline reference hydraulic conductivity of $1.20x10^{-9}$ cm/s, as shown in Figure 6.13. Once the baseline was obtained the permeant was changed to the synthetic wastewater. Initially the hydraulic conductivity decreased slightly. This decrease could be attributed to interlayer absorption of organic molecules present in the wastewater and precipitation of calcite and dolomite as described in Sections 6.3 and 6.5.1 respectively. Once one pore volume of synthetic wastewater had passed, the hydraulic conductivity increased back to its original value. Subsequent permeation of synthetic wastewater only produces a slight increase in hydraulic conductivity to $1.80x10^{-9}$ cm/s after 10 pore volumes. This long-term compatibility testing began on

January 18, 2003 and was finally discontinued February 28, 2004. A final hydraulic conductivity of 1.80×10^{-9} cm/s was observed after 13.5 pore volumes. It was concluded that all long-term changes had occurred and that high pH, phenolic wastewaters produces only slight increases in hydraulic conductivity of bentonite-based barrier systems.

It is evident from the discussions above that there is some degree of mineral alteration associated with the high pH, phenolic wastewater when bentonite-based barrier materials (both soil-bentonite and GCL) come in contact with the wastewater. It is further suggested that the degree of alteration and consequent compatibility issues appears to be slight or perhaps moderate; certainly there is no indication of a major increase in hydraulic conductivity associated with a catastrophic compatibility problem.

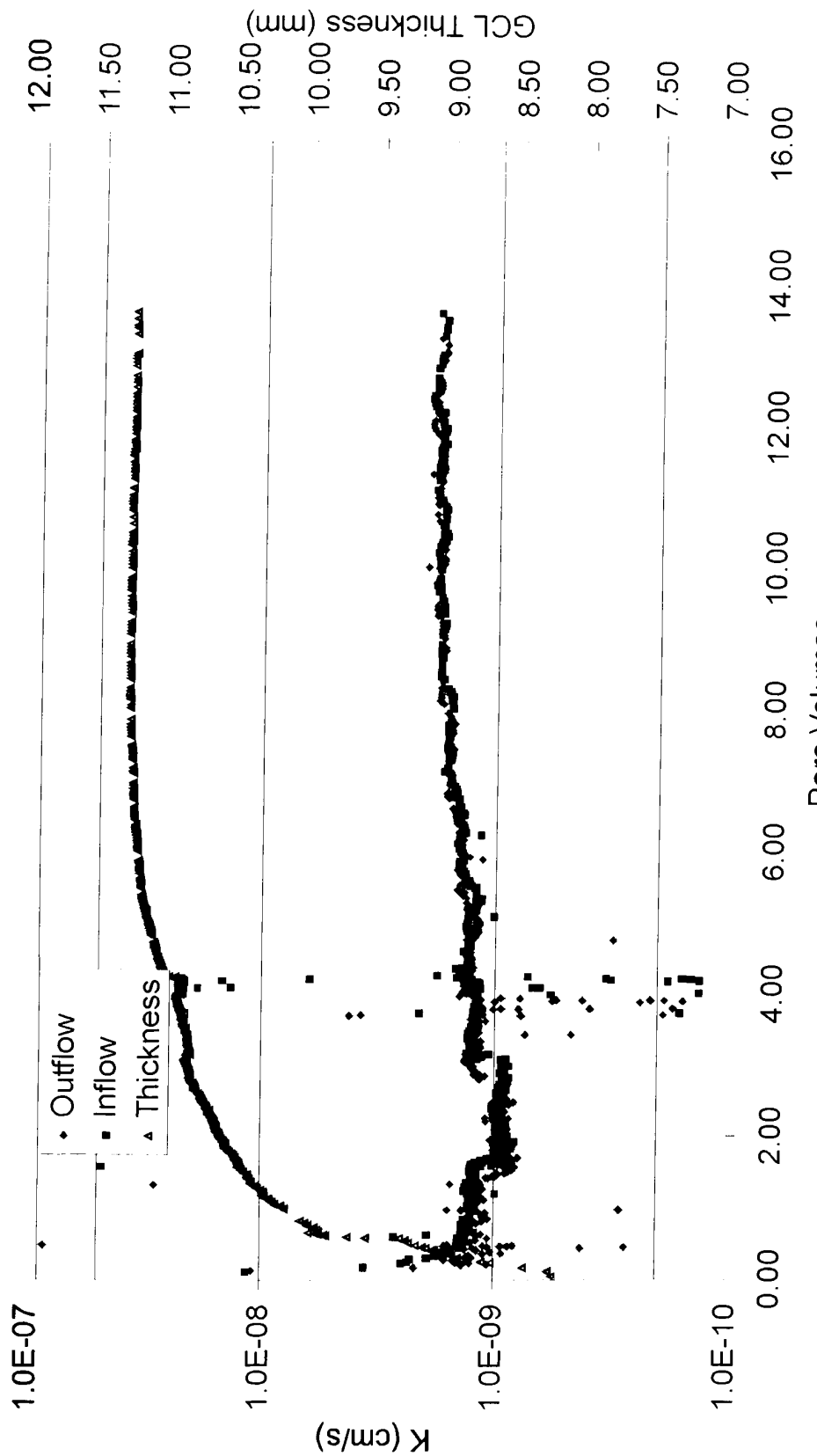

Figure 6.13 - Hydaulic conductivity vs. pore volumes for GCL permeated with synthetic wastewater.

6.6 Application of Pre-Screening Methods to Evaluate Compatibility

Following the discussion of Section 6.5 above, the wastewater acquired from the equalization lagoon was used in the pre-screening methods to evaluate compatibility with bentonite-based barrier materials. The two pre-screening methods were; i) ASTM D 6141; and ii) the alternative method outlined in Chapter 5.

6.6.1 Pre-Screening Methods

The synthetic wastewater was used in the pre-screening testing. The bentonites used were the GCL and the untreated Wyoming bentonite: the same two described in Chapter 3.2.

6.6.1.1 Free Swell

The free swell index of the bentonite in the wastewater was determined according to ASTM D 5890. The free swell index was 28 ml with the GCL bentonite and 19.5 ml with the Wyoming bentonite. The free swell testing of the GCL bentonite can be seen in Figure 6.14. Comparing the free swell indices of the bentonite in the wastewater to their respective distilled de-ionized water reference free swell index (33 ml for GCL bentonite and 35 ml for Wyoming bentonite), S/S_o values of 0.85 and 0.56 respectively were obtained and are shown in Figure 6.15 along with selected data originally presented in Figure 4.16.

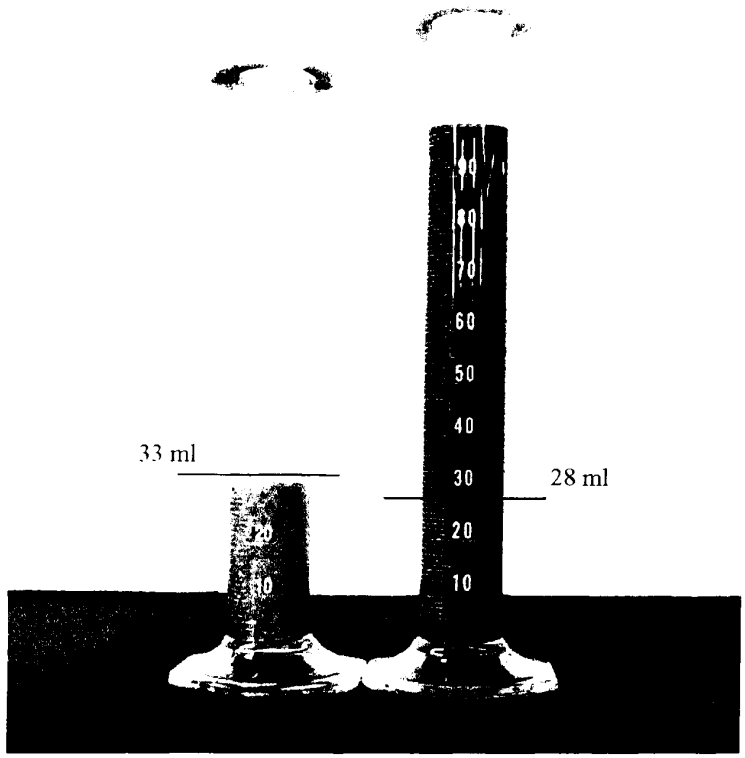

Figure 6.14 - Free swell index of GCL bentonite in distilled de-ionized water and synthetic wastewater.

The k/k_o values represented in Figures 6.15 and 6.17 were obtained from filter press testing. Slurry samples were mixed and placed in a filter press. The hydraulic conductivity of the resulting filter cake was determined and compared to a reference hydraulic conductivity of a filter cake produced with distilled de-ionized water. The test procedure and results have been discussed in Chapter 3.4.4.1 and Chapter 4.2.5.1.

Using this compatibility criterion, it would be expected that the GCL bentonite would not experience a change in hydraulic conductivity, whereas the

Wyoming bentonite might show slight to moderate changes in hydraulic conductivity. As described above, the data suggest that there is a slight change in hydraulic conductivity for both GCL and untreated Wyoming bentonite.

If a GCL were to be used to contain this wastewater, use of the free swell index criteria would suggest that there will be no change in the hydraulic conductivity but, as observed in Section 6.3, there is alteration of the bentonite structure. This would suggest that additional testing should be performed to assess the extent of such structural change and that the hydraulic conductivity of the GCL will not remain unchanged. Additional testing on a GCL sample was performed as described in the previous section and slight changes to the hydraulic conductivity were observed. If untreated Wyoming bentonite were to be used in a bentonite-based liner, this criterion would indicate that additional testing should be performed to determine the extent of the increase in the hydraulic conductivity.

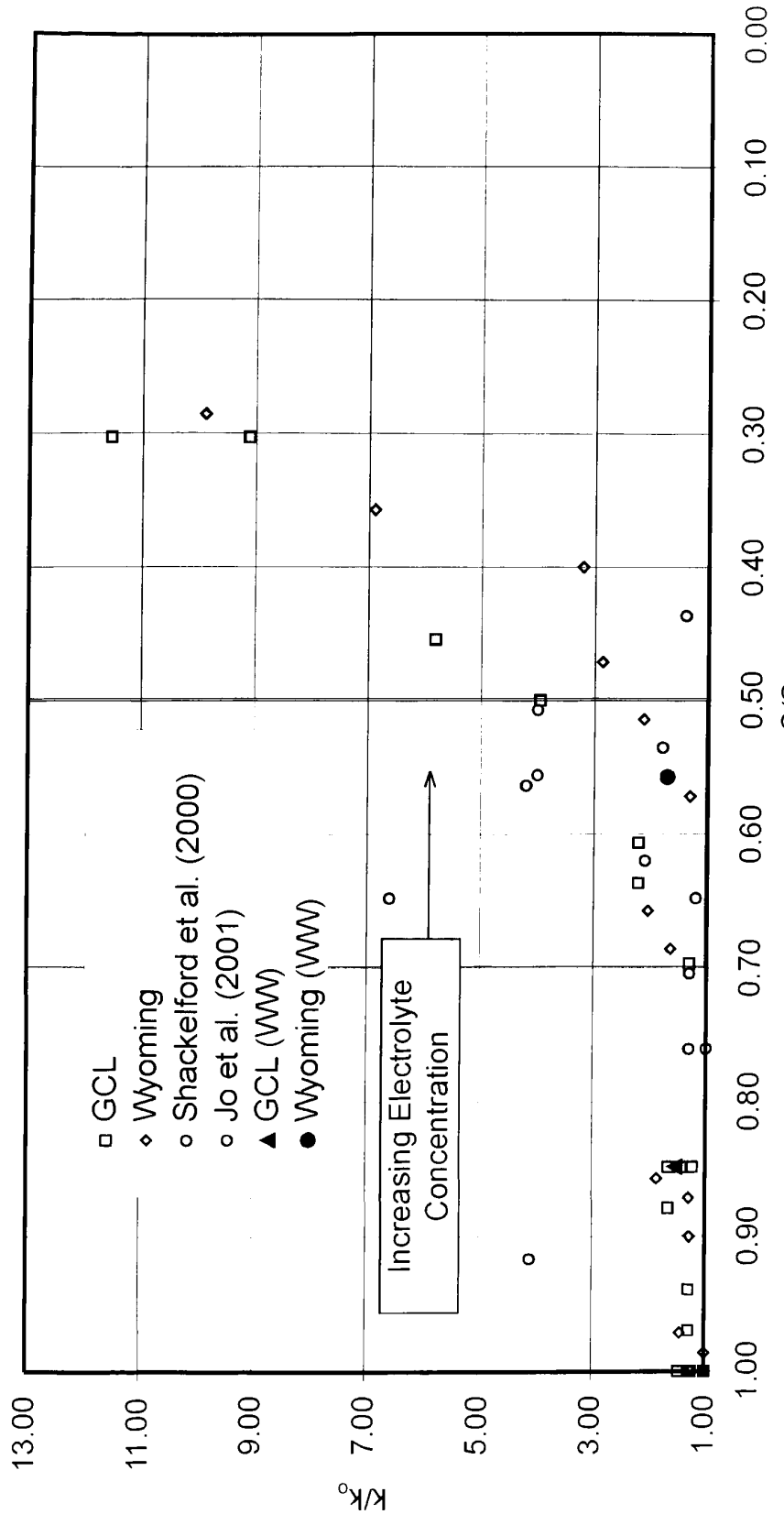

Figure 6.15 - Relative hydraulic conductivity vs. relative free swell (wastewater data).

6.6.1.2 Plastic Viscosity

The plastic viscosity of the slurry mixed with the wastewater was determined according to API-13B. The plastic viscosity was 11 cP with the GCL bentonite and 7 cP with the Wyoming bentonite. The distilled de-ionized reference and the synthetic wastewater slurries can be seen in Figure 6.16.

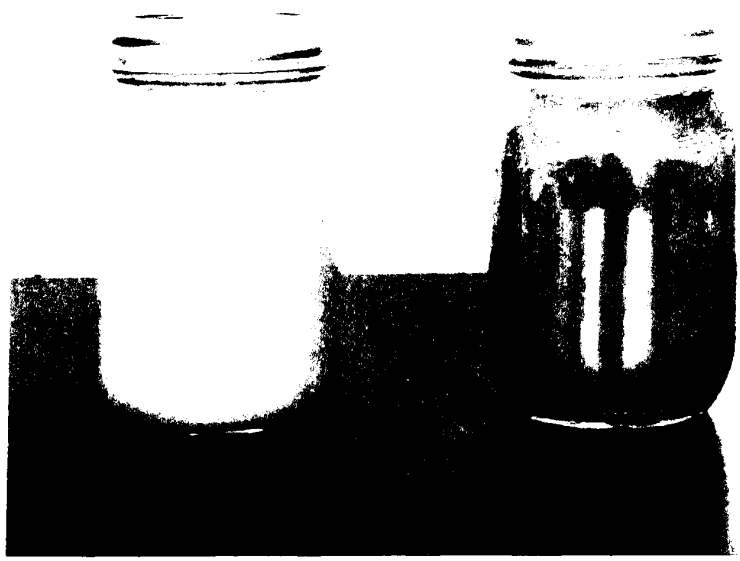

Figure 6.16 – Slurries of GCL bentonite mixed with distilled de-ionized water and synthetic wastewater.

Comparing the plastic viscosity of the slurries mixed with the wastewater to their respective distilled de-ionized water reference plastic viscosity (30 cP for GCL bentonite and 16 cP for Wyoming bentonite), similar PV/PV_o values are obtained (0.37 and 0.44 respectively) and they are plotted in Figure 6.17 over selected data originally presented in Figure 4.19. This compatibility criterion shows that the GCL

and Wyoming bentonite both fall in the intermediate range where slight changes in hydraulic conductivity may be expected. If any of these bentonites were to be used to contain the wastewater, the plastic viscosity pre-screening method would indicate that the wastewater falls in the PV/PV_o range of 0.50 - 0.20 where additional testing should be performed to determine the extent of the increase in the hydraulic conductivity. These slight changes have been observed in large diameter GCL samples tested in flexible wall permeameters and in soil-bentonite samples tested during the initial design compatibility, as described in previous sections.

6.7 Lessons Learned

There is minor alteration of the bentonite when it is exposed to the high pH, phenolic wastewater. The extent of the alteration appears to be minimal and is associated with only slight changes in the hydraulic conductivity. The large change in hydraulic conductivity experienced by the exhumed soil-bentonite liner is still not fully explained, but results are tending towards lower-than-specified bentonite content.

The results from the pre-screening methods support this finding. The ASTM D 6141 method concludes that by using the GCL bentonite, no increases in the hydraulic conductivity should be anticipated and that by using an untreated Wyoming bentonite in a bentonite-based liner, slight to moderate increases in the hydraulic conductivity should be anticipated. The result from the new plastic viscosity method concludes that if either the GCL or untreated Wyoming bentonite

is used, a slight increase in the hydraulic conductivity would be expected – this is exactly as observed during laboratory testing of samples.

In summary, while the existing ASTM D 6141 method tends to provide reasonable agreement with the observations made in this case, it is evident that the proposed plastic viscosity method provides a more consistent agreement. Nevertheless, the use of the free swell index is likely to continue to be the standard as it can be performed in any laboratory due to the simple fact that no special or expensive equipment is needed. In order to use the plastic viscosity pre-screening method, the laboratory must be equipped with a device to measure the viscosity of the soil slurry. Such a device can cost $2,000 used and up to $10,000 new depending on the extra features added to the device. The results presented in this and preceding chapters have highlighted some conditions under which the use of the free swell index would have resulted in unexpectedly high hydraulic conductivity values, which might be a problem in the case of highly sensitive, critical applications.

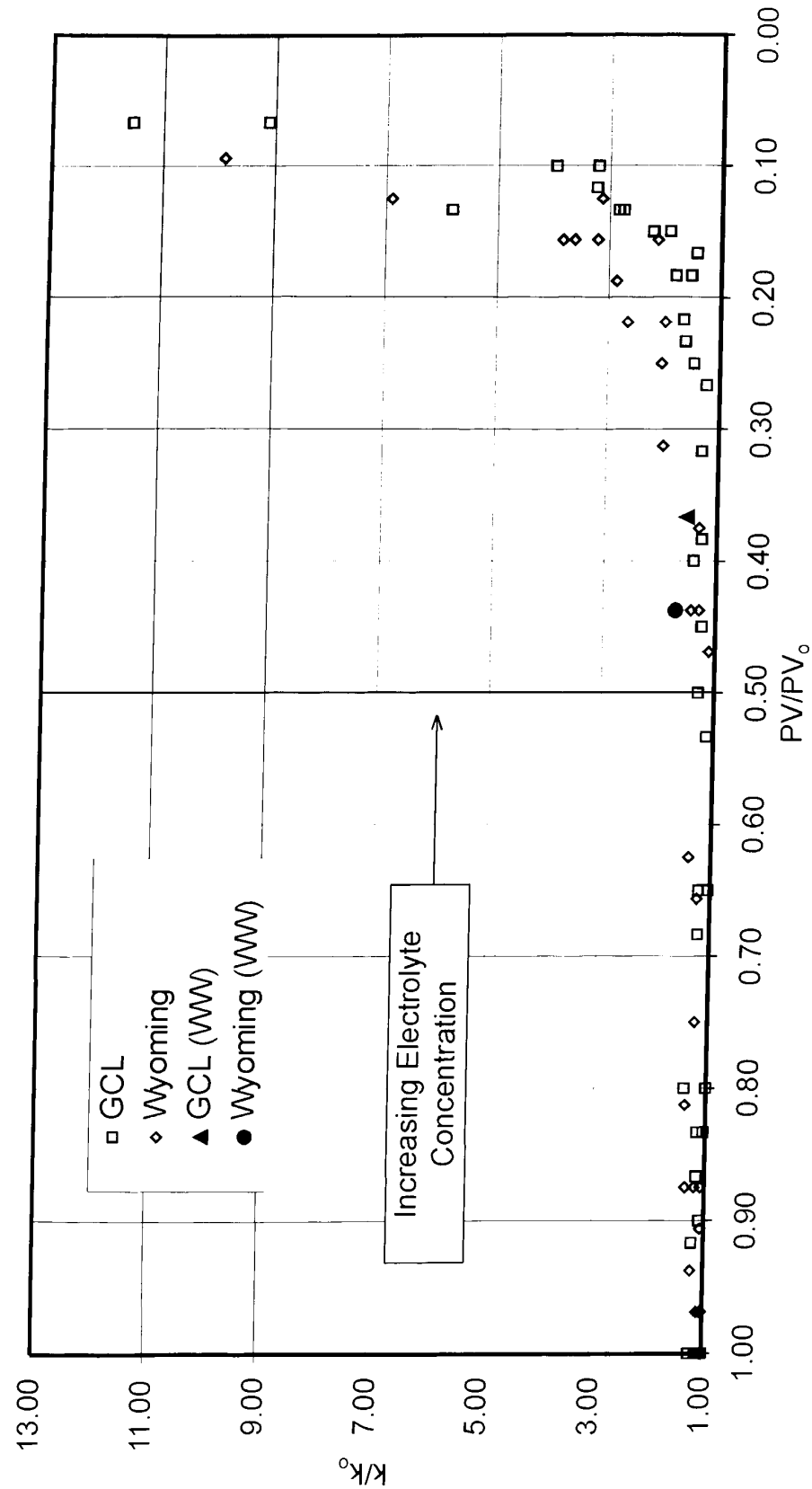

Figure 6.17 - Relative hydraulic conductivity vs. relative plastic viscosity (wastewater data).

Chapter 7 Conclusions and Recommendations

7.1 Introduction

This chapter provides the conclusions with reference to the objectives of the research. Specific emphasis is given to the development of the new alternative pre-screening method involving viscosity testing and fluid loss.

7.2 Conclusions

Following the observations and discussions from the laboratory study of the two bentonites hydrated with electrolyte solutions the following conclusions have been made:

1. Simple index tests such as: free swell, liquid limit, fluid loss, and plastic viscosity are useful to evaluate the potential for compatibility problems when exposed to electrolyte solutions. The index tests that prove to be the most helpful and reliable are fluid loss and the plastic viscosity.

2. Plastic viscosity seems to have some advantages with respect to the above application relative to the free swell index or liquid limits. With increasing electrolyte concentration, free swell indices exhibit an increase followed by a decrease, whereas plastic viscosity exhibits a steady decrease. Liquid limits also

exhibit a steady decrease. This decrease is not as sensitive as with plastic viscosity, and it is more difficult to obtain consistent results for the tests.

3. The fluid loss test can be extended in duration and interpreted to yield approximate values of hydraulic conductivity. These values, while somewhat higher on average than permeameter results, follow the same trend with respect to changes in hydraulic conductivity with changes in the pore water chemistry. Therefore, the authors propose that filter press testing can be used to quickly evaluate potential changes in hydraulic conductivity associated with chemical compatibility.

4. In the field, GCLs under effective stress experience less alteration in the inter-particle structure or fabric than would be the case for the slurries. Changes in hydraulic conductivity in the field situation, therefore, are governed by changes in the DDL thickness and ion exchange. Upon comparing the relative hydraulic conductivity values obtained from the filter press and the values obtained from the permeameters, similar trends were observed with DDL thickness contraction; as the DDL thickness contracts the hydraulic conductivity increases. Changes in the DDL thickness are easy to estimate. The dielectric constant can be measured and the electrolyte concentration of a solution can be determined from the electrical conductivity.

5. The effect of changes in effective stress on the clay fabric is of great importance when observing changes in hydraulic conductivity relative to changes in the DDL thickness. An increase in electrolyte concentration causes greater DDL contraction. This results in a more open structure increasing the hydraulic conductivity. Increasing the effective stress on a clay sample that has experienced

DDL contraction can counteract the open structure and consolidate the sample, thus reducing the hydraulic conductivity, although potentially decreasing the barrier thickness and thus increasing the hydraulic gradient.

6. The new alternative plastic viscosity pre-screening method uses both plastic viscosity and hydraulic conductivity normalized with respect to their "clean water" values to produce a plot that could be used to estimate possible changes in hydraulic conductivity of bentonite associated with compatibility problems. The plot does not give an absolute value of hydraulic conductivity; only the relative change. In measuring the decrease in plastic viscosity of the slurry, a PV/PV_O value greater than 0.5 should be expected to cause little or no change in the hydraulic conductivity. A PV/PV_O value between 0.5 and 0.2 would indicate that incompatibility is possible and alternatives should be considered or additional testing should be carried out. A PV/PV_O value less than 0.2 indicates that a significant compatibility problem may be anticipated and that bentonite should not be used or used cautiously with expert advice.

7. ASTM D 6141 provides similar results. Although the results are more variable, the test incorporates the effects of flocculation, and double layer and interlayer contraction. It is proposed that the viscosity measurement may better represent the actual in-situ performance.

8. The new plastic viscosity method is considered to be better than the existing pre-screening method outlined in ASTM D 6141. Applying either of the above criteria suggests that a few quick and simple tests can be performed to evaluate potential compatibility issues with bentonite. Designers of barrier systems

can use this information to determine whether it is necessary to adopt alternatives to bentonite sealing systems or materials.

9. Although shown to have faults, the use of ASTM D 6141 may still be continued, as it is inexpensive and easy to perform in any laboratory with a graduated cylinder. The plastic viscosity method requires a device to measure the viscosity of a soil slurry; therefore, testing is limited to laboratories that possess such a device.

7.3 Recommendations

During the course of this study, some difficulties were encountered and not all scenarios were considered. The following recommendations are made to improve on further testing and suggest what future testing should be done:

1. A better method should be used to determine the actual hydrated thickness of the GCL in the flexible wall triaxial Permeameter.

2. Plastic viscosity and filter press tests are recommended to be conducted with organic and other inorganic solutions to produce a more extensive list of chemical solutions that can be evaluated for chemical compatibility.

3. Other bentonites or natural clays are recommended to be used in plastic viscosity and filter press testing to expand the use of the pre-screening methods.

4. Analysis of the effects of treated bentonites on the pre-screening methods and the long-term durability of the polymer or other treatments applied to the bentonite clays.

References

Alther, G., Evans, J.C., Fang, H.-Y., and Witmer, K., 1985, Influence of inorganic permeants upon the permeability of bentonite, Hydraulic Barriers in Soil and Rock, ASTM STP 874, A.I. Johnson, R.K. Frobel, N.J. Cavalli, and C.B. Pettersson, Eds., ASTM, Philadelphia, pp. 64-73.

American Petroleum Institute, 1990, Recommended Practice Standard Procedure for Field Testing Water-Based Drilling Fluids, API-13B, 1st Edition, Washington, D.C. 46 p.

American Society for Testing and Materials (ASTM), 1984, Standard Test Method for Liquid Limit, Plastic Limit, and Plasticity Index of Soils (D4318-84), In : 1993 Annual Book of ASTM Standards, Vol 4.08, ASTM, Philadelphia, Pa, pp.682-692.

American Society for Testing and Materials (ASTM), 1995, Standard Test Method for Swell Index of Clay Mineral Component of Geosynthetic Clay Liners (D5890-95), In : 2003 Annual Book of ASTM Standards, Vol 4.08, ASTM, Philadelphia, Pa, pp.1570-1571.

American Society for Testing and Materials (ASTM), 1995, Standard Test Method for Fluid Loss of Clay Component of Geosynthetic Clay Liners (D5891-95), In : 2003 Annual Book of ASTM Standards, Vol 4.08, ASTM, Philadelphia, Pa, pp.1572-1573.

American Society for Testing and Materials (ASTM), 1997, Standard Guide for Screening the Clay Portion of a Geosynthetic Clay Liner (GCL) for Chemical Compatibilty to Liquids (D 4318-84), In : 2003 Annual Book of ASTM Standards, Vol 4.08, ASTM, Philadelphia, Pa, pp.1604-1605.

British Standard Determination of Liquid Limit, Preferred Method using Cone Penetrometers (BS 1377-1990 Test 2(A).

Boldt-Leppin, B., 1995, Soil-bentonite liners modified with organophilic clay, M.Sc. Thesis, Department of Civil Engineering, University of Saskatchewan, Saskatoon.

Chilingarian, G.V. and Vorabutr, P., 1981, Drilling and Drilling Fluids, Elsevier Scientific Publishing Co., New York, 767 p.

Clem, A.G. and Doehler, R.W., 1961, Industrial applications of bentonite, Clays and Clay Minerals, 10: pp. 272-283.

CSR, 1982, Drilling mud and cement slurry rheology manual, Chambre Syndicale de la Recherche et de la Production du Pétrol et du Gaz Naturel, Éditions Technip, Paris, 107 p.

Das, B.M., 1999, Principles of Foundation Engineering, 4th Edition, PWS Publishing Co. Boston, 862 p.

Edil, T.B. and Erickson, A.E., 1985, Procedure and equipment factors affecting permeability testing of a bentonite-sand liner material, Hydraulic Barriers in Soil and Rock, ASTM STP 874, A.I. Johnson, R.K. Frobel, N.J. Cavalli, and C.B. Pettersson, Eds., ASTM, Philadelphia, pp. 155-170.

Egloffstein, T., 1995, Properties and test methods to assess bentonite used in geosynthetic clay liners, Geosynthetic Clay Liners, R.M. Koerner, E. Gartung, and H. Zanzinger, Eds., Balkema, Rotterdam, pp.51-72.

Egloffstein, T., 2001, Natural bentonites-influences of the ion exchange and partial desiccation on permeability of self-healing capacity of bentonites used in GCLs, Geotextiles and Geomembranes, 19: pp. 427-444.

Fernandez, F. and Quigley, R., 1988, Viscosity and dielectric controls on the hydraulic conductivity of clayey soils permeated with water-soluble organics, Canadian Geotechnical Journal, 25(3): pp. 582-589.

Filz, G.M., Henry, L.B., Heslin, G.M., and Davidson, R.R., 2001, Determining hydraulic conductivity of soil-bentonite using the API filter press, Geotechnical Testing Journal, 24(1): pp. 61-71.

Gleason, M., Daniel, D., and Eykholt, G., 1997, Calcium and sodium bentonite for hydraulic containment applications, Journal of Geotechnical and Geoenvironmental Engineering, 123(5): pp. 438-445.

Goldman, L.J., Greenfield, L.I., Damle, A.S., Kingsbury, G.L., Northeim, C.M., and Truesdale, R.S., 1990, Clay Liners for Waste Management Facilities, Pollution Technology Review No. 178, Noyes Data Co., New Jersey, 524 p.

Henry, L.B., Filz, G.M., and Davidson, R.R., 1998, Formation and properties of bentonite filter cakes, Filtration and Drainage in Geotechnical/Geoenvironmental Engineering, Geotechnical Special Publication No. 78, L. Reddi and M. Bonala, Eds., ASCE, New York, pp. 69-88.

Haug, M.D., 1985, Slurry trench cutoffs, The First Canadian Engineering Technology Seminar on: The Use of Bentonite for Civil Engineering Applications, Avonlea Mineral Industries, Regina, SK.

Haug, M.D., 2003, CE 851, Course Notes, Applications in Geoenvironmental Engineering, University of Saskatchewan, Saskatoon.

Haug, M.D. and Boldt-Leppin, B., 1994, Influence of polymers on the hydraulic conductivity of marginal quality bentonite-sand mixtures, Hydraulic Conductivity and Waste Contaminant Transport in Soil ASTM STP 1142, D. Daniel and S. Trautwein, Eds., ASTM, Philadelphia, pp. 407-421.

Haug, M.D., Buettner, W., and Wong, L., 1994, Impact of leakage on precision in low gradient flexible wall permeameter testing, Hydraulic Conductivity and Waste Contaminant Transport in Soil ASTM STP 1142, D. Daniel and S. Trautwein, Eds., ASTM, Philadelphia, pp. 390-406.

Henry, L., Filz, M., and Davidson, R., 1998, Formation and properties of bentonite filter cakes, Filtration and Drainage in Geotechnical/Geoenvironmental Engineering, Geotechnical Special Publication No. 78, L. Reddi and M. Bonala, Eds., ASCE, New York, pp. 69-88.

Jo, H., Katsumi, T., Benson, C., and Edil, T., 2001, Hydraulic conductivity and swelling of non-prehydrated GCLs with single-species salt solutions, Journal of Geotechnical and Geoenvironmental Engineering, 127(7): pp. 557-567.

Kashir, M. and Yanful, E.K., 2001, Hydraulic conductivity of bentonite permeated with acid mine drainage, Canadian Geotechnical Journal, 38: pp. 1034-1048.

McBride, M., 1997, A critique of diffuse double layer models applied to colloidal and surface chemistry, Clays and Clay Chemistry, 45(4): pp. 598-608.

Mitchell, J.K., 1993, Fundamentals of Soil Behavior, 2nd Edition, Wiley, New York, 437 p.

Mitchell, J.K. and Madsen, F.T., 1987, Chemical effects on clay hydraulic conductivity, Geotechnical Practice for Waste Disposal '87, Geotechnical Special Publication No. 13, ASCE, New York, pp. 87-116.

Minase, M., Kondo, M., and Kamon, M., 2001, Evaluation of permeability of bentonite mud cake, Clay Science for Engineering, K. Adachi and M. Fukue, Eds., Balkema, Rotterdam, pp. 267-273.

Osicki, R., Fleming, I.R. and Haug, M.D., 2004a, A simple compatibility testing protocol for bentonite-based barrier systems, Journal of ASTM International, Vol. 1, No. 2 Paper ID JAI11731, Available online at: www.astm.org.

Osicki, R., Fleming, I.R. and Haug, M.D., 2004b, A simple compatibility testing protocol for bentonite-based barrier systems, Advances in Geosynthetic Clay Liner Technology: 2nd Symposium ASTM STP 1456, R.E. Mackey and K. Von Maubeuge, Eds., ASTM, Philadelphia, In press.

Petrov, R.J., Rowe, R.K., and Quigley, R.M., 1997, Selected factors influencing GCL hydraulic conductivity, Journal of Geotechnical and Geoenvironmental Engineering, 123(8): pp. 683-695.

Petrov, R.J. and Rowe, R.K., 1997, Geosynthetic clay liner (GCL) – chemical compatibility by hydraulic conductivity testing and factors impacting its performance, Canadian Geotechnical Journal, 34, pp. 863-885.

Reschke, A.E., 1991, Characterization of bentonites for use in sand-bentonite liner systems, M.Sc. Thesis, Department of Civil Engineering, University of Saskatchewan, Saskatoon.

Reschke, A.E. and Haug, M.D., 1991, The physico-chemical properties of bentonites and the performance of sand-bentonite mixtures, Proceedings: Canadian Geotechnical Conference, Calgary Alberta, Vol. 2, pp. 62-1 – 62-10.

Ross, C.S. and Shannon, E.V., 1926, The minerals of bentonite and related clays and their physical properties, Journal of the American Ceramic Scientist, 9: pp. 78-96.

Rowe, R.K., Petrov, R.J., and Lake, C., 1997, Compatibility testing and diffusion through GCLs, Geotechnical Research Centre Report GEOT-3-97, Department of Civil Engineering, University of Western Ontario, London, Canada, 18 p.

Rowe, R.K., Quigley, R.M., and Booker, J.R., 1995, Clayey Barrier Systems for Waste Disposal Facilities, E & FN Spon, London, 390 p.

Ruhl, J. and Daniel, D., 1997, Geosynthetic clay liners permeated with chemical solutions and leachates, Journal of Geotechnical and Geoenvironmental Engineering, 123(4): pp. 369-381.

Shackelford, C.D., 1994, Waste soil interactions that alter hydraulic conductivity, Hydraulic Conductivity and Waste Contaminant Transport in Soil ASTM STP 1142, D. Daniel and S. Trautwein, Eds., ASTM, Philadelphia, pp. 111-168.

Shackelford, C., Benson, C., Katsumi, T., Edil, T., and Lin, L., 2000, Evaluating the hydraulic conductivity of GCLs permeated with non-standard liquids, Geotextiles and Geomembranes, 18(2-4): pp. 133-162.

Shan, H. and Lai, Y., 2002, Effect of hydrating liquid on the hydraulic properties of geosynthetic clay liners, Geotextiles and Geomembranes, 20: pp. 19-38.

Simpson, B.E., 2000, Evaluation of leachate compatibility to clay soil for three geosynthetic clay liner products, Advances in Transportation and Geoenvironmental Systems Using Geosynthetics, Geotechnical Special Publication No. 103, J.G. Zornberg and B.R. Christopher, Eds., ASCE, New York, pp. 117-128.

Sivapullaiah, P.V. and Savitha, S., 1999, Index properties of illite-bentonite mixtures in electrolyte solutions, Geotechnical Testing Journal, 22(3): pp. 257-265.

Sridharan, A., Rao, S.M., and Murthy, N.S., 1986, Liquid limit of montmorillonite soils," Geotechnical Testing Journal, 9(3): pp. 156-159.

Stern, R. and Shackelford, C., 1998, Permeation of sand-processed clay mixtures with calcium chloride solutions, Journal of Geotechnical and Geoenvironmental Engineering, 124(3): pp. 231-241.

van Olphen, H., 1977, An Introduction to Clay Colloid Chemistry, 2nd Edition, Wiley, New York, 318 p.

Xanthakos, P., 1979, Slurry Walls, McGraw Hill, New York, 622 p.